

C o n t e n t s

MORPHOLOGY 28 (3)

Original Articles

- K. Todorova, I. Ivanov, I. Iliev, L. Kirazov, M. Dimitrova** – Biological Activity of Orally Given Ethyl Acetate Extract from *Cotinus coggygria* in Albino Mice with Solid and Ascites Forms of Ehrlich's Tumor 3
- I. Stefanov, S. Stefanov, N. Tsandev, I. Ivanova, S. Hamza, V. Pilicheva, A. Vodenicharov** – Morphometric Characteristics of the Lymphatic Nodules in the Porcine Gallbladder. 10
- St. Stanchev, A. Iliev, G. Kotov, N. Stamenov, M. Stefanov, B. Landzhov** – Hypertension-Induced Renal Damage in Rat Model – an Electron Microscopic Study 19
- Y. Gluhcheva, E. Petrova, E. Pavlova, A. A. Tinkov, O. P. Ajsuvakova, P. Rashev, M. Gantcheva, I. Vladov, A. V. Skalny** – Cobalt-induced Changes in Iron Homeostasis in Skeletal Muscles of Immature Mice after Perinatal Exposure to Cobalt Chloride 29

Review Articles

- E. Kaisheva** – Microscopic Characteristics for Human Hair Identification. 37

ANTHROPOLOGY AND ANATOMY 28 (4)

Original Articles

- I. Yankova Pandourska, Y. Zhecheva, A. Dimitrova** – Changes in Stature, Weight and Body Mass Index in 3-6-Year-Olds Bulgarian Children (2005 – 2016). 49
- S. Mladenova** – Characteristics of the Basic Anthropometric Features in Children of Preschool Age (3-6 years) from Smolyan Region, Bulgaria. 57
- B. Kirilov** – Eruption of the Permanent Teeth in Bulgarian Children. 67

Ts. Petleshkova, S. Sivkov, A. Baltadjiev, H. Manev, R. Raycheva, P. Timonov – Morphometric Analysis of the Orbital Area in Young Bulgarians with 3D Laser Scanning.	76
K. Makherjee, K. Das – Intra and Inter-Sexual Variation in Second (2D) and Fourth (4D) Digit Length and Ratio (2D:4D) among the Bhandas of Andaman and Nicobar Islands, India: A Cross-sectional Study	83
A. Fasova, A. Baltadjiev, I. Tsrachev, P. Timonov, F. Popova, M. E. Ali – Evaluation of Bilateral Asymmetry in the Proximal and Distal end of Humerus among the Contemporary Bulgarian Population.	96
T. Chia, A. Ajagbe, O. Onigbinde, O. I. Oyeniran, B. Turhan – Repositioning Gross Anatomy Practical for Future Pandemics: A Paradigm Shift from Traditional to Effective Alternatives. . .	103
D. Velkova, E. Kaisheva, D. Gospodinova, W. Dokov – A Case Report Applying Anthropological Methods for Establishing the Sex, Age and Stature in a Case of Dismembered Corpse. . . .	116

Review Articles

G. Temaj – Application of Dermatoglyphics Traits of Population Variation Study	123
Ts. Dimitrova - Role of Dermatoglyphics for Breast Cancer Prevention and Prognosis	130

MORPHOLOGY 28 (3)

Original Articles

Biological Activity of Orally Given Ethyl Acetate Extract from *Cotinus coggygia* in Albino Mice with Solid and Ascites Forms of Ehrlich's Tumor

Katerina Todorova¹, Ivaylo Ivanov², Ivan Iliev¹, Ludmil Kirazov¹, Mashenka Dimitrova^{1}*

¹ *Institute of Experimental Morphology, Pathology and Anthropology with Museum – Bulgarian Academy of Sciences*

² *Department of Medicinal Chemistry and Biochemistry, Medical University – Sofia*

*Corresponding author e-mail: mashadim@abv.bg

Biological activity of ethyl acetate extract from the leaves of *Cotinus coggygia* Scop. (smoke tree) was studied in an *in vivo* model of mice both healthy and developing solid or ascites form of Ehrlich's mammary gland carcinoma. Thus, the toxicity of the extract, applied per os, as well as its possible antitumor activity were evaluated. Clinical and pathomorphological studies were carried out. According to the results, no signs of overall or organ-specific toxicity were found. The extract did not prevent the development of Ehrlich's tumor but reduced the solid tumor grade by enhancing the cells differentiation. Additionally, the herb was shown to possess a mild tissue-protective activity expressed by less pronounced pathological changes in the internal organs. Another beneficial effect of the extract application was the prolonged life expectancy of treated mice.

Key words: *Cotinus coggygia* Scop., plant extracts, Erlich's breast cancer, mouse model, pathomorphology

Introduction

To date the interest in the replacement of conventional chemotherapeutic drugs used as antitumor agents, with natural compounds is growing exponentially, mostly to avoid

unfavorable side effects. Different plants, especially traditionally used over the centuries by mankind, are a good source of active substances with beneficial effects in tumor diseases. *Cotinus coggygia* Scop. (syn. *Rhus cotinus*, European smoketree, Venetian sumach) is a beautiful flowering plant from the family *Anacardiaceae*, widely spread in Europe, including our country, and commonly used in folk and modern medicine. Chemical analyses of the extracts from *C. coggygia* have shown that the plant is rich in polyphenols, glycosylated flavonols, gallic acid and gallotannins [8, 10]. *C. coggygia* extracts were reported to possess antiseptic, anti-inflammatory, hepatoprotective, antioxidant and antitumor activities [4, 8]. Our *in vitro* studies have shown that ethyl acetate extract from *C. coggygia* leaves has a selective effect on the cell viability in different tumor and not tumorigenic human cell lines [5, 6]. On the other hand, the plant is considered poisonous due to the presence of strong allergens in the essential oil.

The mouse model of Ehrlich's mammary gland carcinoma (ascites and solid forms) has proven to be convenient for the *in vivo* studies of therapeutic potential of different preparations [1, 2]. It represents a transplantable malignant tumor exhibiting aggressive behavior and poor differentiation, which can be developed in practically all strains of mice.

The aim of the present study was to evaluate the possible toxicity of the ethyl acetate extract from *C. coggygia* leaves given *per os*, and to characterize its effect on the organs of laboratory mice developing ascites and solid forms of Ehrlich's breast carcinoma.

Materials and Methods

Ethyl acetate extract of *C. coggygia* leaves was obtained exactly as described in our earlier studies [5, 6].

For the study, 42 male albino mice, 20 g body weight (b.w.), were randomly allocated to seven groups (6 mice each), as follows:

- Group 1 – not-treated controls;
- Group 2 – treated daily *per os* with DMSO solution;
- Group 3 – toxicity controls receiving daily a dissolved extract of *C. coggygia per os*;
- Group 4 – mice inoculated with Ehrlich's cells s.c in the hind leg and developing solid tumor;
- Group 5 – like group 4 but receiving daily the extract of *C. coggygia per os*;
- Group 6 – mice inoculated with Ehrlich's cells i. p. and developing ascites carcinoma;
- Group 7 – like group 6 but receiving daily the extract of *C. coggygia per os*.

All the animals were fed and watered *ad libitum* during the whole testing period (20 days). Control group 2 was treated only with the solvent, i.e. 0.2 ml 0.1 % DMSO in Phosphate Buffered Saline (PBS, Sigma) for 20 days. Toxicity controls (group 3) received daily 30mg/kg b.w. extract of *C. coggygia* dissolved in 0.2 ml 0.1% solution of DMSO in PBS for 20 days. The same treatment was applied also in groups 5 and 7. For the development of Ehrlich's carcinoma, animals were inoculated with 1×10^6 cells of the line EAC (Ehrlich's Ascites Carcinoma, maintained by *in vivo* culturing in albino

mice) in PBS s.c. in the hind leg (groups 4 and 5) or i.p. (groups 6 and 7) on the 10th day of the experiment.

The experiments were carried out in the Institute of Experimental Morphology, Pathology and Anthropology with Museum, Bulgarian Academy of Sciences (Permission Nr 11 30 127) in accordance with the national regulation Nr 20/01.11.2012 regarding laboratory animals and animal welfare and European directive 2010/63/EU of the European Parliament.

Observations of the animals were performed daily, regarding the specific signs and symptoms of the tumor disease. Animals' monitoring included also: general condition, appetite, water intake, signs of intoxication, body posture and movements, ataxia, paresis, scratching, etc.

The animals from all groups were sacrificed by cervical dislocation on the 20th day and tissue samples from solid tumors, liver, kidneys, lung, small intestine, brain, spleen and pancreas were extracted, stained with H&E according to the standard methods of histology and examined microscopically (Leica DM 5000B, Wetzlar, Germany) for the presence of morphological signs of toxicity, necrosis or destruction, tumor metastases and inflammatory reactions. Ascites' smears were stained with DiaPath May-Grünwald Giemsa Fast Method and examined under the microscope as above.

Results and Discussion

Ehrlich Ascites Carcinoma (EAC) cell line has been isolated from a spontaneously developed mammary adenocarcinoma in a mouse. It can be maintained by *in vivo* culturing through i.p. injections in virtually every mouse species [reviewed in 9]. Inoculation of experimental animals can be performed both i.p. and s.c. to develop ascites or solid form of the tumor respectively. Ehrlich's carcinoma is a poorly differentiated highly transplantable and rapidly developing tumor, resembling the most sensitive to chemotherapy human breast cancers [9]. It has been widely used to study the possible therapeutic effects of substances of both natural and synthetic origin [e.g. 1, 2].

In our experiments, we chose to apply the ethyl acetate extract of *C. coggygia* leaves orally to evaluate its overall and organ toxicity upon ingestion, since this is the most common way of uptake through teas or tinctures. Actually, we did not expect the extract to be particularly toxic as all the allergens are in the essential oil, which evaporates during the extraction process. Additionally, previous studies showed safe doses of 25-50 mg/kg b.w of *C. coggygia* total flavonoids orally given to mice [11]. In the present study we use a dose of 30 mg/kg b.w.

Clinical observations. All animals monitored during the study were observed for both normal and abnormal behavior and parameters mentioned above. As expected, groups 1 and 2 did not show any abnormal reactions or toxicity signs. The same applied also for group 3-treated with the *C. coggygia* extract. Tumors developed very quickly in other groups (2nd to 3rd day after inoculation), as noted by palpation (solid form) or abdominal circumference (ascites form). The animals from those groups showed characteristic signs of fatigue, lameness with the injected leg, enlarged abdominal circumference (ascites form of the tumor), difficulty in movement, reduced tone and

a significant decrease in activity and general condition. It should be noted that the animals in groups treated with *C. coggygia* extract (5 and 7) showed a preserved food intake and prolonged life expectancy in the range of the experiment, whereas two of the animals of the group 6 and one of the 4th group died before the end of the testing time.

Macroscopically, solid tumors in the groups inoculated s.c. (4 and 5) varied in size independently of whether the mice received extract or not. The same applied also for the volume of ascites in the animals, inoculated i.p. (groups 6 and 7). The internal organs seemed unchanged except for the pancreas which was enlarged in all the animals with developing ascites tumors.

Pathomorphology. No clinical signs of general toxicity or pathohistological evidences for organ toxicity were observed in mice treated only with the extract (group 3) during the 20 days period of the experiment. All the examined organs of those animals did not show any differences from the control groups 1 and 2. Histological studies of the solid tumors (group 4) revealed a pronounced cell anaplasia, cells in different phases of mitosis, rarely pyknotic nuclei and cytoplasm vacuolization, pointing out a low level of apoptosis (**Fig. 1A**). Tumor masses of the animals treated orally with the extract exhibited signs of cell differentiation and maturation in the tumor periphery (**Fig. 1C and D**). Also, cells with karyorrhectic or pyknotic nuclei as well as a substantial

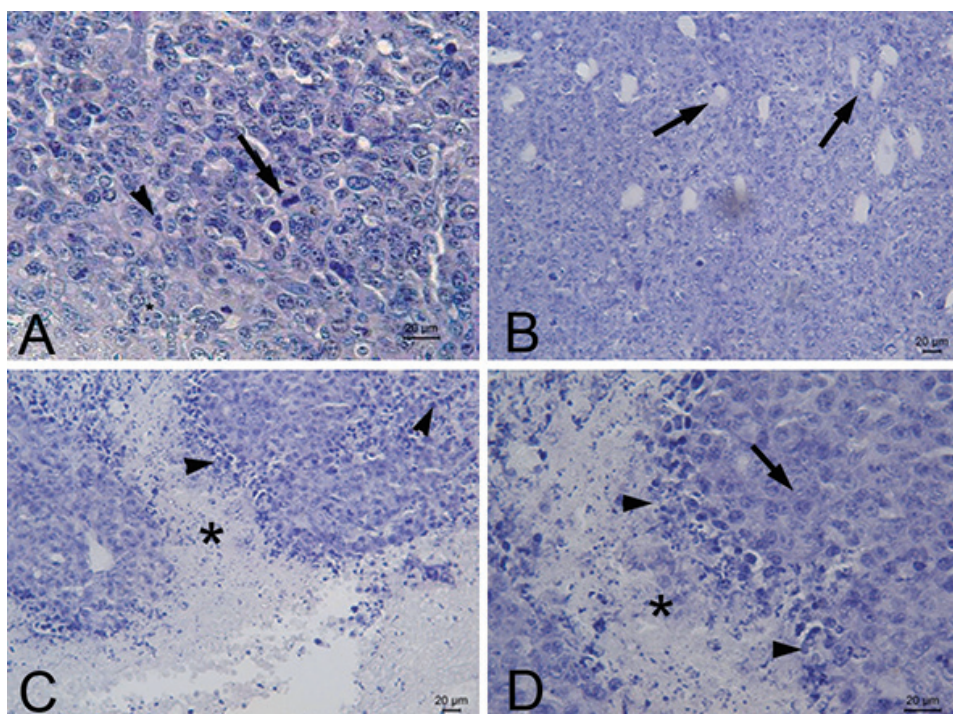


Fig. 1. Solid form of Ehrlich's carcinoma. Mice not treated with *C. coggygia* (A) – anaplasia, cells in different phases of mitosis (arrow), low number of pyknotic nuclei (arrowhead); Mice treated with the extract (B, C, D) – abundant vasculature in the tumor periphery (arrows) (B); C and D – formation of necrotic foci (asterisk) in the central tumor masses, lots of cells with pyknotic or karyorrhectic (apoptotic) nuclei (arrowheads), visible cell differentiation (arrow) in the tumor periphery (D). H&E, scale bar = 20 µm.

vacuolation of the cells were observed (**Fig. 1C and D**), which can be assumed as an indication of apoptotic processes. Necrotic areas in the tumor center were also observed (**Fig. 1C and D**). Neovascularization was visible in the peripheral area with the lumen of the vessels filled with plasma proteins content (**Fig. 1B**). In nonvascular regions formation of hypoxic areas and focal necroses were noticed.

Cell smears of the animals with ascites form of Ehrlich's carcinoma showed mitotic figures and formation of multinucleated giant carcinoma cells. Pyknosis or vacuolation were rare (**Fig. 2A, B**). Visibly, the number of giant cells in the ascites from animals treated with the extract was lower. Leukocytes and mononuclear cells were also presented.

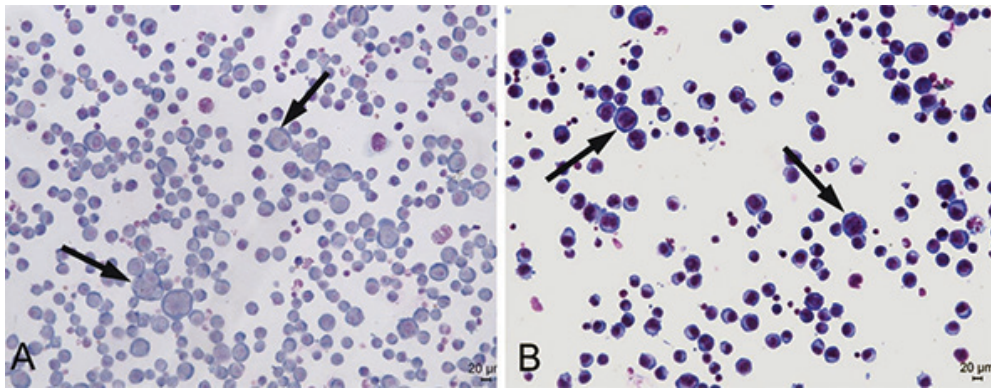


Fig. 2. Ascites form of Ehrlich's carcinoma. Mice not treated with *C. coggygria* (A). Mice treated with the extract (B). Giant carcinoma cells (arrows). May-GrunwaldGiemsa, scale bar = 20 μ m.

Ehrlich's mammary gland carcinoma in mice has been shown to metastasize in the liver, kidney and spleen and different methods have been tested to reduce the tumor spread [e.g. 3]. In our experiment, no metastases were found in the animals with solid form of the tumor (groups 4 and 5), whereas tumor cells infiltrations were found in the kidney and pancreas of mice with ascites form of the tumor (group 6). Liver and spleen also showed pathological changes in the animals not-receiving *C. coggygria* extract. In the liver, enlarged sinusoids with immune cell content but invisible (not enlarged) perisinusoidal spaces (Disse spaces) were observed. Groups of cells with pyknotic nuclei were also seen in the liver lobules (**Fig. 3B**). Otherwise, mice treated with the extract (groups 5 and 7) showed a normal architecture of the liver lobules (**Fig. 3A**). In the spleen, the megakaryocytes population was increased with both normal and dwarf cells, some of which having endomytotic figures (**Fig. 3F**). The animals treated with *C. coggygria* had a lower number of megakaryocytes with normal appearance (**Fig. 3E**). Kidneys of some of the animals with ascites form of the tumor had metastatic tumor infiltrations (**Fig. 3D**). In certain animals enlarged periglomerular spaces due to a shrinkage of the glomeruli were seen as well as disrupted tubules organization (**Fig. 3D**). Those findings should be connected with the aggressive tumor growth and organism exhaustion. No metastases were observed in the animals receiving *C. coggygria* and the structure of kidney parenchyma in those animals appeared preserved (**Fig. 3C**).

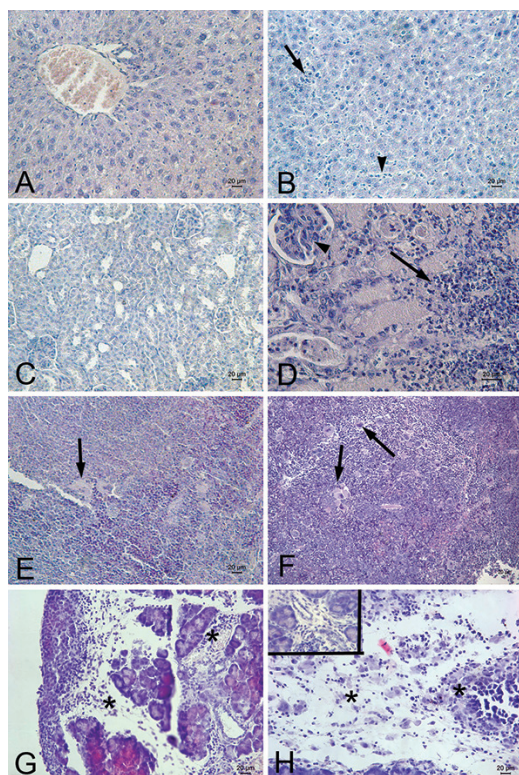


Fig. 3. Pathomorphology of the internal organs of mice, developing ascites Ehrlich's carcinoma. Left (A, C, E, G) – treated with *C. coggygia* extract; Right (B, D, F, H) – not treated with the extract. A – Normal appearance of a hepatic lobule; B – groups of cells with pyknotic nuclei (arrow), enlarged sinusoid with immune cells content (arrowhead). C – Preserved structure of the kidney cortex; D – tumor cells and inflammatory cells infiltrations (arrow) in mice of group 6, renal corpuscles (arrowhead); E – Increased number of megakaryocytes with normal appearance (arrows); F – a large number of normal and dwarf megakaryocytes (arrows), some of which with mitotic nuclei. G and H – Leukocytes and metastatic tumor cells infiltrations in the fibrovascular capsule and pancreatic septa (asterisks); H inclusion – cell spreading in the perivascular spaces and pancreatic ducts in mice of group 6. H&E, scale bar = 20 μ m.

lack of lethal cases for the 10 days post-inoculation period in the groups treated with the extract could be attributed to the herb's protective effect on parenchymal organs.

Acknowledgements: This work is financially supported by the Scientific Fund of Bulgarian Ministry of Education and Science, Grant Nr KP-06-N31/1.

Metastatic Ehrlich's tumor infiltrations were found in pancreatic peripheral exocrine parenchyma more distinct in two mice from the group 6 (**Fig. 3H**). Similar but less pronounced infiltrations were seen also in mice, treated with the extract (**Fig. 3G**).

In general, it can be said that the herb extract mitigates the pathological changes resulting from the tumor development in parenchymal organs. Earlier studies point out the large content of gallic acid and gallotanins in the preparations of *C. coggygia* [8, 10]. Gallic acid (free or liberated from gallotanins by intestinal enzymes) is readily absorbed by the intestinal mucosa and spread with the blood to all organs, forming a major depot in the liver [12]. Biological activity of this compound includes inhibition of tumor cells proliferation and common tissue-protective effects [reviewed in 7]. It can be assumed that the tissue protective activity of the *C. coggygia* extract on the parenchymal organs in our study is due at least in part to gallic acid.

In conclusion, ethyl acetate extract from *C. coggygia* leaves does not show any signs of toxicity by application *per os* in mice at least at a dose of 30 mg/kg b.w. The extract cannot prevent the development and growth of Ehrlich's mammary gland carcinoma but can reduce the solid tumor grade by enhancing the cells differentiation. Additionally, the herb possesses a mild by the less pronounced pathological changes of the internal organs. Also, the

References

1. Aldubayan, M. A., R. M. Elgharabawy, A. S. Ahmed, E. Tousson. Antineoplastic activity and curative role of avenanthramides against the growth of Ehrlich solid tumors in mice. – *Hindawi Oxidative Medicine and Cellular Longevity*, 2019, Article ID 5162687.
2. Ali, A. D., K. N. Badr El-Din, R. F. Abou-El-Magd. Antioxidant and hepatoprotective activities of grape seeds and skin against Ehrlich solid tumor induced oxidative stress in mice. – *Egyptian Journal of Basic and Applied Sciences*, **2**(2), 2015, 98-109.
3. Fadel, M. A, R. El-Gebaly, A. Aly, A. Sallam, O. Sarhan, H. Eltohamy. Preventing of Ehrlich tumor metastasis in liver, kidney and spleen by electromagnetic field. – *Int. J. Phys. Sci.*, **5**(13), 2010, 2057-2065.
4. Gospodinova, Z., N. Bózsity, M. Nikolova, M. Krasteva, I. Zupkó. Antiproliferative properties against human breast, cervical and ovarian cancer cell lines, and antioxidant capacity of leaf aqueous ethanolic extract from *Cotinus coggygria* Scop. – *Acta Medica Bulgarica*, **XLIV**, 2017, 20-25.
5. Iliev, I., I. Ivanov, K. Todorova, M. Dimitrova. Effects of a *Cotinus coggygria* ethyl acetate extract on two human normal cell lines. – *Acta morphol. anthropol.*, **27**(3-4), 2020, 25-29.
6. Iliev, I., I. Ivanov, K. Todorova, D. Tasheva, M. Dimitrova. *Cotinus coggygria* non-volatile fraction affects the survival of human cultured cells. – *Acta morphol. anthropol.*, **28**(1-2), 2021, 23-18.
7. Kahkeshani, N., F. Farzaei, M. Fotouhi, S. S. Alavi, R. Bahramsoltani, R. Naseri, S. Momtaz, Z. Abbasabadi, R. Rahimi, M. H. Farzaei, A. Bishayee. Pharmacological effects of gallic acid in health and diseases: A mechanistic review. – *Iran. J. Basic Med. Sci.*, **22**(3), 2019, 225-237.
8. Matić, S., S. Stanicć, M. Mihailović, D. Bogojević. *Cotinus coggygria* Scop.: An overview of its chemical constituents, pharmacological and toxicological potential. – *Saudi Journal of Biological Sciences*, **23**, 2016, 452-461.
9. Ozaslan, M., I. D. Karagoz, I. H. Kilic, M. E. Guldur. Ehrlich ascites carcinoma. – *Afr. J. Biotech.*, **10**, 2011, 2375-2378.
10. Pollio, A., A. Zarrelli, V. Romanucci, A. Di Mauro, F. Barra, G. Pinto, E. Crescenzi, E. Roscetto, G. Palumbo. Polyphenolic profile and targeted bioactivity of methanolic extracts from Mediterranean ethnomedicinal plants on human cancer cell lines. – *Molecules*, **21**, 2016, 395.
11. Wang, G., J. J. Wang, L. Du, F. Li. Effect and mechanism of total flavonoids extracted from *Cotinus coggygria* against glioblastoma cancer *in vitro* and *in vivo*. – *BioMed Research International*, 2015, Article ID 856349.
12. Zong, L., M. Inoue, M. Nose, K. Kojima, N. Sakaguchi, K. Isuzugawa, T. Takeda, Y. Ogi-hara. Metabolic fate of gallic acid orally administered to rats. – *Biol. Pharm. Bull.*, **22**(3), 1999, 326-329.

Morphometric characteristics of the lymphatic nodules in the porcine gallbladder

Ivaylo Stefanov^{1}, Stefan Stefanov³, Nikolay Tsandev², Ivelina Ivanova¹,
Sevinch Hamza¹, Vanessa Pilicheva¹, Angel Vodenicharov²*

¹ Department of Anatomy, Faculty of Medicine, Trakia University, Stara Zagora, Bulgaria

² Department of Veterinary Anatomy, Histology and Embryology, Trakia University, Stara Zagora, Bulgaria

³ Fifth year student at Medical faculty, Trakia University, Stara Zagora, Bulgaria

* Corresponding author e-mail: ivstefanov@abv.bg

The aim of this study was to estimate the distribution and size of the lymphatic nodules in the wall of gallbladder in pigs at different ages.

A light microscopic observation was performed on the lymphatic tissue localized in *fundus*, *corpus* and *collum vesicae felleae*. We found out that lymphatic tissue in gallbladder is represented by diffuse lymphatic tissue, primary and secondary type of solitary lymphatic nodules as well as aggregated lymphatic nodules. In 2 month-old pigs, only diffuse lymphatic tissue was observed. In 6 month- and 3 year-old animals except for diffuse lymphatic tissue, both primary and secondary lymphatic nodules were defined. The density of nodules in 6 month-old pigs was higher than in 3 year-old ones. In 6 month-old pigs, the diameter of nodules was smaller than in 3 year-old ones.

In conclusion, the solitary and aggregated lymphatic nodules observed form well defined gallbladder-associated lymphoid tissue.

Key words: gallbladder – associated lymphoid tissue, morphometry, pigs

Introduction

Based on the anatomical and functional properties, the mucosal immune system (MIS) can be separated into inductive and effector sites [9]. The migration of immune cells from mucosal inductive to effector tissues via the lymphatic system is the cellular basis for the immune response in the gastrointestinal, the upper respiratory, and female reproductive tracts. Mucosal inductive sites include mucosa-associated lymphoid tissue (MALT) network delivering a continuous source of memory B- and T-lymphocytes that then move to mucosal effector sites [5, 7]. Mucosal effector sites, including the lamina propria regions of the gastrointestinal, the upper respiratory and female reproductive tracts as well as secretory glandular tissues (mammary, lacrimal, salivary, etc.) contain

Ag-specific mucosal effector cells such as IgA-producing plasma cells, and memory B and T cells [1]. The components of MALT include solitary lymphoid nodules, aggregates consisting of several lymphoid nodules and lymphoepithelium (LE) [8].

The uptake of antigen occurs through the lymphoepithelium (LE) by M cells or dendritic cells. Some components of MALT are constitutively present at defined mucosal sites, such as the tonsils; others are with varying location, such as Peyer's patches in the jejunum and ileum, and others are induced by antigen exposure, such as bronchus-associated lymphoid tissue and solitary lymphatic nodules. Recirculating lymphocytes enter MALT through venules in the internodular areas. Receptors on venules regulate the tissue-specific migration of lymphocytes [8].

The structure of the lymphoid tissue in porcine stomach, small and large intestine is well studied [6, 15]. Recently, Stefanov [14] studied the age-dependent distribution and size of lymphatic nodules as components of extrahepatic bile duct associated lymphatic tissue in domestic swine. However, information about the existence and structure of the lymphoid tissue in gallbladder in domestic swine (even in *Nomina Histologica Veterinaria* [12]) is not available.

That's why the aim of the current study is to define the distribution and size of lymphatic nodules (LNs) in the wall of gallbladder in pigs at different ages in order to elucidate the structure of gallbladder-associated lymphoid tissue (GBALT) as another component of mucosa-associated lymphoid tissue.

Materials and Methods

Animals

For this study, gallbladders of 6 pigs at the age of 2 months (22 – 33 kg), 6 pigs at the age of 6 months (92 - 100 kg) and 6 pigs at the age of 3 years (280 - 300 kg) were collected according to the Scientific Project number 13/2017, Medical Faculty, Trakia University, Stara Zagora, Bulgaria. All procedures were carried out in accordance with the Bulgarian legislation regarding animal care (Ordinance 20 of 01.11.2012 on the minimum requirements for the protection and welfare of experimental animals and the requirements for the sites for use, breeding and/or delivery) and Directive 2010/63 / EU of the European Parliament and of the Council of 22 September 2010 on the protection of animals used for scientific purposes.

Material

The tissue samples were obtained from pigs slaughtered at slaughter house for meat consumption. The samples from gallbladder's bottom, body and neck were fixed in 10% aqueous solution of formalin. Then these samples were dehydrated in alcohols and embedded in paraffin. About 5-6 μm thick paraffin serial cross sections were mounted on gelatinized slides, twice placed in xylene, rehydrated by decreasing ethanol concentrations and stained with Haematoxylin and Eosin (H&E) dye.

Histochemical methods for detection of elastic and collagen fibers

Orcein staining method was used to identify elastic fibers (stained in dark brown) but Van Gieson method – for detection of collagen fibers (stained in red).

Morphometric study

The measurements were performed on sections stained with H&E in order to define the size (diameter, height and width in μm) and density (number per cross section) of LNs. The measurements were done by a light microscope (LEICA DM1000, Leica Microsystems, UK) with a digital camera (LEICA DFC 290) and software (LAS V4.10.0 2016).

Statistical analysis

The data obtained were processed by GraphPad Prism 6 for Windows (GraphPad Software, Inc., USA) via one-way analyses of variance (one-way ANOVA) followed by Tukey-Kramer's post-hoc test. The values of the studied parameters were presented as mean \pm SD. P-values < 0.05 were considered statistically significant.

The terminology was consistent with the Nomina Histologica Veterinaria [12].

Results

In the present study, a light microscopic observation was performed on the lymphatic tissue localized in the three parts of the gallbladder: bottom (*fundus vesicae felleae*), body (*corpus vesicae felleae*) and neck (*collum vesicae felleae*).

It was found that the gallbladder-associated lymphatic tissue was represented by diffuse lymphatic tissue (DLT), solitary lymphatic nodules (SLNs) and aggregated lymphatic nodules (ALNs). SLNs and ALNs were absent in 2 month-old pigs but were present in 3 year – and 6 month-old animals. The micromorphometric study allowed calculating the diameter, height and width of SLNs and ALNs (**Table 1**).

In **2 month-old pigs**, DLT is the main lymphoid tissue localized in the propria (*lamina propria mucosae*) below the surface simple columnar epithelium (*lamina epithelialis mucosae*), but SLNs were not observed. The DLT in the propria of the *fundus* of gallbladder was less developed and looser than in the gallbladder's body. In the neck of gallbladder, the DLT was most developed and extends into muscle layer (*tunica muscularis*) of the organ where surrounds the gallbladder's glands (*gll. vesicae felleae*) (**Fig. 1a,b**).

In **6 month-old pigs**, loose DLT was present in the propria of *fundus* filling the connective tissue of the mucosal folds. This group of pigs, unlike 2 month-old pigs, showed well developed SLNs arranged in single row in the propria protruded to the lumen of bladder. These protrusions, covered with unfolded mucosa, were situated between mucosal folds of gallbladder's *corpus* and *collum*. The peripheral part of the LNs penetrates the inner part of the muscle layer at the border with the propria. In most of SLN, *corona lymphonoduli* and germinal center were not defined. Single LNs with distinctive *corona lymphonoduli* and germinal center were observed (**Fig.1c**). Above nodules, between them and *lamina epithelialis mucosae*, a low and wide area of lymphocytes, known as dome, was determined. The DLT in *corpus vesicae felleae* was more developed and denser than those in the *fundus* and was localized in the remaining parts of the propria where LNs were not present. Except of the propria,

the DLT was also observed in the muscle layer surrounding the glandular alveoli. In the *collum vesicae felleae*, the DLT and SLNs were localized in the same manner like in gallbladder's body. However, single (1-2 nodules per cross section) pear-or oval shaped lymphatic nodules were localized deeply in *tunica muscularis*. The SLNs were not surrounded by connective tissue capsule except of those localized in muscle layer which were surrounded by delicate capsule. The basal part of each nodule was separated from underlying muscle layer by delicate connective tissue area containing collagen and elastic fibers, as well as vessels of the microcirculatory bed: arterioles, capillaries and venules. The lymphoid tissue was represented mainly by primary and less secondary SLNs separated by internodular area containing lymphocytes (DLT), collagen and elastic fibers, as well as vessels of microcirculatory bed (**Figs. 1, 2**). The vessels were observed mostly in the basal part of nodules, as well as in domes at the border with peripheral part of nodules and between *corona lymphonodul* and germinal center in secondary LNs.

In *corpus vesicae felleae*, ALNs, consisting of 3 LNs in most cases, were localized in the propria and protruding to the lumen of bladder between mucosal folds (**Fig. 1c**). In the surface epithelium above the ALNs single goblet cells were identified.

The ALNs in gallbladder formed nodular area, internodular area and nodule-associated epithelium (**Fig. 1c**). The internodular area was represented mainly by DLT and vessels of microcirculatory bed. The nodule-associated epithelium was observed to consist of simple columnar epithelium above the nodules and domes, lymphocytes as well as has single or no goblet cells.

Rarely, the base of ALNs together with gallbladder glands formed lymphoglandular complex (LGC) which was formed mostly by diffuse lymphatic tissue and gallbladder's glands (**Fig. 1b**), but single lymphatic nodules were detected near the glands. LGC epithelium was represented by secretory glandular cells, goblet cells and lymphocytes. In *collum vesicae felleae*, ALNs, consisting of 2 LNs, were localized in the propria and protruding to the lumen of bladder between mucosal folds.

Single goblet cells (from 1 to 3 cells) were observed in the surface epithelium above the ALNs. The surface epithelium of the adjacent mucosa contained more goblet cells (**Fig. 1d**).

The diameter of ALNs in *collum vesicae felleae* was bigger than in *corpus vesicae felleae*. In 6 month-old pigs the diameter of ALNs was larger than in 3 year-old animals.

In **3 year-old animals**, the localization of solitary LNs and DLT was similar to 6 month-old pigs.

The main shape of nodules in gallbladder wall was round – their height and width were almost the same (**Table 1**). The diameter of SLNs was largest in the neck, followed by the body, and smallest in the bottom of gallbladder in both groups: of 6 month- and 3 year-old animals. The number of SLNs was highest in the body, followed by the bottom and smallest in the neck of gallbladder in 6 month- and 3 year-old animals. Most LNs showed raised areas called domes, which were observed as low and wide subepithelial regions in the gallbladder of 6 month-old pigs but were better defined in the three parts (bottom, body and neck) of gallbladder in 3 year-old animals. The surface epithelium over the dome region was devoid of folds or only single thin and short folds can be detected. This nodule-associated epithelium overlying the lymphatic

nodules consists of simple columnar epithelium with single goblet cells (**Fig. 1d**). The surface epithelium was infiltrated with lymphocytes (**Fig. 1b**). Therefore the nodule-associated epithelium is kind of lymphoepithelium. The basement membrane of the surface epithelium participating in formation of lymphoepithelium was more porous than that of the surface epithelium between nodule-containing areas.

In 3 year- old animals, ALNs, consisting of 2 lymphatic nodules, were localized in the propria and protruding to the lumen of gallbladder's bottom, body and neck between mucosal folds (**Fig. 1d**). The diameter of ALNs in the neck was the biggest, followed by bottom and body of bladder. Like in 6 month-old pigs, the LGC was formed mainly by DLT around and between gallbladder's glands, but single SLNs were detected near the glands. Lymphoglandular complex epithelium was observed to contain secretory glandular cells, goblet cells and lymphocytes

The number of SLNs in both 3 year- and 6 month-old animals was highest in *corpus*, followed by *fundus* and *collum vesicae felleae*. However, in 6 month-old animals the density of SLNs was significantly higher than in animals at the age of 3 years (**Table 2**).

Discussion

In the current light microscopic study, the detailed information about the structure of gallbladder-associated lymphatic tissue was delivered for the first time. It was revealed that GBALT was represented by DLT, solitary lymphatic nodules – *noduli lymphatici solitarii* [12] similarly to GALT in small and large intestine described by Urmila et al. [15]. With advancing age, the GBALT developed and primary and secondary LNs were seen in the gallbladder. Lymphatic tissue developed until six months. No signs for lymphatic tissue involution were seen at the age of six months in the GBALT. However, such involution was detected at the age of 3 years.

The results showed that the lymphoid tissue forming in the gallbladder of two-month-old pigs was represented by DLT only. The SLNs in gallbladder appeared in pigs at six months of age and were arranged in single row without germinal center, only single LNs showed germinal centers. This finding is similar to the localization of SLN in submucosa of porcine duodenum but is different from their location in jejunum and ileum, where LNs were arranged into two rows [15]. The lymphoid tissue gallbladder had primary and secondary LNs separated by internodular areas. This lymphoid tissue was seen in specimens taken from pigs older than two months.

The current study showed that the diameter of the LNs in gallbladder increased with age from fundus to *collum vesicae felleae* and was similar to diameter of LNs in porcine intestine [15]. Also, they were oval shaped resembling the SLNs in porcine duodenum [15].

The SLNs in gallbladder were not enclosed by connective tissue capsule except those localized in muscle layer which were surrounded by delicate capsule. The lymphoid tissue had mainly primary and less secondary LNs separated by internodular areas containing lymphocytes, vessels of microcirculatory bed and collagen- and elastic fibers. These results correspond to the findings of Urmila et al. [15] in porcine intestine.

As mentioned above, in porcine gallbladder both types of LNs were detected: primary and secondary ones. The secondary LNs showed pale germinal center and dense *corona lymphonoduli*. Similar to porcine intestine, over the LNs areas called domes were observed [15]. In gallbladder, the domes were low and broad. The domes of the jejunal and ileal lymphoid nodules were found to possess broad basal portion and a narrow apical part [15]. According to Neutra et al., [11] the dome contains B- and T-lymphocytes, dendritic cells (DCs) and macrophages. Morfitt and Pohlenz [10] reported that gastric MALT nodules resemble lymphoglandular complexes described in the colon of pigs. The gastric epithelium is devoid of parietal and goblet cells in these areas and releases deep crypts with areas of lymphoepithelium between the lymphoid follicles. Solitary LNs were observed in the submucosa and lamina propria of the lesser curvature of the gastric cardia and of the cardiac fundic diverticulum [6]. Later, in healthy pigs, some authors found that gastric MALT was present in fetal pigs and at birth like the other MALT structures of the gastrointestinal tract [3]. In piglets, they are described as inactive encapsulated aggregates of lymphocytes deep in the submucosa [6]. Green et al. [6] reported that activation of gastric MALT can be induced by colonization of piglets with *Helicobacter pylori*, but not by enteric bacteria or viruses.

The intestinal aggregated lymphatic tissue was described in details by Eurell and Frappier, [4]. Aggregated lymphatic tissue of the intestine contains submucosal lymphatic nodules with high mitotic activity, a zone of small lymphocytes (the *corona lymphonoduli*), internodular region rich in T cells and postcapillary venules through which lymphocytes recirculate, an elevated region (the dome) overlying LNs, and a nodule-associated epithelium. Like in rabbit intestine [11], the ALNs in gallbladder observed in this study form nodular area, internodular area and nodule-associated epithelium.

The LNs were observed near the gallbladder's glands forming LGC. The current study showed that LGC epithelium in porcine gallbladder consisted of glandular secretory cells, goblet cells, intraepithelial leukocytes. The LGCs were present in the *corpus vesicae felleae* of 6 month-old pigs but not in 3 year-old animals. Taking into account the classification of LGCs in porcine intestine [15], we suggest that most LGCs in gallbladder belong to superficial type, because they were localized in *lamina propria mucosae*. Single LGCs were observed deep in the muscle layer of gallbladder's *collum*.

The lymphoepithelium was described on jejunal Peaer's patches, ileal Peaer's patches domes and in LGC in the large intestine [2, 8, 10, 13]. It was reported to consist mostly of enteroabsorptive cells and single M-cells. In gallbladder, the lymphoepithelium, also called nodule-associated epithelium, was presented by simple columnar epithelium infiltrated by lymphocytes. M-cells of lymphoepithelium in gallbladder were not described because they were not the aim of the current study.

The structure of LGCs observed in gallbladder was similar to that of LGCs in porcine intestine described by Morfitt and Pohlenz [10]: LNs and internodular lymphatic tissue penetrated by gallbladder's glands. In the intestine, the LGC epithelium contained goblet cells, enterocytes, enteroendocrine cells, M cells, individual and grouped intraepithelial leukocytes [10], but in gallbladder LGC epithelium consisted of secretory glandular cells, single goblet cells and intraepithelial lymphocytes.

Conclusion

The presence of lymphatic nodules and aggregates forming gallbladder-associated lymphoid tissue defines the gallbladder's mucosa as important part of the mucosal immune system in pigs.

Acknowledgements: With thanks to scientific project № 13/2017, Medical Faculty, Trakia University, Stara Zagora, for delivering of animals for this study.

References

1. **Brandtzaeg, P.** Induction of secretory immunity and memory at mucosal surfaces. – *Vaccine*, **25**, 2007, 5467-5484.
2. **Chu, R. M., R. D. Glock, R. F. Rossand, D. E. Cox.** Lymphoid tissues of the small intestine of swine from birth to one month of age. – *Am. J. Vet. Res.*, **40**(12), 1979, 1713-1719.
3. **Driessen, A., C. Van Ginneken, J. Creemers, I. Lambrichts, A. Weyns, K. Geboes N. Ectors.** Histological and immunohistochemical study of the lymphoid tissue in the normal stomach of the gnotobiotic pig. – *Virchows Arch.*, **441**, 2002, 589-598.
4. **Eurell, J. A., B. L. Frappier.** Dellmann's textbook of veterinary histology, 6th ed. Blackwell Publishing Professional 2121 State Avenue, Ames, Iowa 50014, USA, 2006, pp. 139-143.
5. **Fujihashi, K., P. N. Boyaka, J. R. McGhee.** Host defenses at mucosal surfaces. In: Clinical immunology, ed. Rich R.T, Mosby Elsevier, Philadelphia, 2008, pp. 287-304.
6. **Green W. B., K. Eaton, S. Krakowka.** Porcine gastric mucosa associated lymphoid tissue (MALT): stimulation by colonization with the gastric bacterial pathogen, *Helicobacter pylori*. – *Vet. Immunol. Immunopathol.*, **56**, 1997, 119-131.
7. **Kiyono, H., J. Kunisawa, J. R. McGhee, J. Mestecky.** The mucosal immune system. In: Fundamental immunology, editor Paul W.E., Lippincott Williams & Wilkins, Philadelphia, 2008, pp. 983–1030
8. **Liebler-Tenorio, E. M. R. Pabst.** MALT structure and function in farm animals. – *Vet. Res.*, **37**(3), 2006, 257-280.
9. **McGhee, J. R., K. Fujihashi.** Inside the Mucosal Immune System. *PLOS Biology*, **10**(9), 2012, e1001397. doi:10.1371/journal.pbio.1001397
10. **Morfitt, D. C., J. F. L. Pohlenz.** Porcine colonic lymphoglandular complex: distribution, structure, and epithelium. – *Am. J. Anat.*, **184**, 1989, 41-51.
11. **Neutra, M. R., T. L. Phillips, E. L. Mayer, D. J. Fishkind.** Transport of membrane-bound macromolecules by M cells in follicle-associated epithelium of rabbit Peyer's patch. – *Cell Tissue Res.*, **247**(3), 1987, 537-546.
12. **Nomina Histologica Veterinaria.** 1st edition. International Committee on 5 Veterinary Histological Nomenclature (I.C.V.H.N.) to the World 6 Association of Veterinary Anatomists. Published on the website of the World 7 Association of Veterinary Anatomists, 2017, pp. 30, 31, 51.
13. **Torres-Medina, A.** Morphologic characteristics of the epithelial surface of aggregated lymphoid follicles (Peyer's patches) in the small intestine of newborn gnotobiotic calves and pigs. – *Am. J. Vet. Res.*, **42**, 1981, 232-236.
14. **Stefanov, I. S.** Age-dependent distribution and size of lymphatic nodules as components of extrahepatic bile duct-associated lymphatic tissue in domestic swine – a micromorphometric study. *Bulg. J. Vet. Med.*, ONLINE FIRST ISSN 1311-1477, 2021, DOI: 10.15547/bjvm.2021-0003
15. **Urmila, T. S, P. J. Ramayya, M.S. Lakshmi, A. V. N. Siva Kumar.** Histomorphological studies on Gut Associated Lymphoid Tissue of pig (Susserofa). – *Pharma Innov. J.*, **8**(3), 2019, 97-101.

Table1. Diameter, height (h) and width (w), in μm , of solitary lymphatic nodules (SLNs) and aggregated lymphatic nodules (ALNs) in the wall of gallbladder (*Vesica fellea*).

Parameters	3 year-old pigs Mean \pm SD	6 month-old pigs Mean \pm SD	2 month-old pigs Mean \pm SD
<u>Diameter of SLNs</u>			
<i>Vesica fellea</i> :			
• fundus	382.0 \pm 15.23	360.7 \pm 8.88 D1	-
• corpus	527.1 \pm 27.18 C4	370.9 \pm 32.70 D4	-
• collum	638.6 \pm 20.88 A4,B4	396.7 \pm 13.90 B3,D4	-
<u>Height and width of SLNs</u>			
• fundus (h)	414.5 \pm 17.40	394.8 \pm 23.42	-
(w)	349.5 \pm 19.34	326.6 \pm 18.26	-
• corpus (h)	591.5 \pm 45.29	373.3 \pm 47.02	-
(w)	462.7 \pm 17.54	368.5 \pm 35.31	-
• collum (h)	663.7 \pm 39.74	418.7 \pm 21.08	-
(w)	613.50 \pm 0.32	374.7 \pm 22.83	-
<u>Diameter of ALNs</u>			
<i>Vesica fellea</i> :			
• fundus	628.6 \pm 6.5	-	-
• corpus	805.8 \pm 19.78 C4	930.2 \pm 7.43 D4	-
• collum	820.5 \pm 24.63 A4,B4	1008.0 \pm 10.47 A4,D4	-

A4 ($P < 0.0001$) statistical significant difference between *collum* and *corpus vesicae felleae*

B 3,4 ($P < 0.001$, $P < 0.0001$) statistical significant difference between *collum* and *fundus vesicae felleae*

C4 ($P < 0.0001$) statistical significant difference between *corpus* and *fundus vesicae felleae*

D 1,4 ($P < 0.05$, $P < 0.0001$) statistical significant difference between 6 month- and 3 year- old animals

Table 2. Number (per cross section) of solitary lymphatic nodules (SLNs) in the wall of *Vesica fellea*

Parameters	3 year-old pigs Mean \pm SD	6 month-old pigs Mean \pm SD	2 month-old pigs Mean \pm SD
<u>Number of SLNs</u>			
<i>Gallbladder</i> :			
✓ fundus	8.50 \pm 0.51	11.11 \pm 0.83 D4	-
✓ corpus	11.06 \pm 0.80 C4	13.89 \pm 0.83 C4,D4	-
✓ collum	6.11 \pm 0.83 A4, B3	7.00 \pm 0.77 A4,B4,D2	-

A 4 ($P < 0.0001$) statistical significant difference between *collum* and *corpus vesicae felleae*

B 3,4 ($P < 0.001$; $P < 0.0001$) statistical significant difference between *collum* and *fundus vesicae felleae*

C 4 ($P < 0.0001$) statistical significant difference between *corpus* and *fundus vesicae felleae*

D 2,4 ($P < 0.01$; $P < 0.0001$) statistical significant difference between 6 month- and 3-year-old animals

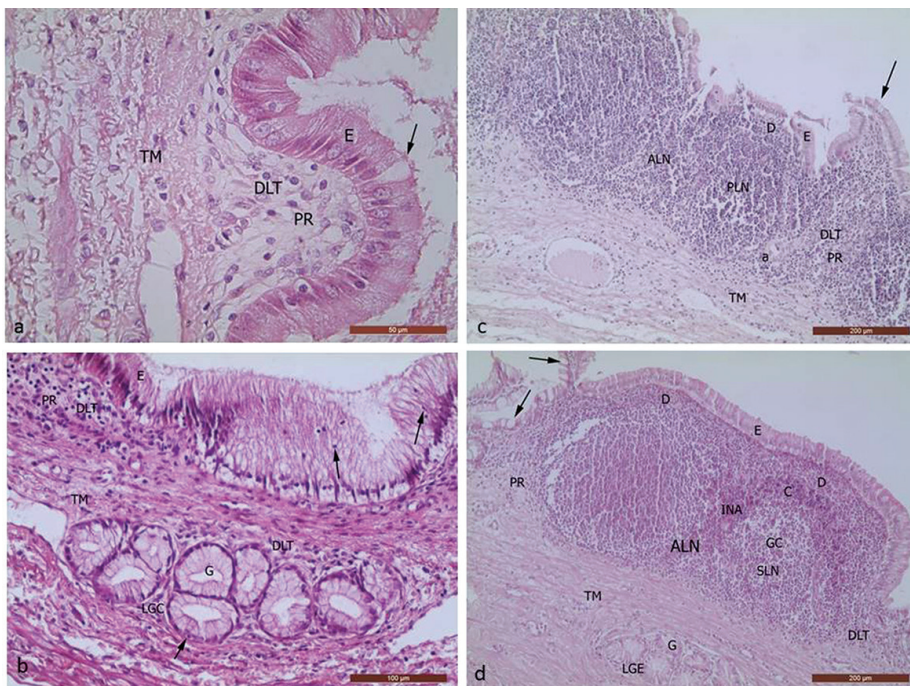


Fig.1. Diffuse lymphatic tissue (DLT), aggregated lymphatic nodules (ALNs), primary (PLNs) and secondary lymphatic nodules (SLNs) as components of gallbladder-associated lymphoid tissue.

a,b – *fundus* and *collum*, respectively of gallbladder in 2-month-old pigs

c – *corpus* of gallbladder in 6-month-old pigs

d – *collum* of gallbladder in 3-year-old-animals

C – *corona* lymphonoduli; GC – germinal center of the nodule, a – arteriola; INA – internodular area; D – dome; LGE – lymphoglandular epithelium; E – *lamina epithelialis mucosae*; PR – *lamina propria mucosae*; TM – *tunica muscularis*; G – *glandulae vesicae felleae*; arrows (a,c,d) – goblet cells (b) – intraepithelial lymphocytes.

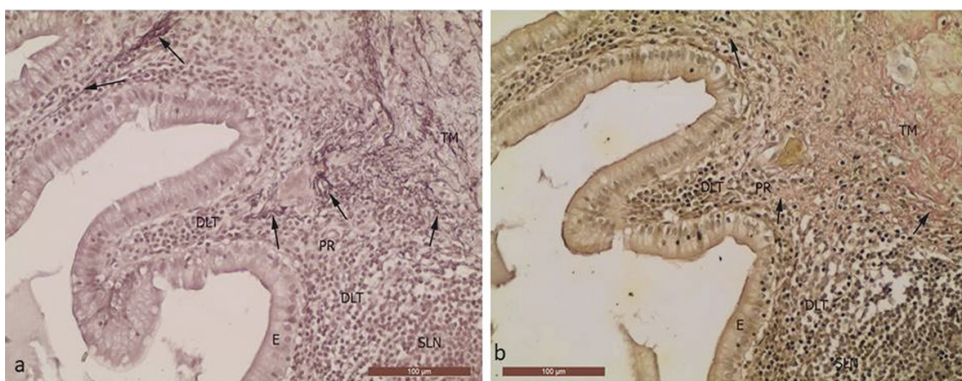


Fig. 2. Elastic (a, arrows) and collagen fibers (b, arrows) within the lymphatic tissue of gallbladder in 6 month-old pigs.

DLT – diffuse lymphatic tissue, SLN – solitary lymphatic nodule,

E – *laminae pithelialis mucosae*; PR – *lamina propria mucosae*; TM – *tunica nuscularis*;

Hypertension-Induced Renal Damage in Rat Model – an Electron Microscopic Study

Stancho Stanchev, Alexandar Iliev, Georgi Kotov, Nikola Stamenov, Mark Stefanov, Boycho Landzhov*

Department of Anatomy, Histology and Embryology, Medical University of Sofia, Bulgaria

* Corresponding author e-mail: dralexiliev@abv.bg

Hypertensive nephrosclerosis is associated with ubiquitously pronounced structural changes in both renal parenchyma and interstitium. Although hypertension-induced renal damage has been well studied, changes appear to be non-specific and can be observed as a result of aging or other underlying pathological condition. The aim of the present study was to investigate the ultrastructural alterations during the initial and chronic phase of hypertension-induced kidney damage. For the present study, we used 6- and 12-month-old spontaneously hypertensive rats and age-matched Wistar rats as controls. A transmission electron microscopic study of the renal cortex was conducted according to a standard protocol. Hypertension-induced kidney damage was associated with prominent changes in the structure of the glomerular filtration barrier, severe podocyte injury, as well as pronounced tubular atrophy. The present work is a detailed ultrastructural study of the renal cortex in a model of hypertension-induced renal damage.

Key words: Kidney, ultrastructure, hypertension, rat

Introduction

Essential hypertension is recognized as a primary risk factor second only to diabetes for the development of chronic renal failure [9]. Hypertension-induced renal damage is associated with a progressive decrease in the functional capacity of the kidney due to numerous morphological alterations in the nephrons and renal interstitium. These changes include severe glomerulosclerosis, hyalinization and sclerosis of interlobular and afferent arterioles, tubular atrophy and an altered balance between collagen synthesis and degradation resulting in the development of renal interstitial fibrosis [2,16]. From an ultrastructural perspective, glomerular damage is characterized by thickening and wrinkling of the glomerular basement membrane (GBM), cytoplasmic vacuolization of the endothelial cells, as well as pronounced alterations in the visceral epithelial cells of Bowman's capsule – the podocytes – shortening and diffuse fusion

of foot processes and loss of podocytes resulting in denudation of the GBM [4, 17, 24]. In addition, podocyte injury has been implicated in the development of hypertensive nephrosclerosis [25]. The deposition of filtered proteins in the proximal tubular segments due to the altered selective permeability of the glomerular filtration barrier (GFB) has potential pro-inflammatory and cytotoxic effects, which contribute to the progression of the tubulointerstitial changes [1]. Tubular atrophy is accompanied by thickening of the tubular basement membranes, increased extracellular space between tubular epithelial cells, as well as substantial injury of the specialized cell membrane structures [7, 12]. However, it appears that renal damage secondary to hypertension is a nonspecific process, as all changes described above can be observed as a result of aging, as well as in the course of different pathological conditions [20, 23]. The lack of certain criteria for demarcation of the etiology of renal structural alterations suggests possible inaccuracy in the evaluation of the histological findings.

The spontaneously hypertensive rat (SHR) is a widely used experimental model of essential hypertension. In this strain, the prolonged and untreated elevated blood pressure provokes ubiquitously pronounced renal morphological changes, which correlate with the observed alterations in case of hypertensive nephrosclerosis in the human population [12].

The aim of the present study was to observe and describe the ultrastructural changes in the GFB and the tubular epithelial cells in the renal cortex in SHR during the initial and chronic phase of hypertensive kidney damage. We analyzed and compared the obtained results with those in age-matched controls.

Materials and Methods

Experimental animals

For the present study, we used two age groups of SHR – 6-month-old (established hypertension) and 12-month old (advanced or late stage hypertension) [12]. We also used two groups of age- and weight-matched control animals – normotensive Wistar rats (WR). Each group consisted of six male rats randomly selected from a large population of SHR and WR in the Laboratory of the Department of Anatomy, Histology and Embryology at the Medical University of Sofia, Bulgaria. The rats were housed in Macrolon cages with free access to food and tap water under controlled environmental conditions (12-h light–dark cycle, room temperature 22 ± 1 °C and humidity $55 \pm 15\%$) in order to diminish the variation. All animal procedures conformed to the guidelines of Directive 2010/63/EU of the European Parliament concerning the protection of animals used for scientific purposes. All experiments were conducted with the approval of the University Committee on Animal Resources (No. 4866). All animals received humane care in compliance with the ‘Principles of laboratory animal care’ formulated by the National Society for Medical Research and the ‘Guide for the care and use of laboratory animals’ prepared by the National Institute of Health (NIH publication No. 86–23, revised 1996). Systolic and diastolic arterial blood pressure was measured through the tail-cuff method on a Model MK-2000ST (Muromachi Kikai Co., Ltd., Tokyo, Japan) and was recorded in all age groups of SHR

and control WR. The mean systolic and diastolic pressure was the average of three separate measurements on each animal (**Table 1**).

Table 1. Mean systolic and mean diastolic blood pressure of 6- and 12-month-old spontaneously hypertensive rats (SHR) and 6- and 12-month-old normotensive Wistar rats (WR). Each group consisted of six animals (n=6) (SD – standard deviation)

Age group	Mean systolic blood pressure (mm Hg) \pm SD	Mean diastolic blood pressure (mm Hg) \pm SD
6-month-old SHR	160 \pm 1.0	100 \pm 2.0
12-month-old SHR	200 \pm 2.0	110 \pm 1.0
6-month-old WR	110 \pm 1.0	80 \pm 2.0
12-month-old WR	120 \pm 2.0	85 \pm 1.0

Tissue preparation

The rats were anesthetized intraperitoneally with Thiopental (Sigma Aldrich Catalogue No. T1022, Sigma Aldrich Chemie GmbH, Taufkirchen, Germany) 40 mg/ kg b.w. The chest cavity was opened and transcardial perfusion was made with 4 % paraformaldehyde (Merck Catalogue No. 1040051000, Merck KGaA, Darmstadt, Germany) in 0.1 M phosphate buffer, pH 7.2 (Merck Catalogue No. 6505-4 L). The abdomen was open through an incision along the midline and the kidneys were rapidly removed and rinsed in oxygenated physiological saline (Merck Catalogue No. 1465690010) for a few minutes. Next, they were fixed in a 10% neutral phosphate buffered formalin solution, prepared under laboratory conditions from 37% formaldehyde solution (Merck Catalogue No. 1040031000) for at least 24 h. Their capsule was removed and the kidneys were sectioned parallel to their long axis. All sections were done in accordance with the standardized methods [14]. Samples were obtained from each kidney, which were then dehydrated in increasing concentrations of alcohol (70%, 80%, 95%, 100%) (Merck Catalogue No. 1009835000), cleared in xylene (Merck Catalogue No. 1082984000) and embedded in paraffin (Merck Catalogue No. 1071511000).

Electron microscopy

After deparaffinization with xylene (Merck Catalogue No. 1082984000), the samples were rehydrated with alcohol (100%, 95%, 80%, 70%) (Merck Catalogue No. 1009835000) and washed in 0.1M phosphate buffer (Merck Catalogue No. 1465920006), pH 7.4, at room temperature. They were briefly treated with 3% glutaraldehyde prepared under laboratory conditions from 25% glutaraldehyde (Merck Catalogue No. 354400) for 30 min. Next, they were post-fixed in 1% osmium tetroxide (Merck Catalogue No. 1245050500) at 4 °C for 2 h. After rinsing in distilled water, the samples were

dehydrated in alcohol (70%, 80%, 95%, 100%) (Merck Catalogue No. 1009835000) and treated for 30 min with propylene oxide (Merck Catalogue No. 8070270100). The samples were then embedded in Durcupan (Fluka Catalogue No. 14040, Fluka Chemie AG, Buchs, Switzerland). Afterwards, all samples were cut with a diamond knife on an ultramicrotome (LKB, Stockholm-Bromma, Sweden) to ultrathin sections (100 nm thick), transferred to copper grids (300 mesh) and contrasted with 2.5% uranyl acetate (Electron Microscopy Sciences Catalogue No. 102092-284, Electron Microscopy Sciences, Hatfield, Pennsylvania, United States), lead nitrate (Merck Catalogue No 1073980100) and sodium citrate (Merck Catalogue No. 1110371000). For the electron microscopic study we used a transmission electron microscope Hitachi model H-500 (Hitachi, Ltd., Tokyo, Japan), with an acceleration voltage of 100 kV. Micrographs were recorded on 3¼" × 4" Kodak electron image plates in accordance with the well-established protocol [5,15]. In order to ensure inter-observer reliability and reproducibility of results, all observations were made by two independent and experienced investigators.

Results

Ultrastructural findings in the GFB

In 6-month-old WR, the three-layered structure of the GFB was well demarcated. The foot processes and the slit diaphragms showed relatively preserved morphology. In a few podocytes, we noted cytoplasmic vacuolization and presence of electron dense inclusions. No significant changes were observed in the structure of the cell nuclei in the visceral layer of Bowman's capsule (**Fig. 1A**). In the older group of normotensive animals, the GFB showed altered morphology. The GBM appeared thickened. A higher number of podocytes were characterized by pronounced cytoplasmic vacuolization, condensation of the chromatin and reduced foot processes. We also observed regions of pathological contacts between the visceral and parietal layers of Bowman's capsule (**Fig. 1B**).

In 6-month-old SHR, the GBM was thicker compared to the age-matched WR. A large population of podocytes showed altered structure – shortening and reduction of foot processes and presence of cytoplasmic electron-dense granules and vacuoles of variable shape. The cell nuclei showed signs of condensation of the chromatin (**Fig. 1C**), which was not seen in 6-month-old normotensive WR. In 12-month-old SHR, the most severe structural alterations were observed in the mid-cortical and juxtamedullary nephrons. We observed prominent thickening of the GBM compared to the age-matched normotensive controls. Podocyte injury was associated with reduction and shortening of the foot processes; the borders of the slit diaphragms were not well demarcated. We also described regions of denudation of the GBM. Some podocytes exhibited features which suggested that they had undergone apoptosis, which was represented morphologically by prominent condensation of the chromatin in the nucleus (**Fig. 1D**).

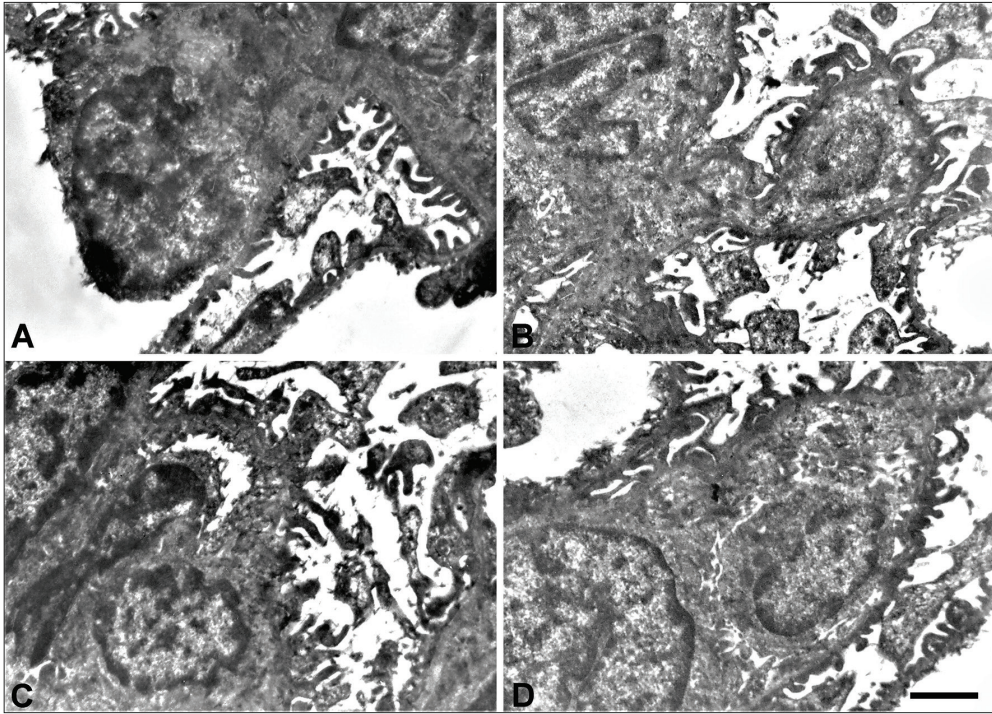


Fig. 1. Electron micrographs of the glomerular filtration barrier (GFB) in 6- and 12-month-old spontaneously hypertensive rats (SHR) and age-matched controls – Wistar rats (WR).

- A. 6-month-old WR. Scale bar – 1.5 μm .
- B. 12-month-old WR. Scale bar – 2.5 μm .
- C. 6-month-old SHR. Scale bar – 1.5 μm .
- D. 12-month-old SHR Scale bar – 2.5 μm .

Ultrastructural findings in the renal tubules

In 6-month-old WR, the basement membranes in the proximal and distal tubular segments were well preserved. We noted the presence of few electron dense granules in the cell cytoplasm. The ultrastructure of the cell nuclei was relatively well preserved, with several nucleoli and a smooth nuclear membrane. Mitochondria presented with well demarcated cristae. We found reduced apical microprojections, as well as presence of narrowed spaces between the interdigitations of the tubular epithelial cells (**Fig. 2A**). In the older group of normotensive animals, the basement membranes of the proximal and distal tubular segments were thickened. Some cells had lost their contact to the underlying basement membrane. The cytoplasm of the tubular cells contained numerous electron dense granules and vacuoles. Initial condensation of the chromatin in the cell nuclei was described, as well as a lower number of mitochondria. There was prominent reduction in the specialized cell membrane structures. The intercellular junctions appeared widened (**Fig. 2B**).

The basement membranes of the proximal and distal tubular segments in 6-month-old SHR were thickened compared to the age-matched WR. A higher incidence of cytoplasmic vacuolization and electron dense accumulations were described. Chromatin in the cell nuclei appeared much more condensed than in 6-month-old WR. Mitochondria with altered morphology were frequently observed. There was increased intercellular space as well as reduction in the number of microvilli compared to the age-matched normotensive group (**Fig. 2C**). In 12-month-old SHR, the proximal and distal tubules were characterized by more severe process of tubular atrophy compared to 12-month-old WR – significant number of electron dense cytoplasmic granules and vacuoles, condensation of the chromatin, indistinguishable morphology and lower number of the mitochondria in the basal infoldings, as well as reduction of the apical microprojections. In addition, the spaces between the interdigitations of the tubular epithelial cells were widest in 12-month-old SHR (**Fig. 2D**).

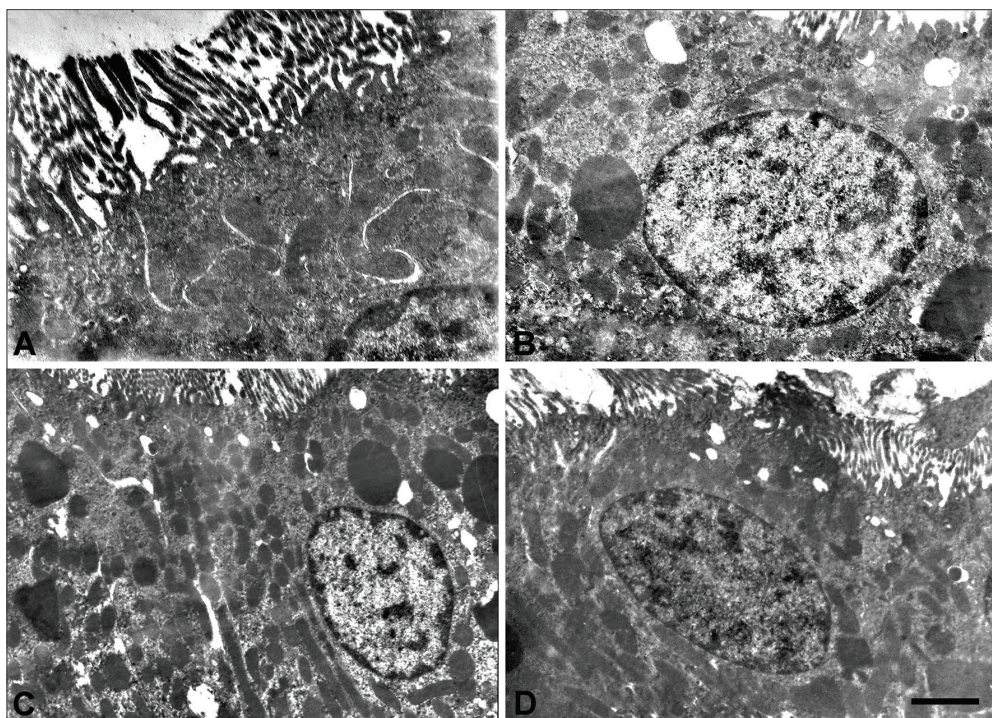


Fig. 2. Electron micrographs of the tubular epithelial cells in 6 and 12-month-old spontaneously hypertensive rats (SHR) and age-matched controls – Wistar rats (WR).

- A. 6-month-old WR. Scale bar – 1.0 μm .
- B. 12-month-old WR. Scale bar – 3.0 μm .
- C. 6-month-old SHR. Scale bar – 3.0 μm .
- D. 12-month-old SHR. Scale bar – 3.0 μm .

Discussion

The present study focuses on the electron microscopic changes in the structural elements of nephrons occurring throughout the process of aging and as a result of the impact of essential hypertension. Our observations revealed that ultrastructural alterations were more severe in the inner rather than the outer cortex in SHR, while no significant differences were found in the renal cortex in WR.

Earlier, Garcia-Pinto et al., 2011 reported that podocyte foot processes and slit diaphragms were better preserved in WR compared to SHR, which is in accordance with the results from the present study. Based on scientific data, the glomerular capillary pressure in the SHR kidney is higher in the inner rather than the outer cortex even in the initial phase of essential hypertension and tends to increase with age [10]. The described hemodynamic difference may explain the more severe structural changes in the inner cortex in SHR, as well as their earlier onset. It is well known that the structural organization of the GFB includes the fenestrated endothelium, the GBM and the podocytes [21]. However, there appear to be morphological differences in the GFB between SHR and WR [6]. These authors reported a smaller diameter in the glomerular endothelial fenestrae in SHR, which were observed during the prehypertensive period. Haensly et al. [10] described an increased incidence of metaplasia of the epithelium lining the parietal layer of Bowman's capsule in SHR compared to WR. The presence of epithelial cells similar to those in the proximal tubule may be explained by the elevated blood pressure or may be a trigger mechanism for the development of hypertension. On the other hand, metaplasia may be considered an age-related alteration, as it was also observed in WR [22].

In the present study, we did not find any morphological changes in the epithelium of the parietal layer of Bowman's capsule in the studied normotensive and hypertensive groups. The main morphological changes in the podocytes in the initial phase of hypertension in SHR include shortened and widened foot processes, as well as accumulation of protein droplets in the cell body and major foot processes. As hypertension advances, some foot processes are effaced [18]. It seems that the trans-membrane protein podocalyxin contributes to the maintenance of the structural integrity of podocytes. The role of this protein has been discussed in the development of renal injury in SHR as it showed decreased expression compared to the normotensive groups [18]. The described fusion of podocyte foot processes containing membrane-limited electron dense inclusions, as well as the pronounced thickening of the GBM in the group of SHR with chronic hypertension are in accordance with the results of Christiansen et al. which also noted the presence of pseudocysts and condensation of the cytoplasm adjacent to the basement membrane [4]. In addition, we also described areas of denudation of the GBM. In case of progressive nephropathy, Fiori et al. described segmental effacement of the podocyte foot processes, which contained vacuoles and dense granules, as well as podocytes characterized by hypertrophy and karyokinesis. The authors also described the presence of subendothelial hyaline inclusions, as well as filamentous structures in the region of the glomerular capillary tufts [11].

The aspects of renal ultrastructural changes in cases of benign and malignant arterial hypertension in the human population have been discussed [19]. The glomerular structural alterations caused by benign hypertension include expansion of the mesangial matrix, as well as mesangial hyperplasia and the presence of lipofuscin inclusions and microvesicles in the cell cytoplasm [19]. Changes initiated by malignant hypertension included narrowed lumens and dense oxyphil basal membranes of the glomerular capillaries due to the accumulation of plasma proteins and fibrin [19]. According to our results, the ultrastructural changes observed in the chronic stage of hypertension in 12-month-old SHR were similar to those described in the setting of malignant hypertension. The described thickening of the GBM was most prominent in the juxtamedullary nephrons in the group of 12-month-old SHR.

In the present study, tubular atrophy in the proximal and distal tubular segments of nephrons was most severe in 12-month-old SHR. It has been reported that cells of the proximal tubules in SHR suffer higher oxidative stress compared to those in WR [28]. Moreover, it has been suggested that proximal tubular segments are more vulnerable and regarded as primary target of injury in the progression of kidney disease [3]. The thickening of the tubular basement membranes and increased space in the region of the interdigitations and basement membranes described by Garcia-Pinto et al. were confirmed by the present study [7]. In addition, we also described pronounced reduction in the specialized cell membrane structures of the tubular epithelial cells as hypertension-induced kidney injury progressed compared to the normotensive controls. One recent study has turned the focus on the ultrastructural changes in the mitochondria and endoplasmic reticulum of the tubular epithelial cells [13]. In addition, evidence in the literature suggests that the functional deficiency of these membrane-limited organelles may play a potential role in the development of arterial hypertension [8,27]. He et al. also described shortening of the mitochondria and widening of the endoplasmic reticulum as signs of injury under hypertensive conditions [26]. Our results supported these findings. Indeed, we noted that the ultrastructural morphology of the mitochondria in the basal infoldings of tubular epithelial cells was altered and hardly distinguishable in 12-month old SHR compared to age-matched WR.

Limitations of the present study existed and should be noted. First, with regard to the renal parenchyma, we only studied the ultrastructure of the renal cortex, but the presence of significant changes in the renal medulla under hypertensive conditions cannot be ruled out. Second, we only used male SHR and WR, in order to eliminate the impact of cyclical hormonal changes in the female organism. Nevertheless, the presence of sex-related differences in the ultrastructure of the kidney under hypertensive conditions as a result of estrogens synthesis in the female organism merits further studies. Last but not least, we did not conduct a quantitative analysis of specific indices of the ultrastructural changes in the GBM and tubular basement membranes, which could potentially provide further evidence of the significance of these findings.

Conclusion

The present work is a detailed study on the specific ultrastructural changes in the GFB and tubular epithelial cells in a rat model of hypertension-induced kidney injury. The obtained results indicate severe glomerulosclerosis represented with thickening of the

GBM and substantial podocyte injury, as well as more prominent tubular atrophy in the proximal and distal tubular segments in the renal cortex under hypertensive conditions as opposed to age-matched normotensive controls.

Acknowledgements: This work is supported by the Bulgarian Ministry of Education and Science under the National Program for Research ‘Young Scientists and Postdoctoral Students’.

References

1. **Abbate, M., C. Zoja, G. Remuzzi.** How does proteinuria cause progressive renal damage? – *J. Am. Soc. Nephrol.*, **17**, 2006, 2974-2984.
2. **Boor, P., T. Ostendorf, J. Floege.** Renal fibrosis: novel insights into mechanisms and therapeutic targets. – *Nat. Rev. Nephrol.*, **6**, 2010, 643-656.
3. **Chevalier, R. L.** The proximal tubule is the primary target of injury and progression of kidney disease: role of the glomerulotubular junction. – *Am. J. Physiol. Renal Physiol.*, **311**, 2016, 145-161.
4. **Christiansen, R. E., O. Tenstad, S. Leh, B. M. Iversen.** Glomerular charge selectivity is impaired in hypertensive nephropathy. – *Nephrol. Dial. Transplant.*, **19**, 2004, 1083-1091.
5. **Evan, A. P., F. C. Luft, V. Gattone, B. A. Connors, D. A. McCarron, L. R. Willis.** The glomerular filtration barrier in the spontaneously hypertensive rat. – *Hypertension*, **3**, 1981, 54-61.
6. **Fiori, M. C., G. P. Ossani, N. R. Lago, C. Amorena, A. J. Monserrat.** Chronic progressive nephropathy: functional, morphological, and morphometrical studies. – *Ren. Fail.*, **32**, 2010, 112-118.
7. **Garcia-Pinto, A. B., V. S. de Matos, V. Rocha, J. Moraes-Teixeira, J. J. Carvalho.** Low-Intensity physical activity beneficially alters the ultrastructural renal morphology of spontaneously hypertensive rats. – *Clinics (Sao Paul)*, **66**, 2011, 855-863.
8. **Glauert, A. M.** Fixation, dehydration and embedding of biological specimens. (Ed. A. M. Glauert), Amsterdam, Elsevier Science, 1984.
9. **Griffin, K.A.** Hypertensive kidney injury and the progression of chronic kidney disease. – *Hypertension*, **70**, 2017, 687-694.
10. **Haensly, W. E., H. J. Granger, A. C. Morris, C. Cioffe.** Proximal-tubule-like epithelium in Bowman's capsule in spontaneously hypertensive rats. Changes with age. – *Am. J. Pathol.*, **107**, 1982, 92-97.
11. **He, X., Y. Liu, K. Usa, Z. Tian, A. W. Cowley Jr., M. Liang.** Ultrastructure of mitochondria and the endoplasmic reticulum in renal tubules of Dahl salt-sensitive rats. – *Am. J. Physiol. Renal Physiol.*, **15**, 2014, 1190-1197.
12. **Hultström, M.** Development of structural kidney damage in spontaneously hypertensive rats. – *J. Hypertens.*, **30**, 2012, 1087-1091.
13. **Inagi, R.** The implication of organelle cross talk in AKI. – *Nephron*, **144**, 2020, 634-637.
14. **Iversen, B. M., K. Amann, F. I. Kvam, X. Wang, J. Ofstad.** Increased glomerular capillary pressure and size mediate glomerulosclerosis in SHR juxtamedullary cortex. – *Am. J. Physiol.*, **274**, 1998, 365-373.
15. **Jarad, G., J. H. Miner.** Update on the glomerular filtration barrier. – *Curr. Opin. Nephrol. Hypertens.*, **18**, 2009, 226-232.
16. **Kato, T., N. Mizuguchi, A. Ito.** Characteristics of podocyte injury in malignant hypertensive nephropathy of rats (MSHRSP/Kpo strain). – *Biomed. Res.*, **36**, 2015, 313-321.
17. **Kretzler, M., I. Koeppen-Hagemann, W. Kriz.** Podocyte damage is a critical step in the development of glomerulosclerosis in the uninephrectomised-desoxycorticosterone hypertensive rat. – *Virchows Arch.*, **425**, 1994, 181-193.

18. **Lee, H., Y. Abe, I. Lee, S. Shrivastav, A. P. Crusan, M. Hüttemann, U. Hopfer, R. A. Felder, L. D. Asico, I. Armando, P. A. Jose, J. B. Kopp.** Increased mitochondrial activity in renal proximal tubule cells from young spontaneously hypertensive rats. – *Kidney Int.*, **85**, 2014, 561-569.
19. **Liang, M.** Hypertension as a mitochondrial and metabolic disease. – *Kidney Int.*, **80**, 2011, 15-16.
20. **Lim, A. K. H.** Diabetic nephropathy – complications and treatment. – *Int. J. Nephrol. Renovasc. Dis.*, **15**, 2014, 361-381.
21. **Lu, W., S. Liu, Z. Zhao, Y. Liu, T. Li.** The effect of connective tissue growth factor on renal fibrosis and podocyte injury in hypertensive rats. – *Ren. Fail.*, **36**, 2014, 1420-1427.
22. **McLaren, K. M., M. K. MacDonald.** Histological and ultrastructural studies of the human juxtaglomerular apparatus in benign and malignant hypertension. – *J. Pathol.*, **139**, 1983, 41-55.
23. **Rule, A. D., H. Amer, L. D. Cornell, S. J. Taler, F. G. Cosio, W. K. Kremers, S. C. Textor, M. D. Stegall.** The association between age and nephrosclerosis on renal biopsy among healthy adults. – *Ann. Intern. Med.*, **152**, 2010, 561-567.
24. **Schwartz, M. M.** The role of podocyte injury in the pathogenesis of focal segmental glomerulosclerosis. – *Ren. Fail.*, **22**, 2000, 663-684.
25. **Sun, D., J. J. Wang, W. Wang, J. Wang, L. N. Wang, L. Yao, Y. H. Sun, Z. L. Li.** Human podocyte injury in the early course of hypertensive renal injury. – *World J. Clin. Cases*, **26**, 2019, 3698-3710.
26. **Treuting, P. M., S. M. Dintzis, K. S. Montine.** Comparative anatomy and histology: a mouse, rat, and human atlas. (Eds. P. M. Treuting, S. M. Dintzis, K. S. Montine) Massachusetts, Academic Press, 2017.
27. **Walker, P. D., T. Cavallo, S. M. Bonsib.** Ad Hoc Committee on Renal Biopsy Guidelines of the Renal Pathology Society. Practice guidelines for the renal biopsy. – *Mod. Pathol.*, **17**, 2004, 1555-1563.
28. **Young, C. N., X. Cao, M. R. Guraju, J. P. Pierce, D. A. Morgan, G. Wang, C. Iadecola, A. L. Mark, R. L. Davisson.** ER stress in the brain subfornical organ mediates angiotensin-dependent hypertension. – *J. Clin. Invest.*, **122**, 2012, 3960-3964.

Cobalt-induced Changes in Iron Homeostasis in Skeletal Muscles of Immature Mice After Perinatal Exposure to Cobalt Chloride

Yordanka Gluhcheva^{1}, Emilia Petrova¹, Ekaterina Pavlova¹, Alexey A. Tinkov², Olga P. Ajsuvakova^{2,3}, Pavel Rashev⁴, Mary Gantcheva^{1,5}, Ivelin Vladov¹, Anatoly V. Skalny^{2,3}*

¹ *Institute of Experimental Morphology, Pathology and Anthropology with Museum, Bulgarian Academy of Sciences, Sofia, Bulgaria*

² *PM Demidov Yaroslavl State University, Yaroslavl, Russia*

³ *IM Sechenov First Moscow State Medical University, Moscow, Russia*

⁴ *Institute of Biology and Immunology of Reproduction "Acad. Kiril Bratanov", Bulgarian Academy of Sciences, Sofia, Bulgaria*

⁵ *Acibadem City Clinic, Sofia, Bulgaria*

* Corresponding author e-mail: ygluhcheva@hotmail.com

Perinatal exposure to CoCl₂ induced significant time-dependent 11.3-fold and 88.9-fold increase in accumulation of the metal in the muscles of the treated immature day 18 and day 25 animals, respectively. The muscle samples of day 25 metal-exposed mice accumulated 4.44-fold higher cobalt (Co) levels compared to the day 18 experimental animals. Iron (Fe) content was also increased but the difference was significant only for day 25 mice probably due to the reduced TfR1 expression found in day 18 Co-exposed mice and increased in day 25 treated animals. Surprisingly, hepcidin showed the same expression pattern – decrease in day 18 and an increase in day 25 Co-exposed mice. Alterations in Fe homeostasis may be of significant importance for myogenesis, physical performance, skeletal muscle regeneration and in ageing may contribute to skeletal muscle atrophy.

Key words: cobalt chloride, iron, iron-regulatory proteins, skeletal muscle

Introduction

Cobalt (Co) is an essential trace element, environmental pollutant and a hypoxia-mimicking agent. Food is the main source of exposure to Co for infants, children and adults. The only known biological function of organic Co is its role as metal component of vitamin B₁₂, cyanocobalamin, whereas inorganic cobalt compounds have been described as toxic for the environment and humans following excessive exposure [14].

The effect of cobalt chloride (CoCl_2) as a hypoxia-mimicking agent on muscle fiber development and regeneration are controversial. Recent studies show that *in vitro* CoCl_2 suppresses myoblast differentiation in a dose-dependent manner [20]. Hypoxia-induced muscle wasting is a phenomenon frequently reported in several environmental and pathological conditions, such as exposure to high altitudes, prolonged immobilization, chronic obstructive pulmonary disease, exercise, and anemia [2]. On the contrary, hypoxic preconditioning with CoCl_2 enhances physical performance and protects muscle from exercise-induced oxidative damage via GSH, HO-1 and MT-mediated antioxidative capacity [19]. The same authors also demonstrate an increase in mitochondrial biogenesis, glucose uptake and metabolism by aerobic respiration in skeletal muscle, which leads to increased physical performance in CoCl_2 -preconditioned rats [20]. There are concerns about Co being misused as blood doping agent by athletes to enhance aerobic performance [15] and some energy drinks may contain high amounts of vitamin B_{12} [7]. Exercise and physical activity on the other hand reduce endogenous iron (Fe) content in the skeletal muscles. Iron homeostasis in the skeletal muscles has not been extensively characterized. The tissue contains from 10 to 15% of body iron, mainly in the form of heme-iron bound myoglobin. Fe released during muscle fiber damage must be promptly removed to limit its oxidative effect, however, iron must become available during skeletal muscle repair to allow the synthesis of myoglobin [3]. Fe is shown to accumulate in the skeletal muscles with senescence and disuse atrophy [8, 10].

There are scarcity data [11] on the *in vivo* effects of Co exposure on skeletal muscle Fe content as well as on the related risk health effects. Alterations in Fe homeostasis and specifically Fe deficiency contribute to skeletal muscle dysfunction and exercise intolerance [11]. Combined conditions of hypoxia and iron deficiency are the most detrimental for skeletal myocytes in the context of morphology alterations and expression of atrophy markers [11].

The aim of the study was to assess cobalt accumulation and iron redistribution and Fe-regulatory proteins transferrin receptor 1 (TfR1) and hepcidin expression in skeletal muscles after perinatal exposure to cobalt chloride.

Material and Methods

Animal Model

Experimental animals were purchased from the Experimental and breeding base for laboratory animals (EBBLA) – Slivnitsa, Bulgaria and left to acclimatize for a week prior treatment. Pregnant ICR (Institute of Cancer Research) mice were subjected to a daily dose of 75 mg cobalt chloride/kg body weight ($\text{CoCl}_2 \cdot 6\text{H}_2\text{O}$) for 2-3 days before delivery and treatment continued until day 25 after delivery. The compound was dissolved and administrated with drinking tap water. Animals were fed a standard diet and had access to food ad libitum with strong control of the feeding regime. Our previous experience showed no significant gender differences neither in body weight nor in haematological parameters and the experimental groups consisted of both male and female mice. The mice were maintained in the Institute's animal breeding facility at

23 ± 2°C and 12:12 h light/dark cycle in individual standard hard-bottom polypropylene cages. The suckling mice were sacrificed by decapitation after etherization on postnatal days 18 (n=4) and 25 (n=6). Femur muscles were excised, weighed and stored at -20°C prior to ICP-DRC-MS analysis. Age-matched mice obtaining regular tap water were used as a control group (n=5 for day 18 and n=4 for day 25 mice). The experiment was carried out in accordance with guidelines EU Directive 2010/63/EU for animal experiments. All applicable international, national, and/or institutional guidelines for the care and use of animals were followed.

ICP-DRC-MS Analyses of Cobalt and Iron Content in Muscles

Prior to analysis 50-100 mg of the studied tissue samples were subjected to digestion in concentrated HNO₃ (Sigma-Aldrich, Co., USA) in the Berghof SW-4 DAP-40 microwave system (Berghof Products + Instruments GmbH, Eningen, Germany). The digested samples were transferred into 15 mL polypropylene test tubes and adjusted to the final volume of 15 mL with deionized water (18 MΩ cm, Milli-Q, Millipore, Bedford, MA, USA) and thoroughly mixed up by shaking in the closed test tubes.

Analysis of Co and Fe levels in the samples was performed using inductively-coupled plasma mass spectrometry with dynamic reaction cell technology (ICP-DRC-MS) at NexION 300D spectrometer (Perkin Elmer, USA) equipped with ESI SC-2 DX4 autosampler (Elemental Scientific Inc., Omaha, NE, USA). Co and Fe content in the studied samples was expressed as µg/g wet weight.

Calibration of the system was performed using standard solutions with different concentrations of Co and Fe prepared from Universal Data Acquisition Standards Kits (PerkinElmer Inc., Shelton, CT 06484, USA). Internal online standardization was performed using 10 µg/L Yttrium (Y) and Rhodium (Rh) Pure Single-Element Standard (PerkinElmer Inc., Shelton, CT, USA) prepared on a matrix containing 8% 1-butanol (Merck KGaA, Gernsheim, Germany), 0.8% Triton X-100 (Sigma-Aldrich Co., St. Louis, MO, USA), 0.02% tetramethylammonium hydroxide (Alfa Aesar, Ward Hill, MA, USA) and 0.02% ethylenediaminetetraacetic acid (Sigma-Aldrich Co., St. Louis, MO, USA). Laboratory quality control was performed via permanent analysis of the certified reference material (GBW09101, Shanghai Institute of Nuclear Research, Shanghai, China). The recovery rate for Co and Fe elements was within the interval of 92-104% and 95-107%, respectively.

Enzyme-linked Immunosorbent Assay (ELISA) for Transferrin Receptor 1 (TfR1) and Hepcidin

Muscle tissue homogenates were analysed using mouse TFR1 ELISA kit and Hepcidin ELISA kit (Wuhan Elabscience Biotechnology Co., Ltd, China) according to the manufacturer's instructions. The optical density was read at 450 nm on ELISA Reader GDV (GIO. DE VITA EC., Italy). The final concentrations were determined using Curve Expert 1.4 software and are expressed in ng/g for TfR1 and in pg/g for hepcidin.

Statistical Analysis

The obtained data were processed using Statistica 10.0 (Statsoft, Tulsa, OK, USA). The results from the hematological and biochemical analyses are presented as mean value ±

SD. Data on Co and Fe content in the studied samples are expressed as median and the respective 25 and 75 percentile boundaries (interquartile range). Statistical significance between the experimental groups was assessed using Mann-Whitney U-test at the level of significance of $p < 0.05$.

Results

Prenatal and early postnatal exposure to CoCl_2 resulted in a significant metal ion accumulation in the muscles of the experimental suckling mice (**Table 1**). Day 18 Co-exposed mice accumulated 11.3-fold higher levels of Co compared to the untreated age-matched control group. The increase in 25-day-old Co-exposed animals was found to be 88.9-fold in comparison to the control values. The muscle samples of day 25 metal-exposed mice accumulated 4.44-fold higher Co content compared to the day 18 experimental animals suggesting a significant time-dependent effect. At the same time, no significant difference in muscle Co content was observed in control animals of different age.

Table 1. Co Content ($\mu\text{g/g}$) in Muscles of Day 18 and 25 Control and Co-exposed Mice

Sample	d18	d25
control	0.016 (0.010-0.049)	0.009 (0.005-0.025)
Co-treated	0.18 (0.16-0.20) *	0.80 (0.25-0.93) *

Data are presented as mean \pm SD. Asterisk (*) signifies significant difference at $p < 0.05$ between age-matched control and CoCl_2 -exposed mice.

Simultaneous analysis of Fe content in the muscle tissue also showed an increase upon Co exposure (**Table 2**). Although being insignificant, in day 18 metal-treated mice Fe was elevated by 15.8% compared to the untreated control animals. Significant increase by 39.1% was observed in day 25 CoCl_2 -treated immature mice. The muscle tissue of day 25 metal-exposed mice contained significantly higher Fe levels by 55.2% compared to day 18 Co-treated mice which suggests Co-induced Fe accumulation in the target organ.

Table 2. Fe Content ($\mu\text{g/g}$) in Muscles of Day 18 and 25 Control and Co-exposed Mice

SampleW	d18	d25
control	12.12 (10.72-12.89)	15.65 (12.97-17.76)
Co-treated	14.03 (12.79-16.68)	21.77 (21.09-44.85) *

Data are presented as mean \pm SD. Asterisk (*) signifies significant difference at $p < 0.05$ between age-matched

Immunological analysis of the expression of the Fe-regulatory proteins TfR1 and hepcidin showed similar pattern. Both proteins expression was decreased in day 18

mice following CoCl_2 exposure and increased in day 25 metal-treated experimental animals. The elevated TfR1 concentration in muscles of day 25 Co-exposed mice (**Fig. 1**) corresponded to the significant increase in Fe content in this tissue. Surprisingly, hepcidin concentration was insignificantly (2.7%) reduced in day 18 Co-exposed mice while a 3-fold increase was observed in day 25 metal-treated animals (**Table 3**).

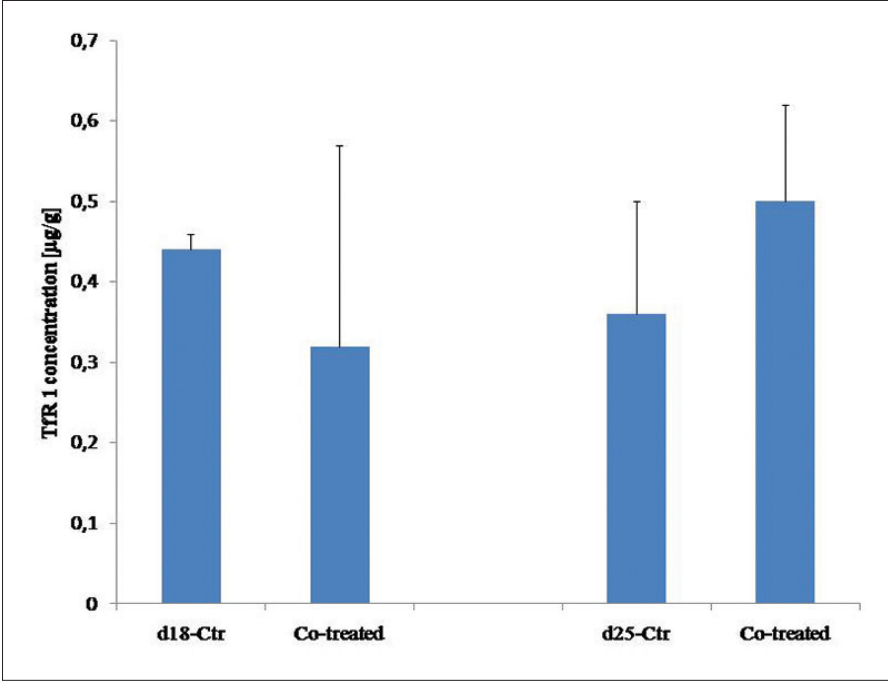


Fig. 1. TfR 1 concentration (ng/g) in skeletal muscle homogenates of day 18 and 25 control and Co-treated mice.

Table 3. Heparidin concentration (pg/g) in Skeletal Muscle Homogenates of day 18 and 25 Control and Co-Treated Mice

Experimental groups	Control	Co-exposed	Change
Day 18	157.45±10.68	153.20±106.07	~ 2.7% ↓
Day 25	62.35±48.01	183.25±4.31	~ 3-fold ↑

Data are presented as mean ± SD.

Discussion

Prenatal and early postnatal exposure to CoCl_2 resulted in a significant time-dependent metal ion accumulation in the muscles of the experimental immature mice. Our results are in agreement with data reviewed by Simonsen et al. [21] showing that Co content in skeletal muscles increases with time. The elevated Co content altered endogenous muscle Fe concentration and induced changes in Fe-regulatory protein expression. Although Fe homeostasis is tightly controlled, its alterations in the skeletal muscles leading to Fe overload are not fully elucidated. Literature data show that Fe content in skeletal muscles of healthy individuals is comparable to that of the liver. High tissue Fe stores are associated with impaired muscle contractivity and muscle endocrine function, insulin resistance and Fe-dependent oxidative stress [6]. The oxidative stress induced by Fe overload results in delayed muscle regeneration with decreased in size myofibres and reduced expression of myoblast differentiation biomarkers [9]. In a mouse model of Fe overload Reardon and Allen observed reduced skeletal muscle weight and reduced exercise capacity [16]. As suggested by Hofer et al. [9] increase in Fe content possibly contributes to muscle atrophy with ageing or disuse. In our study we also find an age-dependent significant increase in Fe content in skeletal muscles of suckling mice upon perinatal exposure to CoCl_2 . The results suggest that Co administration enhanced Fe accumulation in the target organ. Our results for increased Fe content following CoCl_2 exposure of immature mice correspond to our previously published experimental data for other organs [5]. The elevated intracellular Fe may be a source for free radical generation. It may contribute to the generation of hydroxyl radical via Fenton reaction, oxidative modification of proteins and lipids, lipid peroxidation, etc. [10].

Alterations in Fe homeostasis are mediated by changes in Fe-related proteins. Barrientos et al. demonstrate the critical role for TfR1 for skeletal muscle development as its inactivation alters normal muscle energy metabolism [1]. According to Corna et al. TfR1 protein levels are virtually undetectable in healthy skeletal muscle and substantially increase after injury [3]. In addition, Robach et al. show that when hemoglobin content is increased during enhanced erythropoiesis, myoglobin expression in the skeletal muscles is down regulated due to body Fe mobilization and acquisition by the erythrocytes [17]. The same authors also find significant reduction in Fe-related proteins TfR1 and ferritin. These results are in agreement with our data for the reduced TfR1 in day 18 CoCl_2 -exposed mice. Altered muscle oxygen homeostasis as well as the increased Fe demands for muscle fiber development possibly serve as a feed back mechanism leading to increased TfR1 in day 25 Co-treated mice. As evidenced by Corna et al. [3], TfR1 expression parallels the appearance of novel fibers. This is also supported by Kobak et al. [11] who demonstrated that in hypoxia, increased expression of Atrogin1 and MuRF1 was associated with an increased expression of TfR1, reflecting intracellular iron demand in cultured *in vitro* rat skeletal myocytes. In our study, the observed elevation of TfR1 level in day 25 CoCl_2 -exposed mice may be responsible for significantly increased Fe content in these animals. Robach et al. [18] demonstrate increased Fe accumulation and up regulation of TfR1 and ferroportin despite significantly reduced hepcidin levels in healthy volunteers treated with recombinant erythropoietin (rhEpo) suggesting that muscle Fe homeostasis is mediated by other factors as erythropoietin. At systemic level Fe metabolism is regulated by

hepcidin. It is mainly produced in the liver but is also found in the skeletal muscles [13]. Diet and physical activity regulate both iron accumulation and hepcidin expression. The significant Fe storage in skeletal muscle tissue of day 25 CoCl₂-exposed mice in our experimental model in parallel with the increased hepcidin level suggests that Fe accumulation is possibly regulated by hepcidin-independent mechanism. A markedly increased expression of hepcidin during hypoxia is also demonstrated by Dziegala et al. [4] in cultured skeletal myocytes. Kulik-Rechberger et al. [12] find high hepcidin levels in newborns and hypothesize that it may be due to high ferritin level at that age.

Conclusion

Prenatal and early postnatal exposure to CoCl₂ resulted in a significant metal ion accumulation in the muscles of the experimental immature mice altering endogenous muscle Fe content and inducing changes in Fe-regulatory protein expression. The results suggest that changes in Fe homeostasis may be one of the mediators of CoCl₂ effects on myogenesis, physical performance, skeletal muscle regeneration and in ageing may contribute to skeletal muscle atrophy.

Acknowledgements: The study was supported by Grants No. DNTS/Russia 02/1/14.06.2018 from the Bulgarian National Science Fund and No. 18-54-18006 from the Russian Foundation for Basic Research.

References

1. Barrientos, T., I. Laothamatas, T. R. Koves, E. J. Soderblom, M. Bryan, M. A. Moseley, D. M. Muoio, N. C. Andrews. Metabolic catastrophe in mice lacking transferrin receptor in muscle. – *EBioMedicine*, 2, 2015, 1705-1717.
2. Chen, R., T. Jiang, Y. She, J. Xu, C. Li, S. Zhou, H. Shen, H. Shi, S. Liu. Effects of cobalt chloride, a hypoxia-mimetic agent, on autophagy and atrophy in skeletal C2C12 myotubes. – *BioMed Res. Int.*, 2017, 2017, 7097580 <https://doi.org/10.1155/2017/7097580>
3. Corna, G., I. Caserta, A. Monno, P. Apostoli, A. A. Manfredi, C. Camaschella, P. Rovere-Querini. The repair of skeletal muscle requires iron recycling through macrophage ferroportin. – *J. Immunol.*, 197, 2016, 1914-1925.
4. Dziegala, M., M. Kasztura, K. Kobak, J. Bania, W. Banasiak, P. Ponikowski, E. A. Jankowska. Influence of the availability of iron during hypoxia on the genes associated with apoptotic activity and local iron metabolism in rat H9C2 cardiomyocytes and L6G8C5 skeletal myocytes. – *Mol. Med. Reports*, 14, 2016, 3969-3977.
5. Gluhcheva, Y., E. Pavlova, E. Petrova, A. A. Tinkov, O. P. Ajsuvakova, M. G. Skalnaya, I. Vladov, A. V. Skalny. The impact of perinatal cobalt chloride exposure on extramedullary erythropoiesis, tissue iron levels, and transferrin receptor expression in mice. – *Biol. Trace Elem. Res.*, 194, 2020, 423-431.
6. Halon-Golabek, M., A. Borkowska, A. Herman-Antosiewicz, J. Antosiewicz. Iron metabolism of the skeletal muscle and neurodegeneration. – *Front. Neurosci.*, 13, 165, Mar. 2019, doi: 10.3389/fnins.2019.00165
7. Higgins, J. P., T. D. Tuttle, C. L. Higgins. Energy beverages: content and safety. – *Mayo Clin. Proc.*, 85, 2010, 1033-1041.

8. Hofer, T., E. Marzetti, J. Xu, A.Y. Seo, S. Gulec, M. D. Knutson, C. Leeuwenburgh E. E. Dupont-Versteegden. Increased iron content and RNA oxidative damage in skeletal muscle with aging and disuse atrophy. – *Exp. Gerontol.*, **43**, 2008, 563-570.
9. Ikeda, Y., A. Satoh, Y. Horinouchi, H. Hamano, H. Watanabe, M. Imao, M. Imanishi, Y. Zamami, K. Takechi, Y. Izawa-Ishizawa, L. Miyamoto, T. Hirayama, H. Nagasawa, K. Ishizawa, K.-I. Aihara, K. Tsuchiya, T. Tamaki. Iron accumulation causes impaired myogenesis correlated with MAPK signaling pathway inhibition by oxidative stress. – *FASEB J.*, **33**, 2019, 9551-9564.
10. Jung, S. H., L. R. DeRuisseau, A. N. Kavazis, K. C. DeRuisseau. Plantaris muscle of aged rats demonstrates iron accumulation and altered expression of iron regulation proteins. – *Exp. Physiol.*, **93**, 2007, 407-414.
11. Kobak, K., M. Kasztura, M. Dziegala, J. Bania, V. Kapuśniak, W. Banasiak, P. Ponikowski, E. A. Jankowska. Iron limitation promotes the atrophy of skeletal myocytes, whereas iron supplementation prevents this process in the hypoxic conditions. – *Int. J. Mol. Med.*, **41**, 2018, 2678-2686.
12. Kulik-Rechberger, B., A. Kosciesza, E. Szponar, J. Domsud. Hepcidin and iron status in pregnant women and full-term newborns in first days of life. – *Ginek. Pol.*, **87**, 2016, 288-292.
13. Kwapisz, J., A. Slomka, E. Zekanowska. Hepcidin and its role in iron homeostasis. – *EJIFCC*, **20**, 2009, 124-128.
14. Leyssens, L., B. Vinck, C. Van DerStraeten, F. Wuyts, L. Maes. Cobalt toxicity in humans. A review of the potential sources and systemic health effects. – *Toxicology*, **387**, 2017, 43-56.
15. Lippi, G., M. Franchini, G. C. Guidi. Cobalt chloride administration in athletes: a new perspective in blood doping? – *Br. J. Sports Med.*, **39**, 2005, 872-873.
16. Reardon, T. F., D. G. Allen. Iron injections in mice increase skeletal muscle iron content, induce oxidative stress and reduce exercise performance. – *Exp. Physiol.*, **94**, 2009, 720-730.
17. Robach, P., G. Cairo, C. Gelfi, F. Bernuzzi, H. Pilegaard, A. Viganò, P. Santambrogio, P. Cerretelli, J. A. L. Calbet, S. Moutereau, C. Lundby. Strong iron demand during hypoxia-induced erythropoiesis is associated with down-regulation of iron-related proteins and myoglobin in human skeletal muscle. – *Blood*, **109**, 2007, 4724-4731.
18. Robach, P., S. Recalcati, D. Girelli, C. Gelfi, N. J. Aachmann-Andersen, J. J. Thomsen, A. M. Norgaard, A. Alberghini, N. Camprostrini, A. Castagna, A. Viganò, P. Santambrogio, T. Kempf, K. C. Wollert, S. Moutereau, C. Lundby, G. Cairo. Alterations of systemic and muscle iron metabolism in human subjects treated with low-dose recombinant erythropoietin. – *Blood*, **113**, 2009, 6707-6715.
19. Saxena, S., D. Shukla, S. Saxena, Y. A. Khan, M. Singh, A. Bansal, M. Sairam, S. K. Jain. Hypoxia preconditioning by cobalt chloride enhances endurance performance and protects skeletal muscles from exercise-induced oxidative damage in rats. – *Acta Physiol. (Oxf)*, **200**, 2010, 249-263.
20. Saxena, S., D. Shukla, A. Bansal. Augmentation of aerobic respiration and mitochondrial biogenesis in skeletal muscle by hypoxia preconditioning with cobalt chloride. – *Toxicol. Appl. Pharmacol.*, **264**, 2012, 324-334.
21. Simonsen, L. O., H. Harbak, P. Bennekou. Cobalt metabolism and toxicology – a brief update. – *Sci. Total Environ.*, **432**, 2012, 210-215.
22. Wagatsuma, A., M. Arakawa, H. Matsumoto, R. Matsuda, T. Hoshino, K. Mabuchi. Cobalt chloride, a chemical hypoxia-mimicking agent, suppresses myoblast differentiation by downregulating myogenin expression. – *Mol. Cell. Biochem.*, **470**, 2020, 199-214.

Review Articles

Microscopic Characteristics for Human Hair Identification

Emilia Kaisheva

Department of General and Clinic Pathology, Forensic Medicine and Deontology, Medical University – Varna

* Corresponding author e-mail: emiliakaisheva@gmail.com

Identification of human hairs is required for a variety of reasons and under different circumstances. They are one of the main items of evidence examined in a number of crimes, helping to reveal the perpetrator, the victim and the mechanism of the crime. This often requires identification of hair samples, which is done using a variety of methods. Among these, the macroscopic and microscopic examination of the hair is of particular importance. On this basis, a number of features of the individual from whom the hairs originate are determined, namely their species, race, sex, etc. This article has been prepared to provide a brief presentation of the main morphological characteristics of the hair and their role in its identification. Although, to date there are much more precise methods of examination, we believe that the determination of the morphological characteristics of the hair retains its importance in hair identification.

Keywords: hair, identification, morphology, microscopy

Introduction

Identification of human hairs is required for a variety of reasons and under different circumstances. Everyday, between 80 and 100 hairs fall off each person's scalp and onto various objects in the environment. They are one of the main items of evidence examined in a number of crimes – murder, rape, traffic accident, etc., helping to reveal the perpetrator, the victim and the mechanism of the crime [37]. This often requires identification of hair samples, which is done using a variety of methods. Among these, the macroscopic and microscopic examinations of the morphological characteristics of the hair are of particular importance. On this basis, a number of features of the individual from whom the hairs originate are determined, namely their species, race, sex, etc. [3, 8, 34]. The microscopic characteristics of hair have not been a mainstream topic of research in scientific journals for the last ten years, so they seem somewhat overlooked or disregarded.

This article has been prepared to provide a brief presentation of the main morphological features of the hair and their role in hair identification. For more accurate identification it is important to look not only at individual features in isolation, but also at their contribution to an overall pattern.

Discussion

Examination for microscopic features must always include examination of hair shafts along their length from root end to tip end using a brightfield light microscope. Light microscopy is a valuable, nondestructive analytical technique for forensic professionals that enables visual differentiation of patterns in hair microstructure along the length of a hair. Some examiners will also make cross-sections, to establish more details.

To observe adequately the microscopic characteristics of a hair, the sample must be placed in a medium of refractive index similar to that of the hair itself (the average refractive index of hair is approximately 1.55). A synthetic semi-permanent mounting medium with a refractive index of around 1.52 is recommended. Using a mounting medium with a refractive index much different from that of hair will result in excessive shadows and contrast that will tend to mask the internal characteristics of a hair [34].

Both low- and high-power microscopic examinations are necessary in the comparison of hairs. Microscopic examinations at magnifications around 10x, of both unmounted and mounted hairs, are useful for a more general outlook. Whereas a more in depth observations of mounted hairs is done with a variety of magnifications, generally around 50x, 100x, 250x and 400x. The use of high-power (large numerical aperture) objectives, allows for the examination and comparison of the fine detail present in such characteristics as pigmentation and cuticular scales.

In general, the characteristics observed by light microscopy are related to the features of the hair structure – cuticle, cortex and medulla, cross-section, hair diameter, type of hair root and tip, and various changes acquired over time as a result of cosmetic treatment, disease or traumatic effects, the effects of insects, fungi, bacteria, etc. [1, 2, 3, 13,18,37, 43, 45].

The hair shaft can be most roughly described as three cylinders inserted into each other: the medulla or core running along the central axis; the cortex which is the main component; and the cuticle, which is the outer covering [3, 47].

The **medulla** is formed as a column of cells which, during hair formation, collapse in such a manner that the medulla appears as a network of cellular connections and spaces that are filled with air [20, 34].

Medulla is not present in all human hairs. When it is present its appearance varies slightly among the hairs of a given individual but considerably from individual to individual, the main differing characteristics being: thickness, continuity and opacity.

Medulla “continuity” refers to the variations in its visual shape along the length of the hair shaft [3, 8, 9, 27, 34], which are presented in **Table 1** and **Figures 1-4**.



Fig. 1. Absent

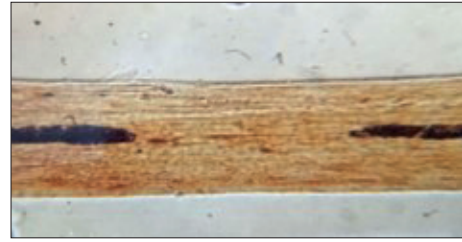


Fig. 2. Fragmentary



Fig. 3. Discontinuous



Fig. 4. Continuous

Table1. Variations of the characteristic „continuity“ of the medulla

Absent	hairs with no visible medulla, including those hairs with no visible medulla due to heavy pigmentation
Continuous	the medulla extends along the axis of the shaft with no interruption
Discontinuous (interrupted)	the lengths of the visible medulla are greater than the lengths of its indiscernible portions
Fragmentary	the lengths of the indiscernible portions of the medulla exceed the lengths of the discernible portions
Different combinations of these variations	the medulla has one type in one section of the shaft and a different type in another

Human head hairs generally have no medulla or have fragmented ones; they very rarely show continuous medullation. Exception is found in the Mongoloid race whose medulla is usually continuous. Thus, the racial affiliation of the individual can be determined by the type of medulla.

Opacity is the second characteristic, and it refers to the appearance of the medulla as viewed with transmitted light under light microscopy. The medulla can be translucent and opaque [27, 34]. The variations are presented in **Table 2**.

The thickness of the medulla also varies in hairs from different individuals. It is usually not large, 1-2 cells in diameter, and does not exceed one-third the width of the hair shaft. In human hairs the medulla is indistinct, narrow and often interrupted. In

contrast, in animal hairs the medulla is usually distinct, wide (more than one-third of the hair shaft), continuous, and much less frequently interrupted [1, 3, 19]. This can be used to identify the species affiliation of the examined hairs, whether they originate from a human or an animal.

Table 2. Variations of the characteristic „opacity“ of the medulla

Absent	hairs with no visible medulla, including those hairs in which the medulla is obscured due to heavy pigmentation
Opaque	when the medulla is filled with air
Translucent	when the medulla is filled with liquid
Opaque/Translucent	when there are both opaque and translucent segments along the medulla shaft

For this purpose, the so-called medullary index, the ratio between the diameter of the medulla and that of the whole hair, is determined. For human hairs, it is less than 0.33.

There is evidence that the medullary index of human hairs varies with age, becoming progressively greater at older ages [21, 23], but does not correlate with a person’s race or sex [40].

This index can also serve to determine the regional origin of the hair, with a well-defined medulla in head hairs, a weak or absent medulla in pubic hairs, and often a double medulla in beard hairs [27, 34].

The **cortex** is the next, outermost layer of the hair fiber. Its microscopic examination determines: cortex cells; texture; pigment – type of pigment, shape and size of granules, arrangement, distribution, density, etc.

Cortical texture refers to the appearance of the cortex as viewed in a longitudinal mount. The cortex may have no apparent texture (absent), it may demonstrate a streaky texture (present), or the ability to observe the cortical texture may be obstructed due to heavy pigmentation (obscured) [27].

The cortex is composed of spindle-shaped cells aligned parallel to the axis of the hair shaft and closely packed together [8, 9, 32, 47]. In some hairs, small structures called cortical fusi [8, 9, 15, 28], air inclusions that appear dark by transmitted light microscopy but have a bright appearance by reflected light [12], are observed between them. They may occur throughout the length of the hair shaft but they are rarely seen at the tip. Most often they are found just above the root [24, 25, 32]. The variates of this feature in different hairs are presented in **Table 3**.

Another feature to consider in relation to the cortex is the presence or absence of ovoid bodies. Ovoid bodies are well-defined aggregations of pigment that can have a spheroidal or oblong shape [8, 9, 27]. Their presence in head hairs is not uncommon, but neither are they ever-present. The variates relate to their quantity in the hair shaft (**Table 3**).

Determination is made by counting the ovoid bodies for each field of view. If the average number counted per field is less than 10, it is categorized as ‚Few‘. If the average number is 10 or more, it is categorized as ‚Many‘ [27].

Table 3. Microscopic Characteristics of Hair Cortex

Cortical Textute	Absent – no apparent texture Present – a streaky texture Obscured – the ability to observe the cortical texture may be obstructed due to heavy pigmentation
Cortical Fusi	Absent – absence of cortical fusi Root Only – presence of cortical fusi in the root only, or in the root and in the proximal end of the hair only Rare – low concentration of cortical fusi along the length of the shaft Common – greater concentration of cortical fusi along the length of the shaft Profuse – high concentration of cortical fusi along the shaft Obscured – inability to observe the presence of cortical fusi due to the presence of heavy pigmentation.
Ovoid Bodies	Absent – absence of ovoid bodies Few – presence of a small number of ovoid bodies in the shaft Many – presence of numerous ovoid bodies in the shaft Obscured – inability to observe the presence of ovoid bodies due to obstruction by heavy pigmentation.
Cortical Pigment	
Pigment Density (the abundance of pigment granules observed under light microscopy)	Absent (no pigment) Light to medium Medium to heavy Heavy to opaque Opaque
Pigment Granule Size	Absent/obscured (or no pigment – white or grey hairs, or impossible to separate into individual pigment granules using light microscopy) Fine Coarse
Pigment Distribution (distribution and concentration of the pigment granules in various areas of the hair shaft)	Absent – no pigment in the hair shaft (e.g. white or grey hair) Uniform – the pigment is evenly distributed across the cortex of the hair shaft Peripheral – the pigment is concentrated in the outer edges of the shaft One-sided – the pigment is concentrated on one side of the shaft Central – the pigment is concentrated (or appears to be concentrated) in the centre of the shaft Random – the pigment is found in greater concentrations in some areas of the shaft and in lesser concentrations in other areas of the shaft, with no recognizable pattern Other – pigment distribution that does not include any of those vitiate categories

Pigment Shape (the appearance of the pigment granules when they are concentrated in a mass that has a recognizable form)	Aggregate	Absent – the absence of pigment (e.g. a white or grey hair), or a pigmented hair that exhibits no aggregation of pigment Streaked – aggregation in the form of streaks Clumped – aggregation in the form of clumps Other – aggregation that cannot be categorized as Streaked or Clumped, or hairs with a mixture of streaked and clumped aggregates
Pigment Size	Aggregate	No aggregates Small streaks Large streaks Small clumps Medium clumps Large clumps Other

In pigmented hairs, cortical cells also contain pigment granules. These are not expected to be found in the medulla or cuticle, but in practice pigment can be found in both. The presence of pigment in the cuticle is commonly observed in individuals with heavily pigmented hairs [27].

There are two types of pigments in the granules, black-brown coloured eumelanin, giving a dark color, and reddish-yellow pheomelanin giving a light color [19, 20, 24], and human hairs, unlike animal hairs, are characterized by homogeneous pigmentation along their entire length [30].

Hair color is not only determined by the color, density, and distribution of pigment granules in the cortex, but also by the amount of melanin polymer in each granule. In dark hairs, the granules are of eumelanin, brown or black in colour, elliptical or oval in shape, 0.8-1.0 μm in length and 0.3-0.4 in diameter [18, 28, 38, 39, 41, 44]. In light hairs, the granules are of pheomelanin, yellow or red in colour, smaller and more spherical, 0.2 μm [40]. They are not observable with light microscopy because of their small size [27, 38].

Pigment characteristics important for hair identification are presented in **Table 3**.

The identification significance of these pigment features is determined by the possibility of determining the racial affiliation of the individual from whom the examined originate. In the European hair the pigment granules are moderately dense with fairly even distribution, while in the African there are densely distributed pigment granules arranged in prominent clumps. In the Asian, the medulla is often broad and continuous, and the pigment granules are densely distributed and often arranged in large patchy clumps or streaks [30].

It is usual in human hairs for the pigment granules to be located at the periphery of the cortex towards the cuticle, except in red hair where they are more centrally located [8, 9, 18].

The **cuticle** is the outermost layer of the hair shaft [14, 17, 18, 25]. It is composed of flattened, imbricated, scale cells that overlap like tiles on a roof [31], sloping outwards, with a free edge pointing towards the tip of the hair shaft [3, 8, 9, 33, 34, 47].

When examining the cuticle, attention is paid to its colour, thickness, inner margin, outer margin, features of the cells – shape, size, contour, convexity /unevenness/, presence of adhesions (**Table 4**).

The thickness of the cuticle may serve as a defining feature in identifying the racial origin of the individual, the source of the hairs, as it establishes a difference between representatives of the major races. It is thickest in hairs of the Mongoloid race – 2.1-4.59 μm , thinner in the Caucasoid race – 1.81-3.59 μm and thinnest in the Negroid race – 1.14-3.43 μm [18, 27].

The scale counts are relatively constant for the hair cuticle of a given individual, but can vary between individuals [3, 11]. The scale count may also vary (although less markedly) on an individual depending on site. The count is significantly smaller (i.e. the scales further apart) for scalp hair than for hairs from other areas such as pubis, face, and chest. Smaller scale numbers are seen in younger people and for facial, axillary, and abdominal hairs of females as compared with the same areas in males [46].

Table 4. Microscopic Characteristics of Hair Cuticle

Cuticle thickness	Thin (cuticle thickness of less than 2,5 μm) Thick (cuticle thickness of 2,5 μm or greater); varies (cuticle thickness varies along the shaft at or near the widest diameter) Non apparent (cuticle not easily measured due to indistinct inner cuticle margin)
Inner cuticle margin (the border between the cuticle and the cortex)	Indistinct (when the inner margin of the cuticle is not visible or is not well defined) Distinct (when the border between the cuticle and the cortex is clearly visible and is well defined) Varies (when the inner cuticle margin varies in its distinctness due to a variation in pigment density along the inner margin)
Outer cuticle scale profile (condition of the cells on the surface of the cuticle)	Smooth (cuticle profile that is even or flat) Serrated (cuticle profile that is saw-toothed) Ragged (cuticle profile that is uneven and irregular); Looped – when the scales are curved at their distal edges so that they arch at the edge of the shaft Other – hairs that have a combination of the above cuticle profiles, or hairs that have a cuticle profile that cannot be categorized as Smooth, Serrated, Ragged or Curved.
Pigment in the cuticle	Present (more commonly in heavily pigmented hairs) Absent (generally the cuticle is not pigmented and if melanin inclusions are detected they should be considered a rare and diagnostically valuable feature)

The free edge of the cells defines the pattern or drawing of the cuticle by forming lines specifically located transversely and longitudinally along the hair shaft. If the cells of the cuticle are arranged in even rows, the lines will have little waviness; if the cells are irregularly arranged, the waviness will be pronounced.

The shape and arrangement of the cells varies from species to species. For non-human hairs, the arrangement or pattern and how this varies along the length of

individual hairs is among the most useful characteristics for species identification. For human hairs, this pattern shows no significant differences between individuals [16], but its difference with patterns in animals can be used for species identification[3, 6].

There are three basic cuticle patterns – coronal (crown-like), spinous (petal-like) and imbricate (flattened). Combinations and variations of these types are possible. The crown-like scale pattern is found in hairs of very fine diameter and resembles a stack of paper cups. It is commonly found in the hairs of small rodents and bats, but rarely in human hairs. The petal-like scales are triangular in shape and protrude from the hair shaft. This pattern is found in the hairs of cats, mink, seals, etc. It is never found in human hairs. The imbricate or flattened cuticle type consists of overlapping scales with narrow margins. They are commonly found in human hairs, but also in many animal hairs [8].

Hair diameter: Another indicator by which human hairs can be typed, each hair is measured in several places and the largest measured value is taken as the thickness of the hair in question. This value helps to differentiate hairs from different body areas and also from hairs of the same body area from persons of different racial groups. For example, Caucasian scalp hair is described as having a moderate shaft diameter, Negroid scalp hair as having a moderate to fine shaft diameter with considerable variation, and Mongoloid scalp hair as having a coarse shaft diameter with little or no variation [4, 10, 34].

Cross-section shape: This is an indicator whose identification value is not accepted unambiguously by researchers [3, 34].

Opponents of this indicator point out that the cross-sectional shape is variable from hair to hair and along individual hair shafts (especially in brittle and curly hair) [40].

Conversely, proponents of the study argue that variation in cross-sectional shape in human hairs is predictable and consistent provided sections from similar types of hair and of equivalent longitudinal appearance are used; cross-sections reveal a number of microscopic features more clearly than can be seen in a longitudinal mounts; and cross-sectional shape is of value for racial origin determination [34].

According to Ogle et al. [27], the appearance of most cross-sectional features does not provide additional data for the purpose of hair identification and comparison, but rather adds a different perspective to those already established. However, a cross-section can aid in the accurate identification of a trait, which is difficult with longitudinal observation. Cross-sectioning is better at determining pigment or medulla distribution, cortical texture, etc. Cuticle thickness, pigment density, and pigment size can usually be easily diagnosed in longitudinal view by an experienced examiner.

The main cross-sectional characteristics of human hairs are: cross-sectional shape and area, cuticle thickness, cortical texture, size, pigment density and distribution [27].

According to Blume-Peytavi et al. the cross-section shape variates are Round, Oval, Triangular, Flat, Kidney, and Teardrop. The triangular shape is seen often in beard hairs and rarely in scalp hairs, i.e. it can be used to determine the regional origin of the examined hair (which part of the body it originates from) [4].

The cross-section shape of the hair also varies depending on racial origin. In Caucasoid hairs, the cross-section is elliptical in shape, corresponding to straight or wavy hair; in Mongoloid hairs, it is usually circular, corresponding to straight hair [36].

In contrast, Negroids have an elongate elliptical or even ribbon-like cross-sectional shape [4, 10, 24].

The cross-sectional area is also determined. It has been found that this area in hairs from different regions of the head has some variation, but still the differences are less than those between different people.

The thickness of the cuticle is measured and it is categorized as Thin, Thick, and Varies, the shape of the medulla – general shape of its cross-section, its size in relation to the cross-sectional size of the whole hair, and its arrangement – median to the hair shaft or asymmetrical, the type of cortical texture – absent, present, obscured [27], and the pigment characteristics – colour and hue, density, shape and size of granules, distribution of pigment in the cross-section (uniform, peripheral, central and one-sided).

Hair root: the variates here represent the growth stage of the hair at the time of its removal or loss from the body and include: Absent, Anagen (active growth phase), Catagen (transitional phase between anagen and telogen phases), and Telogen (terminal stage prior to the hair falling out of the hair follicle) [3, 27].

Examination of the hair root is important because if the hair is pulled from the scalp during the Anagen phase will have an epithelial sheath adhering to the root. If it is pulled during the Catagen phase there may or may not be such a sheath, whereas if the hair is pulled during the Telogen phase there will be no adherent parts of the epithelial sheath [3, 27].

The growth phase of the hair root influences the identification by the presence of such epithelial sheath, making it possible to analyze the DNA present in the nuclei of the adherent epithelial cells and therefore to personalize the hair under study with very high probability [12].

The nucleated cells of the root epithelial sheath also assist in determining the sex of the individual that is the source of the corresponding hairs by determining the so-called sex chromatin (Barr bodies) [38].

Distal tip of the hair: the appearance of the distal hair tip can be used to determine whether it is in its natural state or whether there is some cosmetic/traumatic influence on it. The acquired characteristics of this tip are the result of various morbid or cosmetic effects as well as the adverse effect of certain environmental factors [3, 5, 7, 22, 31, 34, 38, 41, 42, 48].

Variates of the distal tip are: Natural Taper, Rounded Taper, Square Cut/Straight Edge, Angled Cut/Straight Edge, Square Cut/Rounded Edge, Angled Cut/Rounded Edge, Split, Frayed, Crushed, Singed, Broken, and Other[34].

Natural hair has a thin needle-like tip. When cut, the tip becomes square with a straight edge, gradually smoothing over time to a tapered shape. Whether there is a pronounced straight edge or the presence of a cone can determine the length of the time interval between the shearing of the hair and its examination [3].

In so-called 'weathering', as a result of environmental factors, abrasion and splitting of the hair ends with longitudinal splitting of the hair is observed [7, 27, 48].

Hair is also damaged to varying degrees when dried with a hair dryer, i.e. when exposed to higher temperatures, rough combing, the use of curling, straightening, discolouring or colouring agents, depending on their type and composition. These

mainly affect the surface of the hair and are clearly visible under light microscopy – pigment deposition in the cuticle, lifting and breaking of the edge of the cuticle cells until they fall off completely, stripping of the underlying cortex, etc. [5, 7, 22, 31, 33, 38, 41, 42].

Conclusion

Although many investigators believe that morphological analysis of hair is only limited evidentiary value and that its outcome is highly dependent on the training and ability of the investigator, our experience has shown that by considering and taking into account readings for all or most of the microscopic hair characteristics listed above, it is possible to obtain a fairly accurate result when identifying and comparing hair samples.

In all cases where the examiner seeks to be thorough, microscopic examination followed by direct comparison is essential. Light microscopy should be the first test to be performed after receiving the hair sample in the laboratory. This type of examination has a number of advantages over other methods of hair identification: it does not require expensive equipment and consumables; it is not destructive to the sample; it allows for initial screening of the samples, taken from the scene, for suitable ones to then be subjected to more expensive and specific tests.

Perhaps its main advantages, from a forensic point of view, are: contamination of the material does not spoil its examination under light microscope, which often happens in the case of mitochondrial DNA testing (most of the samples from the crime scene are already contaminated); light microscope can be performed on hairs that have not been plucked, but have shedded naturally. This is significant because, such hairs are free of the cellular material attached to the hair root, and cannot be used for nuclear DNA testing. Being that most of the hair material evidence that enters a forensic laboratory is from naturally shedded hairs and nDNA material from plucked hairs is often scarce, light microscopy becomes even more valuable a method for examination.

Therefore, despite the development of science to date and the application of much more precise methods of examination (nDNA, mDNA, etc.), the determination of the morphological characteristics of the hair retains its importance in hair identification.

References

1. **Amit, C., T. Navodita.** A Study on The Presence of Medulla Types of Hair Among the Young Jaat Residents of Western Uttar Pradesh. – J. Forensic. Sci.& Criminal Inves., **10**(4), 2018, 555795. Doi: 10.19080/JFSCI.2018.10.555795
2. **Bednarek, J.** An attempt to establish objective criteria for morphological examinations of hairs using the image analysis system. – Probl. Forensic. Sci., LVI, 2004, 65-77.
3. **Bersegants, L. O., M. F. Vereshtaka.** Morphological features of human hair in the aspect of forensic medical examinations. Moscow, Medicine, 1982, 11-58, 139-156.
4. **Blume-Peytavi, U., A. Tosti, D. A. Whiting, R. M. Trüeb.** Hair Growth and Disorders. Springer, 2008, 1-10.
5. **Bottoms, E., E. Wyatt, S. Comaish.** Progressive changes in cuticular pattern along the shafts of human hair as seen by scanning electron microscopy. – Br. J. Dermatol, **86**(4), 1972, 379-384.

6. **Brunner, H., B. J. Coman.** The Identification of Mammalian Hair. Melbourne, Inkata Press, 1974, 5-17.
7. **Dawber, R.** Diseases of the Hair and Scalp. Oxford, Blackwell Science Ltd, 1997, 239-299, 466-483.
8. **Deedrick, D. W., S. L. Koch.** Microscopy of hair part I: A practical guide and manual for human hairs, Forensic Science Communications [Online]. (January 2004a).
9. **Deedrick, D. W., S. L. Koch.** Microscopy of hair part II: A practical guide and manual for animal hairs, Forensic Science Communications [Online]. (July 2004b).
10. **Franbourg, A., P. Hallegot, F. Baltenneck, C. Toutain, F. Leroy.** Current research on ethnic hair. – J. Am. Acad. Dermatol., **48**(6), 2003, 115-119.
11. **Gamble, L. H., P. L. Kirk.** Human hair studies, II. Scale counts.– J. Crim. Law Criminal., **31**(5), 1940, 627-636.
12. **Harding, H. W. J., G. E. Rogers.** Forensic hair comparison in South Australia. – J. Forens. Sci. Soc., **24**, 1984, 339-340.
13. **Harland, D. P., R. J. Walls, J. A. Vernon, J. M. Dyer, J. L. Woods, F. Bell.** Threedimensional architecture of macrofibrils in the human scalp hair cortex. – J. Struct. Biol., **185**(3), 2014, 397-404.
14. **Harland, D. P., J. A. Vernon, R. J. Walls, J. L. Woods.** Transmission electron microscopy staining methods for the cortex of human hair: A modified osmium method and comparison with other stains. – J. Microsc., **243**(2), 2011, 184-196.
15. **Hausman, L. A.** The cortical fusi of mammalian hair shafts. – Am. Naturalist, **66**, 1932, 461-470.
16. **Hausman, L. A.** A comparative racial study of the structural elements of human head hair. – Am. Naturalist, **59**(665), 1925, 529-538.
17. **Khumalo, N. P.** African hair morphology: Macrostructure to ultrastructure. – Int. J. Dermatol., **44**(1), 2005, 10-12.
18. **Koch, S. L., M. D. Shriver, N. G. Jablonski.** Variation in human hair ultrastructure among three biogeographic populations. – J. Struct. Biol., **205**(1), 2019, 60-66.
19. **Kolowski, J. C., N. Petrich, M. M. Wallace, P. R. Deforest, M. A. Prinz.** A comparison study of hair examination methodologies. – J. Forens. Sci., **49**(6), 2004, 1253-1255.
20. **Kornisheva, V. G., G. A. Yezhkov.** Head hair and scalp pathology. St. Petersburg, Foliant, 2012, 7-18, 137-149.
21. **Langia, H. S.** Increase in medullary index of human hair with the passage of time. – J. Crim. Law Criminal. Pol. Sci., **57**(2), 1966, 221-222.
22. **Lee, Y., Y. D. Kim, H. J. Hyun, L. Q. Pi, X. Jin, W. S. Lee.** Hair shaft damage from heat and drying time of hair dryer. – Ann. Dermatol., **23**(4), 2011, 455-462.
23. **Luell, E., V. E. Archer.** Hair medulla variation with age in human males. – Am. J. Phys. Anthropol., **22**(2), 1964, 107-110.
24. **Menkart, J., L. J. Wolfram, I. Mao.** Caucasian hair, Negro hair and wool: similarities and differences. – J. Soc. Cosmet. Chem., **17**, 1996, 769-787.
25. **Nagase, S., Y. Kajiura, A. Mamada, H. Abe, S. Shibuichi, N. Satoh, T. Itou, Y. Shinohara, Y. Amemiya.** Changes in structure and geometric properties of human hair by aging. – J. Cosmet. Sci., **60**(6), 2009, 637-648.
26. **Noback, C. R.** Morphology and phylogeny of hair. – Ann. NY Acad. Sci., **53**(3), 1951, 476-491.
27. **Ogle, R. R., Jr., M. J. Fox.** Atlas of Human Hair: Microscopic Characteristics, CRC Press LLC, 1998, 24-40.
28. **Ortonne, J. P., G. Prota.** Hair melanins and hair color: ultrastructural and biochemical aspects. – J. Invest. Dermatol., **101**(1), 1993, 82-89.
29. **Ortonne, J. P., J. Thivolet.** Hair melanin and hair color. In: Hair Research. (Ed C. E. Orfanos, W. Montagna and G. Stuttgen). Berlin and Heidelberg: Springer-Verlag, 1981, 146-162.

30. **Preedy, V. R.** Handbook of hair in health and disease. Wageningen Academic Publishers, 2012, 40-47.
31. **Price, V. H.** The role of hair care products. In: Hair Research. (Ed. C.E.Orfanos, W.Montagna and G.Stuttgen). Berlin, Berlin and Heidelberg: Springer-Verlag, 1981, 501-506.
32. **Randebrook, R. J.** Neue erkenntnisse uber den morphologischen aufbau des menschlichen haares. – J. Soc. Cosmet. Chem., **15**, 1964, 691-706.
33. **Robbins, C. R.** Chemical and physical behavior of human hair. New York: Springer, 2012, 5th ed., 25-58.
34. **Robertson, J.** Forensic Examination of Hair, Taylor & Francis, 1998, 5-255.
35. **Robertson, J.** The forensic examination of fibres and hairs. In: Expert Evidence. (Ed. I. Freckleton, H.Selby). Sydney, The Law Book Company, 1995, 3903-4255.
36. **Rook, A.** Hair II Racial and other genetic variations in hair form. – Br. J. Dermatol., **92**(5), 1975, 599-600.
37. **Saferstein, R.** Criminalistics. Upper Saddle River, NJ, Prentice Hall, 2001, 178-219.
38. **Santos Nogueira, A. C., I. Joekes.** Hair color changes and protein damage caused by ultraviolet radiation. – J. Photochem. Photobiol. B., **74**(2-3), 2004, 109-117.
39. **Schiaffino, M. V.** Signaling pathways in melanosome biogenesis and pathology. – Int. J. Biochem. Cell Biol, **42**(7), 2010, 1094–1104.
40. **Seta, S., H. Sato, B. Miyake.** Forensic hair investigation. In: Forensic Science Progress, 2, (Ed. A. Maehly, R. L.Williams), Berlin: Springer-Verlag, 1988, 47-166.
41. **Swift, A. J.** The histology of keratin fibres. In: Chemistry of Natural Protein Fibres. (Ed. R.S.Asquith). New York, Plenum Press, 81-146.
42. **Swift, A. J.** The hair surface. In: Hair Research. (Ed. C.E.Orfanos, W.Montagna, G.Stuttgen). Berlin, Berlin and Heidelberg: Springer-Verlag, 1981, 65-72.
43. **Vaughn, M. R., E. Brooks, R. A. van Oorschot, S. Baindur-Hudson.** A comparison of macroscopic and microscopic hair color measurements and a quantification of the relationship between hair color and thickness. – Microsc. Microana, **15**(3), 2009, 189-193.
44. **Wasmeier, C., A. N. Hume, G. Bolasco, M. C. Seabra.** Melanosomes at a glance. – J. Cell Sci., **121**(24), 2008, 3995-3999.
45. **Westgate, G. E., N. V. Botchkareva, D. J. Tobin.** The biology of hair diversity. – Int. J. Cosmet. Sci., **35**(4), 2013, 329-336.
46. **Wyatt, E. H., J. M. Riggott.** Scanning electron microscopy of hair. Observations on surface morphology with respect to site, sex and age in man. – Br. J. Dermatol., **96**(6), 1977, 627-633.
47. **Yang, F. C., Y. Zhang, M. C. Rheinstädter.** The structure of people's hair. – PeerJ., **14**(2), 2014, 619.
48. **Zimina, Yu. V.** Differential diagnosis of hair of different anatomical areas of the human body by micromorphological features. St. Petersburg, Publishing house SPbMAPo, 2008, 3-21.

ANTHROPOLOGY AND ANATOMY 28 (4)

Original Articles

Changes in Stature, Weight and Body Mass Index in 3-6-Year-Old Bulgarian Children (2005 – 2016)

Ivaila Yankova Pandourska, Yanitza Zhecheva, Albena Dimitrova*

Institute of Experimental Morphology, Pathology and Anthropology with Museum, Bulgarian Academy of Sciences, 1113 Sofia, Bulgaria

*Corresponding author e-mail: anthropologyvaila@gmail.com

The aim of the study is to follow up trends in the stature, weight and body mass index (BMI) in 3-6-year-old children from Sofia during the period 2005-2016 and to assess the prevalence of underweight, overweight and obesity.

From 2004 to 2005 and 2014 to 2016, two independent cross-sectional anthropological studies of children visiting kindergartens in Sofia were carried out. Stature and body weight were measured and BMI was calculated. The children were classified as underweight, normal, overweight and obese according to the International Obesity Task Force BMI cut-offs proposed by Cole and Lobstein.

The children measured during the period 2014-2016 have lower but similar values of the stature, body weight and BMI to those of children from the first survey (2004-2005). The statistically significant differences are not observed. An increase of frequencies of underweight and overweight and a decrease of the incidence of obesity in 3-6-year-old children are detected.

Key words: children, anthropometric measurements, BMI, underweight and overweight, secular changes

Introduction

The anthropological characteristic of the population of each country is an indicator of the specifics of the socio-economic living conditions during its historical development and in the present.

Secular trend presents changes in the consecutive generations, mostly observed in growth, development and maturation of children and adolescents, or in adult sizes [7].

The changes depend on both the genetic potential of the population and environmental factors, notably the level of socio-economic living conditions.

In some developed countries, secular changes slow down [4] or stabilize at a certain age and age of menarche, while in other ones it still continues [1, 2].

The absence of changes in the rate of growth and development in certain years shows that either living conditions stop improving or that they already allow the full expression of genetic potential [23].

Secular growth changes to higher stature, body weight and earlier maturation are also associated with improved nutrition and health care [4, 9, 15, 24, 25] and could be referred to the health status of a population with mostly positive, progressive tendencies. Unfortunately these positive trends lead to some negative consequences such as the increasing body fat content as one of the results of the modern way of living (reduced physical activity along with unfavorable changes in dietary habits) [18].

The risk of being overweight and obese during adolescence and adulthood begins in early childhood. Overweight and childhood obesity are a risk factor for a number of health problems (respiratory, cardiovascular, musculoskeletal, metabolic, endocrine, etc.) [10, 20].

A relative increase in the prevalence of overweight and obesity in early childhood are observed worldwide in the period 1990–2010 [6]. Along with being overweight in the current generation of children and adolescents in developed countries, a serious problem is the increased incidence of underweight, which, although to a lesser extent, also carries a risk of health complications [13, 27].

The frequency of overweight and obesity is constantly increased, but a number of studies have found slowed down or even stabilized percentage of overweight and obese children after the 2000s. This is observed mostly in the younger children (up to 7-10 years) [8, 22, 26].

The aim of the study is to follow up trends in the stature, weight and body mass index in 3-6-year-old children from Sofia during the period 2005-2016 and to assess the prevalence of underweight, overweight and obesity.

Materials and Methods

Two independent cross-sectional anthropological studies of children visiting kindergartens in Sofia were carried out during the periods 2004 - 2005 and 2014 - 2016. A total of 640 participants (320 boys and 320 girls) were included in the first study and 870 (451 boys and 419 girls) in the second one. Stature was measured in standing position with stadiometer to the nearest 0.1 cm by Martin-Saller's classical methods [12]. Body weight was measured using digital scale Tanita to the nearest 0.1 kg. Body mass index (BMI) was calculated by the formula: $BMI = \text{body weight (kg)} / \text{stature (m)}^2$. The participants were classified as underweight, normal, overweight and obese according to the International Obesity Task Force (IOTF) cut-offs of BMI proposed by Cole and Lobstein [5].

Written informed consent from the parents of each child who voluntarily participated in the studies was obtained. The investigations were approved by the Ethical Committee

of Institute of Experimental Morphology, Pathology and Anthropology with Museum – Bulgarian Academy of Sciences and were conducted in agreement with the principles of the Declaration of Helsinki for human studies of the World Medical Association [28].

The metrical data were analyzed by SPSS software, version 16. Student's t-test was used to compare stature, weight and BMI between two investigated cohorts. The comparison of the frequency of underweight, overweight and obesity between the different years was performed with a chi-square test. Statistical significance was considered at $p \leq 0.05$.

Results and Discussion

The statistical data of basic anthropometric features and BMI in 3-6-year-old children are presented on **Table 1**.

The stature of the boys from the first sample (2004-005) varies between 101.20 cm at the age of 3 and 121.28 cm at the age of 6 years. In the boys from the second

Table 1. Statistical data for stature, weight and BMI in 3-6-year-old children (2005-2016)

Features	Age	Years	Boys					Girls				
			n	mean	SD	decade changes	p	n	mean	SD	decade changes	p
Stature (cm)	3y	2005	80	101.20	4.30	- 1.44	0.03*	80	98.99	3.89	- 0.6	0.37
		2016	103	99.76	4.66			102	98.39	4.92		
	4y	2005	80	107.70	4.13	- 0.99	0.18	80	106.52	5.39	- 0.07	0.94
		2016	100	106.71	5.20			100	106.45	5.39		
Body weight (kg)	3y	2005	80	114.66	4.97	- 0.79	0.28	80	113.91	4.97	- 0.79	0.28
		2016	128	113.87	5.18			111	113.12	4.95		
	6y	2005	80	121.28	4.93	0.21	0.79	80	120.40	5.16	- 0.97	0.19
		2016	120	121.49	5.74			106	119.43	4.80		
BMI (kg/m ²)	3y	2005	80	16.33	2.11	- 0.55	0.07	80	15.48	1.79	- 0.33	0.24
		2016	103	15.78	1.93			102	15.15	1.98		
	4y	2005	80	18.35	3.09	- 0.32	0.53	80	17.96	2.68	- 0.24	0.55
		2016	100	18.03	3.60			99	17.72	2.59		
	5y	2005	80	21.06	3.97	- 0.7	0.18	80	20.01	3.72	0.12	0.82
		2016	127	20.36	3.16			110	20.13	3.68		
	6y	2005	80	23.86	4.26	- 0.6	0.31	80	22.87	3.93	- 0.52	0.31
		2016	120	23.26	4.0			106	22.35	3.09		
	3y	2005	80	15.91	1.43	- 0.09	0.65	80	15.76	1.26	- 0.16	0.36
		2016	103	15.82	1.25			102	15.60	1.18		
	4y	2005	80	15.75	1.83	- 0.01	0.97	80	15.76	1.48	- 0.17	0.44
		2016	100	15.74	1.87			99	15.59	1.43		
	5y	2005	80	15.92	1.87	- 0.28	0.23	80	15.38	1.42	0.26	0.33
		2016	127	15.64	1.46			110	15.64	2.02		
	6y	2005	80	16.14	2.04	- 0.46	0.08	80	15.72	2.04	- 0.09	0.75
		2016	120	15.68	1.69			106	15.63	1.59		

* Statistically significant differences at $p \leq 0.05$

study (2014-2016) it is between 99.75 cm and 121.49 cm, respectively. The increment is higher in boys investigated during the period 2014-2016 (21.73 cm) compared to those investigated within 2004-2005 (20.08 cm). The body weight range is from 16.33 kg to 23.86 kg (2004-2005) and from 15.78 kg to 23.26 kg (2014-2016). The weight of boys from both cohorts increased between 3 and 6 years of age with 7.5 kg.

The stature of the girls from the first study ranged from 98.99 cm at 3 years to 120.40 cm at 6 years, as the increment is 21.41 cm. In the group of girls from second study, the stature increased from 3 (98.39 cm) to 6 (119.43 cm) years with 21.04 cm. The body weight of the girls measured in 2004-2005 ranged from 15.48 kg (at the age of 3) to 22.88 kg (at the age of 6), and girls measured in 2014-2016 weigh from 15.15 kg to 22.35 kg. Weight gain is 7.4 kg in the first sample and 7.2 kg in the second one.

The difference in stature of both boys and girls from each cohort is from a few millimeters to about 1.4 cm, and in body weight: from 0.100 kg to 0.700 kg.

In children investigated during the periods 2004-2005 and 2014-2016, the values of the indicator of nutritional status – BMI are within a normal range (18.5 kg/m² – 25.0 kg/m²) and remain relatively constant for a decade.

There are no significant differences in stature, weight and BMI in boys and girls in all age groups between 2005 and 2016, with the exception of 3-year-old boys, in which statistically significant differences are observed in stature (p=0.03).

For each age group in both genders, the mean values of stature, weight and BMI decreased slowly for a decade. The opposite trend is observed only in the stature of 6-year-old boys (0.21 cm) and in the weight and BMI of 5-year-old girls (0.12 kg and 0.26 kg/m² respectively).

Table 2 presents the incidence of underweight, normal weight, overweight and obesity in children studied in 2004-2005 and 2014-2016.

The frequency of underweight children in both genders investigated in 2004-2005 is 11.9%. The highest incidence of underweight is at the age of 3 (17.5%) in boys and

Table 2. Frequency of the categories nutritional status according BMI cut-offs of Cole and Lobstein

Boys											
Age	Years	n	Underweight		Normal weight		Overweight and obesity				χ^2 (df = 3)
							Overweight		Obesity		
			n	%	n	%	n	%	n	%	
3y	2005	80	14	17.5	60	75.0	4	5.0	2	2.5	1.56
	2016	103	17	16.5	76	73.8	9	8.7	1	1.0	
4y	2005	80	11	13.8	63	78.8	3	3.8	3	3.8	3.52
	2016	100	18	18.0	73	73.0	8	8.0	1	1.0	
5y	2005	80	7	8.8	62	77.5	8	10.0	3	3.8	2.82
	2016	127	21	16.6	90	70.9	13	10.2	3	2.4	
6y	2005	80	6	7.50	62	77.5	8	10.0	4	5.0	6.03
	2016	120	14	11.7	99	82.5	6	5.0	1	0.8	

Girls											
Age	Years	n	Underweight		Normal weight		Overweight and obesity				χ^2 (df = 3)
							Overweight		Obesity		
			n	%	n	%	n	%	n	%	
3y	2005	80	11	13.8	63	78.8	5	6.2	1	1.2	1.40
	2016	102	17	16.7	81	79.4	3	2.9	1	1.0	
4y	2005	80	11	13.8	53	66.2	16	20.0#	0	0.0	10.10#
	2016	99	14	14.1	76	76.8	6	6.10	3	3.0	
5y	2005	80	6	7.5	68	85.0	3	3.8	3	3.8	5.26
	2016	110	11	10.0	81	73.6	14	12.7	4	3.6	
6y	2005	80	10	12.5	56	70.0	11	13.8	3	3.8	6.79
	2016	106	7	6.6	87	80.2	12	11.3	0	0.0	

Statistically significant differences at $p \leq 0.05$

at the age of 3 and 4 (13.8%) in girls. The prevalence of underweight among preschool boys and girls studied in 2014-2016 is 15.7% and 11.9% respectively, as the highest frequency is observed at the age of 4 (18.0%) in boys and at the age of 3 (16.7%) in girls. The incidence of underweight decreased with age in both studies. Over 70% of the children from the investigated cohorts have normal weight and 3.0 to 20.0% are overweight. In children from the first study the incidents of overweight rise to 10% and 13.8% in 6-year-old boys and girls and in children from the second one – to 10% and 12.7% in 5-year-old boys and girls, after that the frequency decreases. In both studies the children with obesity are less than 5.0%. There are significant differences only in group of overweight girls at the age of 4 ($p \leq 0.05$).

Discussion

The periodic conduct of similar studies provides a possibility to follow the tendencies in children and adolescents' growth and development for certain periods of time in different socio-economic living conditions.

Our study demonstrates slow-down trends for stature, weight and BMI in 3-6-year-old children from Sofia. The comparative analysis of the data from the two studies shows that the children measured in the period 2014-2016 have lower values of the stature, weight and BMI, but close to those of the children from the first study (2004-2005). Statistically significant differences only in the group of 3-year-old boys are observed. Similar trends in basic anthropometric features are detected in some other populations as well [4, 16, 21]. The data from other countries are consistent in reporting a positive trend. In children under the age of 5 the secular changes in stature, weight and BMI are the smallest and increase with age and reach a maximum during the puberty [18, 19, 29]. Positive and negative changes are recorded for different ages and decades in Novi Sad sample between 1991 and 2001, and after 2001. A modest increase of height and weight during the investigated period, especially in preschool children are established. According to the authors, the changes in anthropometric characteristics reflect the changing socio-economic and political situation in the country after the 1990s [17].

An important aspect of monitoring of the children's health is the investigation of their nutritional status and determination of the frequency of its extreme forms – underweight and obesity.

Comparing the children in both studies an increase of the frequency of underweight is detected, with the exception of 3-year-old boys, and 6-year-old girls. The prevalence of overweight in boys also increases, except 6-year-olds, and decreases in girls, except 5-year-olds. The incidence of obese children decreases in boys, whereas in 3 and 5-year-old girls it remains relatively constant and decreases in 6-year-olds. Similar to our results for children from early childhood, preschool and school age are established in England, Netherlands, Czech Republic and others [11, 14, 22, 26]. Van Jaarsveld and Gulliford reported stabilization in the incidence of obesity in 2-10-year-old English children between 2004 and 2013, but not in older 11-15-year-old students [26]. A relatively constant incidence of obesity was also found by Sigmund et al. for Czech children for the period 2005-2015 [22]. Decrement of the frequency of overweight and obese children in 2002-2011 in Italy was reported by Brambilla et al. They also found an increase in prevalence of underweight children [3].

Conclusion

For the investigated period (2004/2005 – 2014/2016), detention in stature, body weight and BMI in early childhood and preschool children are established. An increase of the frequency of underweight and overweight and a decrease of the incidence of obesity is detected in 3-6-year-old children.

The information obtained could be used to assess the real health risks of children from early childhood and preschool age, and to develop adequate programs and policies to improve the living conditions and health of the younger generation in the country.

Acknowledgements: To our colleagues who helped to carry out the survey, the teams of the kindergartens, the children who participated in the survey and their parents.

References

1. **Ayatollahi, S. M. T., S. Pourahmad, Z. Shayan.** Trend in physical growth among children in southern Iran, 1988–2003. – *Ann. Hum. Biol.*, **33**(4), 2006, 510-514.
2. **Bodzsár, É. B., A. Zsákai, N. Mascie Taylor.** Secular Growth and Maturation Changes in Hungary in Relation to Socioeconomic and Demographic Changes. – *J. Biosoc. Sci.*, Cambridge University Press, **48**(2), 2016, 158-173.
3. **Brambilla, P., M. Vezzoni, R. Lucchini, L. Acerbi, A. Brambilla, G. Brandolini, P. Rogari, G. Cassavia.** Is the prevalence of overweight reducing at age 5-6 years? Ten years data collection in ASL Milano 2. – *Ital. J. Pediatr.*, **38**, 2012, 24.
4. **Cole, T. J.** The secular trend in human physical growth: a biological view. – *Econ. Hum. Biol.*, **1**, 2003; 161-168.
5. **Cole, T. J., T. Lobstein.** Extended international (IOTF) body mass index cut-offs for thinness, overweight and obesity. – *Pediatric Obesity*, **7**, 2012, 284-294.
6. **De Onis, M., M. Blössner, E. Borghi.** Global prevalence and trends of overweight and obesity among preschool children. – *Am. J. Clin. Nutr.*, **92**, 2010, 1257-1264.

7. **Farkas, A., M. Szmodis.** About the Secular Growth Trend. – *Biomed. J. Sci. & Tech. Res.*, **17**(4), 2019. BJSTR. MS.ID.003043.
8. **Franssen, S. J., M. F. van der Wal, P. Jansen, M. van Eijnsden.** Thinness and overweight in children from Amsterdam: a trend analysis and forecast. – *Ned. Tijdschr. Geneesk.*, **159**, 2015, A8967.
9. **Hovels, O.** Growth, maturation and environment. – *Fortschritte der Kieferorthopädie*, 1990, **51**(2), 61-69.
10. **Kirchengast, S.** Biocultural aspects of gender differences in body composition and obesity during childhood and adolescence. – *Anthrop. Anz.*, **66** (3), 2008, 337-348.
11. **Lateva, M., S. Galcheva, W. de Witte, V. Iotova.** Preschool children – obesity and risk behaviours. Trends from 2009 to 2013. – *Scripta Scientifica Medica*, **45**(3), 2013, 39-42.
12. **Martin, R., K. Saller.** Textbook of Anthropology. – Stuttgart, Gustav Fischer Verlag, Band I, 1957. (Lehrbuch der Anthropologie) [in German].
13. **Martinez-Vizcaíno, V., M. S. López, P. M. Martínez, M. S. Martinez, B. N. Pacheco, F. S. Aguilar, F. Rodríguez-Artalejo.** Trends in excess weight and thinness among Spanish schoolchildren in the period 1992-2004: the Cuenca study. – *Public Health Nutr.*, **12**(7), 2008, 1015-8.
14. **Mitova, Z., R. Stoev, L. Yordanova.** Nutritional Status in 9-15-years-old Schoolchildren from Sofia, Bulgaria /1984-2002/. – *Acta morphol. anthropol.*, **19**, 2012, 246-249.
15. **Murata, M., I. Hibi.** Nutrition and the secular trend of growth. – *Horm. Res.*, **38**(1), 1992, 89-96.
16. **Oprîşescu, I., L. C. Gherghel, C. Minculescu.** Secular Trend of Growth in Height, Weight and Body Mass Index in Young Romanians Aged 18-24 Years. – *Procedia - Social and Behavioral Sciences*, **117**, 2014, 622-626.
17. **Pavlica, T. M, R. S. Rakić, B. K. Popović, V. P. Puškaš, V. S. Božić-Krstić.** Secular trend in height and weight among children from Novi Sad (Serbia), 1971–2017 – *Glasnik*, **53**, 2018, 131-140.
18. **Photiou, A., J. H. Anning, J. Mészáros, I. Vajda, Z. Mészáros, A. Sziva, A. Prókai, N. Ng.** Lifestyle, body composition, and physical fitness changes in Hungarian school boys (1975-2005). – *Res. Q Exerc. Sport*, **79**(2), 2008, 166-73.
19. **Pop, R.M., A. Tenenboun, M. Pop.** Secular Trends in Height, Body Mass and Mean Menarche Age in Romanian Children and Adolescents, 1936-2016. – *Int. J. Environ. Res. Public Health*, **18**(2), 2021, 490.
20. **Reilly, J. J., E. Methven, Z. C. McDowell, B. Hacking, D. Alexander, L. Stewart, C. J. H. Kelnar.** Health consequences of obesity. – *Arch. Dis. Child*, **88**, 2003, 748-752.
21. **Sedlak, P., J. Pařízková, D. Samešová, M. Musálek, H. Dvořáková, J. Novák.** Secular Changes in Body Build and Body Composition in Czech Preschool Children in the Context of Latent Obesity. – *Children*, **8**, 2021, 18, <https://doi.org/10.3390/children8010018>
22. **Sigmund, E., D. Sigmundová, P. Badura, L. Trhlíková, A. M. Gecková.** Time trends: a ten-year comparison (2005–2015) of pedometer-determined physical activity and obesity in Czech preschool children. – *BMC Public Health*, **16**, 2016, 560.
23. **Sussanne, Ch., E. Bodzsar.** Patterns of secular changes of growth and development. – In: *Secular growth changes in Europe* (Eds. E. B. Bodzsar, C. Susanne), Eötvös Univ. Press, Budapest, 1998, 5-26.
24. **Tanner, J. M.** The secular trends towards earlier physical maturation. – *Tijdsch. Soc. Geneesk.*, **44**, 1966, 524-538.
25. **Tanner, J. M.** Growth as a measure of the nutritional and hygienic status of a population. – *Horm. Res.*, **38** (1), 1992, 106-115.
26. **van Jaarsveld, C. H. M., M. C. Gulliford.** Childhood obesity trends from primary care electronic health records in England between 1994 and 2013: population-based cohort study. – *Arch. Dis. Child*, **100**, 2015, 214-219.

27. **Vignerova, J., L. Humeníková, M. Paulová, J. Riedlová.** Prevalence of overweight, obesity and low weight in the Czech child population up to 18 years of age in the last 50 years., – *J. Public Health*, **16**, 2008, 413-420.
28. **World Medical Association.** Declaration of Helsinki – Ethical Principles for Medical Research Involving Human Subjects. – *WMJ*, **54**(4), 2008, 122-125.
<https://www.wma.net/policies-post/wma-declaration-of-helsinki-ethical-principles-for-medical-research-involving-human-subjects/>
29. **Zhang, Y. Q., H. Li, H. H. Wu, X. N. Zong.** Secular trends in weight, height and weight for height among children under 7 years in nine cities of China, 1975-2015: results from five repeated cross-sectional surveys. – *BMJ Open*, **9**(10), 2019, e029201.

Characteristics of the basic anthropometric features in children of preschool age (3-6 years) from Smolyan region, Bulgaria

Silviya Mladenova

University at Plovdiv "Paisii Hilendarski", Branch – Smolyan

*Corresponding author e-mail: silviاملadenova.sm@uni-plovdiv.bg

The aim of the present study is to make characteristic of the basic anthropometric features for evaluation of the physical development of contemporary generation preschool children from Smolyan region, Bulgaria in age and gender aspects. A transversal anthropometric study of 330 children from both sexes aged between 3 to 6 years from state kindergartens of Smolyan district, Bulgaria was performed in the period 2017-2019. Height, weight, chest circumference and head circumferences of each child have been measured. The results show unevenness, heterochrony and gender dimorphism both in relation to the absolute values of the indicators and in relation to the rate and reached growth velocity and confirm the general biological regularities of growth in this age period. The observed specific peculiarities in the growth processes are a reflection of the influence of hereditary and environmental factors, operating in the studied population.

Key words: preschool children, height, weight, chest and head circumferences

Introduction

It is known that the different stages in ontogenesis are real reflection of the chain of events in the process of individual growth and development. Each of these stages is characterized by unique and specific combination of biological features which are influenced by a complex of various environmental and genetic factors. The influence of these factors changes during different ages [3, 6, 7, 8, 9, 11, 19, 22], but are especially more pronounced in early childhood [2, 5, 10, 17, 25, 26]. The genetic and environmental influences manifest themselves by morphometric differences in basic anthropometric features, like as height, weight, body diameters, circumferences, body segments and proportions [5, 6, 16, 20, 24, 28], body composition, fat mass and nutritional status [1, 12, 27, 29, 30], different growth velocity and gender differences [13, 15, 27].

The **purpose** of the present study is to characterize of the basic anthropometric features for evaluation of the physical development such as height, weight, chest and head circumferences of preschool children between 3-6 years of age from Smolyan region, Bulgaria in age and gender aspects.

Materials and Methods:

A transversal anthropometric study of 330 children (161 boys and 169 girls), aged between 3-6 years from eight state kindergartens of Smolyan district, Bulgaria was performed in the period 2017-2019. The average age of the children is 3.5, 4.5, 5.5 and 6.5 years. For example, 4-years old are considered the children at age 4.0 years to 4.99 years (**Table 1**).

Table 1. Characteristics of the sample by age and sex

Age (years)	Sample A (2017-2019) Number		
	Boys	Girls	All
3 y.	23	28	51
4 y.	36	44	80
5 y.	49	53	102
6 y.	53	44	97
Total	161	169	330

All studied children are clinically healthy and are of Bulgarian origin. They were examined during their morning classes in kindergartens.

All ethical principles for medical research involving human subjects according Declaration of Helsinki have been adhered [23]. The design of the study has been approved by the Regional Inspectorate of Education of the Bulgarian Ministry of Education and Science in Smolyan and by the Ethics Committee of Filial Smolyan at Plovdiv University. The informed written consent was obtained from parents of all children participating in the study.

Four main indicators for physical development have been measured for each child, as per the methods of Martin-Saller[4]: height (cm), weight (kg), chest circumference and head circumference (cm). The height is measured by original anthropometer GPM (Siber-Hegner Company, Swiss), with a precision up to 0.1cm, and the weight by body composition scale analyzer Tanita BC 465 (Tanita, Japan), with precision up to 0.100 g. The chest and head circumferences were measured by a millimeters band with a precision up to 0.1 cm. The differences in average values in investigated features between both sexes and absolute year increament were calculated. Also the growth velocity (%) was calculated by the relevant formula: $(X_2 - X_1) \times 100 / (X_2 + X_1)$, where X_2 is the mean value of a feature for the given age and the X_1 is the mean value of the same feature for the previous age.

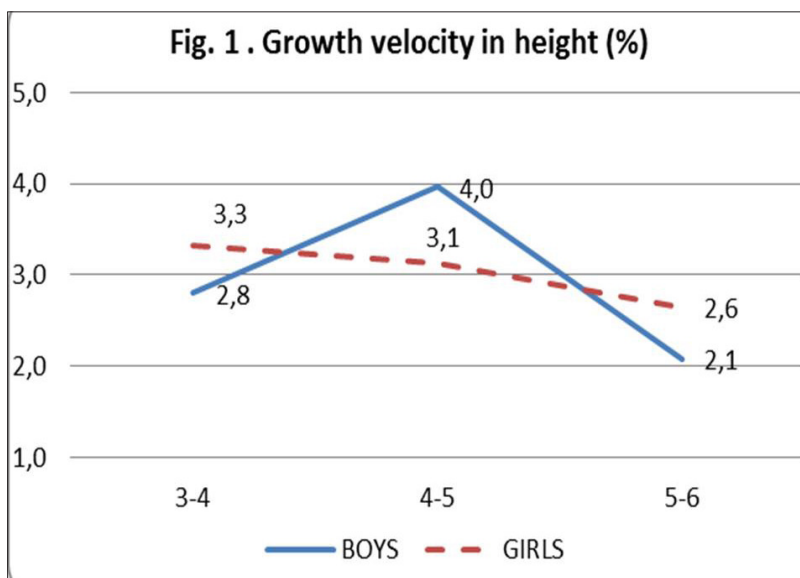
The data have been processed through statistical software suite Statistica 12.0 (StatSoft Inc.), by using analysis of variance. The differences between age and sex groups were evaluated by Student's T-test, with level of significance of $p \leq 0.05$.

Results

The basic statistical characteristics of the height, weight, chest and head circumferences at preschool age Smolyan children are presented in **Table 2**. The growth velocity (%) and inter-sex differences are presented in **Figures 1-5**.

According to the acquired results, **the height** of the present generation of children in preschool age is intensively increasing in both genders (**Table 2**). The average height of the **girls** at age of 3 years is 98.6 ± 4.6 cm. Until they reach to age of 6 years, the height is increased with totally 19.7 cm and reaches value of 118.3 ± 4.7 cm. The absolute year increment is between 6.1 and 6.8 cm per year. The growth velocity varies from 2.6% - 3.3%, and for the girls, it is highest in the period between 3-4 years (**Fig. 1**).

For **boys** at age of 3 years, the average height is 100.8 ± 5.9 cm, where it is intensively increasing and reaches values of 120.3 ± 5.7 cm at age of 6 years. The average annual growth in height is intensive during the entire period and the highest values are observed at age between 4 and 5 years, where the height is increased, on average, by 8.8 cm. The growth velocity for the boys varies from 2.1% to 4%, and it is highest at age between 4-5 years. The high growth velocity decrease for both genders at age between 5-6 years (**Fig. 1**).



During the entire studied growth period, the boys are taller than the girls, where the difference in the height are smallest during the 4th year (1.2 cm), and largest, and statistically significant among the children at age of 5 years, where the difference goes up to 3.2 cm in favour of the boys ($p \leq 0.05$) (**Fig. 5**).

In relation to **body weight** (**Table 2**) the results show that at age of 3 years the weight of the girls is 15.7 ± 2.1 kg, and the boys is 16.1 ± 2.1 kg. The weight is intensively growing during the studied period, where for the boys at age of 6 years, it reaches average values of 24.3 ± 6.2 kg, and for the girls, 25.2 ± 7.0 kg. The absolute

Table 2. Statistical characteristics of basic anthropometric measurements in 3-6-year old children

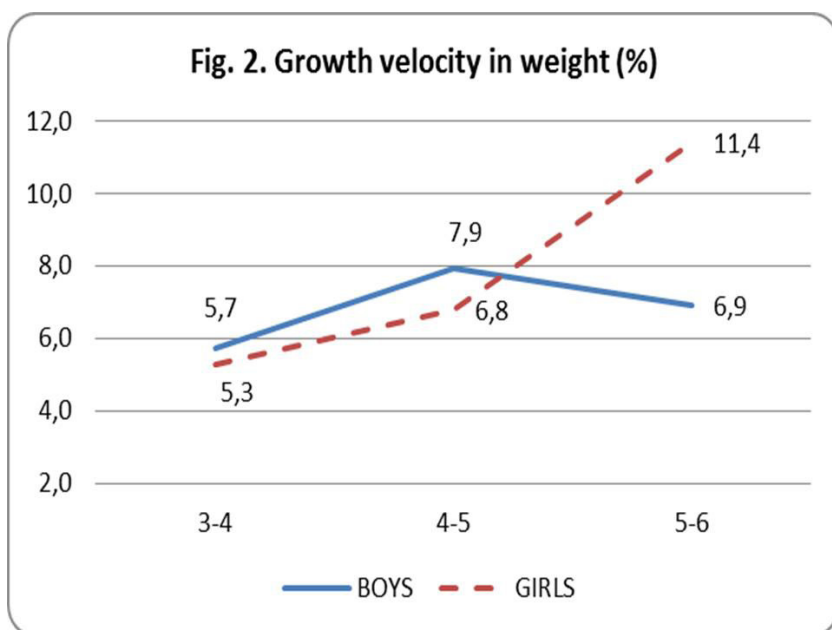
	BOYS			GIRLS					
age (years)	N	Mean	SD	N	Mean	SD	Differ. ♂/♀ (absolute values)	T-Student ♂/♀	p-level ♂/♀
Height (cm)									
3 y.	23	100.8	5.92	28	98.63	4.79	2.2	1.49	0.142
4 y.	36	106.6	3.94	44	105.4	5.50	1.2	1.06	0.290
5 y.	49	115.4	4.16	53	112.2	5.68	3.2*	3.13	0.002*
6 y.	53	120.3	5.69	44	118.3	4.65	2.0	0.80	0.424
Weight (kg)									
3 y.	23	16.10	2.13	28	15.73	2.08	0.37	0.56	0.573
4 y.	36	18.05	2.39	44	17.48	3.68	0.57	0.80	0.423
5 y.	49	21.16	3.37	53	20.03	4.03	1.13*	2.23	0.027*
6 y.	53	24.31	6.15	44	25.19	7.03	- 0.88	0.65	0.511
Chest circumference (cm)									
3 y.	23	52.53	2.71	28	52.40	1.85	0.13	0.17	0.859
4 y.	36	54.51	2.63	44	52.87	3.75	1.64*	2.21	0.029*
5 y.	49	57.02	3.48	53	54.12	5.96	2.90*	2.95	0.003*
6 y.	53	58.08	3.76	44	58.96	7.45	- 0.88	0.73	0.465
Head circumference (cm)									
3 y.	23	50.26	1.41	28	49.80	1.32	0.46	1.18	0.243
4 y.	36	51.11	2.10	44	50.34	2.29	0.77	1.55	0.124
5 y.	49	51.57	1.47	53	50.64	1.25	0.93*	3.01	0.003*
6 y.	53	52.22	3.76	44	51.52	1.34	0.70*	2.36	0.019*

Note: N – number of investigated persons; Mean – average values; SD – standard deviation; Diff. – differences between both sexes T-Student ♂/♀ – values of criteria of Student test; p<0.05* – statistical significance on differences between both sexes.

year increment in the weight for boys varies, average by 2.0 to 3.2 kg, while for the girls varies from 1.8 kg to 5.2 kg. Generally, for the monitored preschool period, the girls grow in weight averagely by 9.5 kg and the boys by 8.2 kg.

The growth velocity of the weight for boys is highest at the age between 4-5 years, when it reaches 7.9%. For the girls, the growth velocity of the body mass is close to that for the boys up to age of 5 years, than it sharply increases and reaches values of 11.4% at age between 5-6 years (**Fig. 2**).

In relation to gender differences, the boys are heavier compared to the girls at same age in the period between 3 to 5 years, where the gender differences have statistical significance only among the children at age of 5 years (p≤0.05). During the 6 year



of their growth, the girls are insignificantly heavier than the boys, which is a result in the jump of body mass accumulation in the period between 5-6 years as well as to significantly higher weight growth speed for girls during that period (**Fig. 5**).

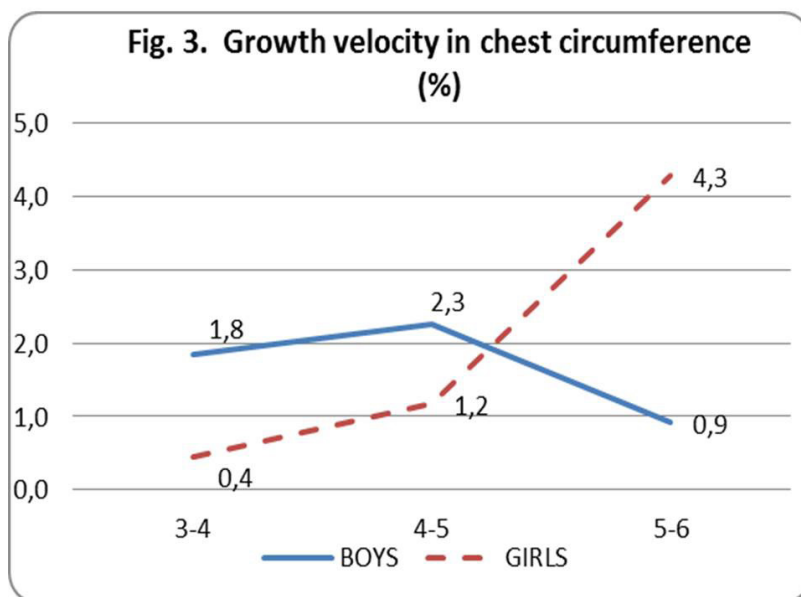
Chest circumference (**Table 2**) is the third main anthropometric indicator, which is used for evaluation of the healthy physical development of the individual in epidemiological studies. Our results show that at age of 3 years, the average chest circumference for boys is 52.5 ± 2.7 cm and for girls it is 52.4 ± 1.9 cm, where at age of 6 years, it reaches values of 58.1 ± 3.8 cm for the boys and respectively, 59.0 ± 7.5 cm for the girls. Generally, the chest circumference increase by 5.55 cm for boys and by 6.56 cm for girls for the period from 3 to 6 years of age.

For the boys the average year increment of the chest circumference increases between 1.1 cm to 2.5 cm, while the growth velocity is highest at age 4-5 years (2.3%) and lowest, respectively, at age between 5-6 years (0.9%).

For the girls, the average year increment of the chest circumference is rather uneven – between 0.5 to 4.8 cm, where the growth velocity varies between 0.4% for age 3-4 years up to 4.3% for age 5-6 years (**Fig. 3**).

In inter-sex aspect, the boys are with larger chest circumference in comparison to the girls during the age between 3 to 5 years, where the differences have statistical significance among the children at age of 4 and 5 years ($p < 0.05$). But during the 6th year, the girls insignificantly outrun the boys in terms of that indicator, which is related to the higher average year increment and to the higher growth velocity for the girls in that period (**Fig. 5**).

The **head circumference** (**Table 2**) is the other very important anthropometric indicator for evaluation of the physical development of children. The head circumference of the studied boys at age of 3 years is with average value of 50.3 ± 1.4 cm and for the girls at age of 3 years, respectively 49.8 ± 1.3 cm. For both genders, this indicator grows



with the age, where at age of 6 years for the boys, it reaches average values of 52.2 ± 3.8 cm and for the girls – 51.5 ± 1.3 cm.

In relation to the average year increment, the most intensive increase of the head circumference for the boys is observed at age between 3-4 years (0.9 cm), and the highest growth velocity during the same period is observed as well – respectively 0.8% (**Fig. 4**).

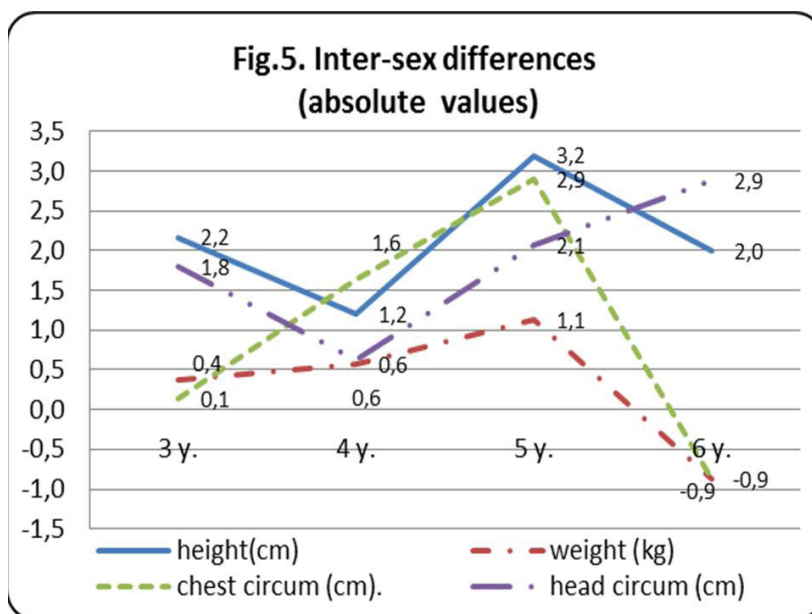
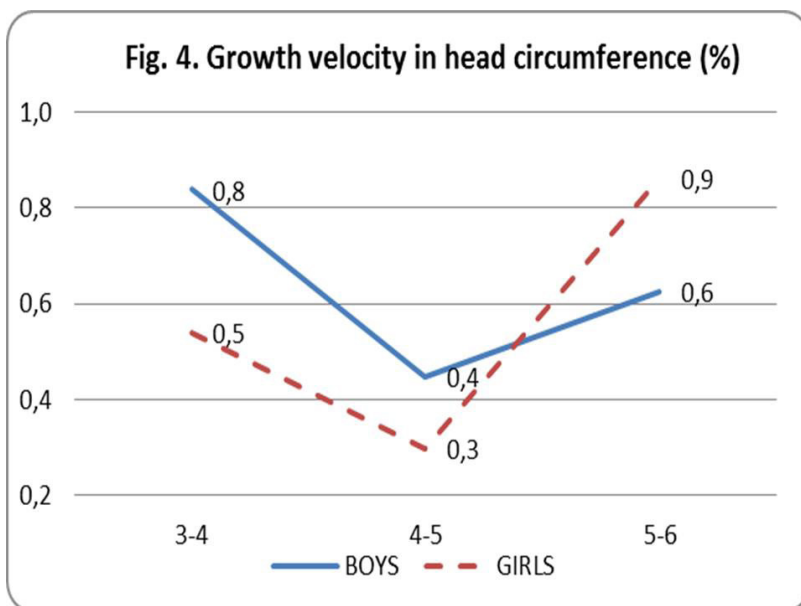
For the girls, the highest average year increment of the head circumference is observed at age between 5-6 years, which corresponds to the highest growth velocity of the indicator (0.9%) (**Fig. 4**). During the remaining age periods, the head circumference grows with slower rate for both genders, which is characteristic for the head features, and as a result of that, the growth of the head circumference for the entire period for the boys is with average total value of 1.96 cm and for the girls 1.72 cm.

In inter-gender aspect, the boys are with larger head circumference compared to the girls for the entire studied period, where the differences are largest and statistically significant among the children at age between 5 and 6 years ($p \leq 0.05$) (**Fig. 5**).

Discussion

In this work we present, for the first time, new data of growth of the height, weight, chest and head circumferences of today preschool children from Smolyan region, Bulgaria at age between 3-6 years.

Investigated children in this study are in average age of 3.5, 4.5, 5.5 and 6.5 years. For example, as we write in section Materials, 4 years old children are considered the children at age 4.0 years to 4.99 years. We used this age grouping to be able to make a correct comparison with similar data of other Bulgarian preschool children who are group in the same way [30]. In contrast, in our previous publications we used an age group according to which, for example, 4-year-olds are children aged 3.5 to 4.49 [9]. The age



grouping of the data, as well as the few similar data for Bulgarian children in this age period are limiting factors in this study which limited our possibility for comparison of data. The only possible comparison at this stage was with similar data for Sofia city of Zhecheva, Yankova [30], due to the identical research methodology and age grouping.

Anthropometric data on different physical characteristics of children and the dynamics of their growth in preschool age were published earlier by other Bulgarian authors. They mainly affect children from the capital Sofia, Plovdiv and some other

towns in Bulgaria [5, 10, 13,14, 15, 16, 18, 20, 21, 24, 25]. Data on children from rural kindergartens are very rare in the native anthropological literature [5]. The data for the children from Smolyan district, aged from 3 to 6 years, studied in the period 1996/1998, were published in our earlier survey [9]. But in general, the anthropometric data for contemporary children in this age group are very rare.

In relation to the growth processes of the studied features during the critical preschool period, our results show unevenness in the growth of various indicators and heterochrony for both genders in relation to almost all features. An intensive growth of the **body height** for both genders is observed, which is characterized by uneven course among the boys and even course among the girls. The largest growth in height is observed at age between 4-5 years for both genders.

In relation to weight, the age dynamics is characterized with more even course, where the average annual increase is within the range of 2 to 3 kg, while among the girls, the gaining of body mass during that period is uneven and at age between 5-6 years, a sharp growing jump of 5.2 kg on average annual base is observed.

In relation to **chest circumference**, the absolute year increase is smooth and significantly more even among the boys (from 1 to 2.5 cm), while among the girls, once again, we observe unevenness and significant increase in the period between 5-6 years. Due to the fact that the chest circumference reflects the growth of the thorax, respectively provides information about the growth process of some body diameters (transversal and sagital diameters of the thorax).

In relation to **head circumference**, reflecting the development of the brain section of the skull, the growth is different in time for the two genders. For the boys, the largest increase of the head circumference takes place at age between 3-4 years, while for the girls, once again, the process takes place at age between 5-6 years.

Our present new data on the height and weight of preschool children in Smolyan region are very close to the data for Sofiapreschool children, published by Zhecheva and Yankova [30]. The comparison that we made with the previously published data of the authors for the body height showed that Smolyan preschool children differ slightly and insignificant in height from their Sofia coevals. The comparison between body weight on children from two territorial groups showed that the current 3- and 4-year-old boys and the 4- and 5-year-old girls from Smolyan and Sofia have practically the same body weight. But the 5-year-old and 6-year-old Smolyan boys are slightly heavier average with 0.8-1.0 kg than their Sofia peers ($p \geq 0.05$). The Smolyan girls are heavier than their Sofia coevals in 6 years of age, when the difference reaches 2.8 kg and is statistically significant ($p \leq 0.05$).

In summary, our results about age and gender differences in the dynamics of the growth of the main anthropometric indicators (height, weight, chest and head circumference) show unevenness, heterochrony and gender dimorphism both in relation to the absolute values of the indicators and in relation to the rate of growth and reached growth velocity. While among the boys, the peaks in increase of body height, body weight and chest circumference for the studied period (age 3-6 years) match in time and are observed to take place at age between 4-5 years, and for the head circumference, at age between 3-4 year, for the girls, the increase in the body height is most significant in the period between 3 to 5 years, while their weight, chest and head circumference increase at age between 5 and 6 years of their development. These results are also confirmed by earlier data of other authors [29, 30].

Our results confirm uneven and not simultaneous increase of various body segments, uneven and not simultaneous grow rates and pronounced sexual dimorphism in period between 3-6 years of age. It is more pronounced in boys, both in growth dynamics and in absolute dimensions of the studied measurements.

Our results confirm the general biological regularities of growth in that age and their peculiarity is a reflection of the influence of the hereditary and environmental factors, operating in the studied population.

Our results once again show the complex character of the growth processes, which are presented, in various extent, in the various morphological systems of the body during the different stages of the ontogenesis and are different for the two genders. Most probably these differences are related to the influence of the specific hereditary factors, dominating the growth of the studied indicators in that age as well as with the different ecosensitivity of the body to environmental factors in the earlier critical stages of the development, which will be a subject of our future studies.

Acknowledgements: The present study was performed by partial financial support of Fund "Scientific Researches" of Plovdiv University "Paisii Hilendarski", within contracts SP 17 – FS – 024 and FP 21 – FS – 003.

References

1. **Andreenko, E., M. Nikolova.** Topical Distribution of the Subcutaneous Fat Tissue on some Parts and Regions of the Body in Children and Adolescents from South Bulgaria. – *Biotechnology & Biotechnological Equipment*, **24** (1), 2010, 342-346.
2. **Dundova, R., D. Kalaikov, B. Zahariev.** Influence of some medico-social factors on the physical development of children in Bulgaria up to 3 years of age. II. Influence of education, social group, visit nurseries and the number of children in the family. – *Pediatrics*, **1**, 1991, 79-83. [in Bulgarian].
3. **Godina, E.** Dynamics of human growth and development processes: spatial - temporal aspects. *DSc Thesis*, Moscow, 2001 [In Russian].
4. **Martin, R., K. Saller.** Lehrbuch der Anthropologie. Stuttgart: Gustav Fisher Verlag, 1957, 1-661 [in German].
5. **Mikhov, H., M. Mikhova, A. Kaleva, G. Mandradziev, E. Enev.** The physical development of preschool children from some Plovdiv and Rhodope villages in 1960/1961. – *Hygiene*, **4**, 1963, 58-65. [In Bulgarian].
6. **Mitova, Z.** Influence of Age and Sex on the Growth of Different Body-segments in 9-15-Year-old Schoolchildren from Sofia (Bulgaria). – *Acta morphol. anthropol.*, **26** (3-4), 2019, 81-87.
7. **Mladenova, S., M. Nikolova, E. Godina.** Socioeconomic factors and their role in the processes of intragroup differentiation of certain morphological characteristics in children and adolescents from the Smolyan region (Bulgaria). – *Proceedings with Scientific papers from Conference Anthropology on the Threshold of the III Millennium*. Moscow, **2**, 2005, 686-697.
8. **Mladenova, S., M. Nikolova.** Intragroup differences in morphological characteristics in children and adolescents from Smolyan region based on social and economic factors. – *Journal of Anthropology*, Sofia, **4**, 2002, 55-58.
9. **Mladenova, S.** Anthropological characteristics of the growth and development of children and adolescents from Smolyan region in modern living conditions. *PhD Thesis*, Plovdiv, 2003, 1-199 [In Bulgarian].
10. **Mladenova, S.** Influence of some factors on the main indicators of newborns physical development in Smolyan region (1980-2008). – *Anniversary Book «Biological Sciences for a Better Future»*, Plovdiv University, 2012, 171-185. [in Bulgarian].

11. **Nikolova, M.** Genetic and environmental bases of morphological variability.– *Monographs*, Plovdiv, 2000, 1-200.
12. **Nikolova, M., E. Godina, D. Mollova.** A Comparison of Plovdiv and Moscow Children's Height, Weight and BMI Values. – *Acta morphol. anthropol.*, **15**, 2010, 212-216.
13. **Nikolova, M., I. Petrov.** Gender differences in the growth rate of recognition of children from 3 to 7 years. – *Scientific Research of Plovdiv Univeristy "Paisii Hilendarski"*, **20**(4), 1982, 375-388 [In Bulgarian].
14. **Nikolova, M., L. Popova.** Percentage graphic norms for body length, body weight and head circumference of children up to 6 years of age. – *Scientific Research of Plovdiv Univeristy "Paisii Hilendarski"*, **27**(6), 1989, 275-285 [In Bulgarian].
15. **Nikolova, M., M. Ilieva.** Somatometric growth differences between boys and girls from 3 to 7 years. – *Scientific Research of Plovdiv Univeristy "Paisii Hilendarski"*, **20**(4), 1982, 351-362 [In Bulgarian].
16. **Pavlov, S., I. Petrov, M. Tzirovski, A. Geshev, T. Matev, M. Nikolova, M. Bachvarova, et al.** On the changes in the body growth of the children from the kindergartens in Plovdiv for the period 1953/1956-1977. – *Pediatrics.*, **1**, 1980, 58-63. [In Bulgarian].
17. **Petraviciene, I., R. Grazuleviciene, S. Andrusaityte, A. Dedele, M. Nieuwenhuijsen.** Impact of the Social and Natural Environment on Preschool-Age Children Weight. – *Int. J. Environ. Res. Public Health*, **15**, 2018, 449.
18. **Stanimirova, N., L. Peneva, C. Baltova.** Physical and puberty development of Bulgarian children from 0 to 18 year of age. Norms and Reference curves. *Books*, Sofia, 2007, 1-118 [In Bulgarian].
19. **Tanner, J. M.** Interaction of heredity and environmental factors in controlling growth. In: *Education and Physical Growth* (Ed. J.M. Tanner), 2nd Edition, London, Hodder and Stoughton, 1978, 90-111.
20. **Tineshev, S., M. Nikolova.** Body diameters in 3-6 years old children from Plovdiv. – *Glasnik Antropološkog društva Srbije*, **48**, 2013, 19-28.
21. **Tsirovski, M.** Growth dynamics of 45 body traits in children from Plovdiv from birth to three years of age. Part I – boys; Part II – girls. – *Scientific Research of Plovdiv Univeristy "Paisii Hilendarski"*, **11** (5), 1973, 261-288 [In Bulgarian].
22. **Wolanski, N.** Genetic and ecological factors in human growth. – *Hum. Biol.*, **42**(3), 1970, 349-368.
23. **World Medical Association Declaration of Helsinki.** Ethical principles for medical research involving human subjects. – *JAMA*, **310**(20), 2013, 2191-2194.
24. **Yankova, I., Y. Zhecheva.** Growth and Proportionality of Body and Extremities' Length during Childhood. – *Acta morphol. anthropol.*, **21**, 2015, 149-153.
25. **Yankova-Pandourska, I., R. Stoev, Y. Zhecheva, A. Dimitrova.** Influence of Economic and Social factors on the Body Dimensions in Newborns. – *Acta morphol. anthropol.*, **26**(1-2), 2019, 121-127.
26. **Yurko, G., L. Veremkovich, O. Silina.** Criteria for assessing the influence of certain environmental factors on the body of preschool children. – *Hygienic aspects of health care for children and adolescents*. Moscow, **1984**, 11-12 [In Russian].
27. **Zhecheva, Y.** Body Weight and Body Composition in Children at the Age of 3-6 Years. – *Acta morphol. anthropol.*, **14**, 2009, 73-80.
28. **Zhecheva, Y.** Waist Circumference as an Indicator of Body Nutritional Status in Children Aged 3 to 6 Years. – *Acta morphol. anthropol.*, **15**, 2010, 230-235.
29. **Zhecheva, Y., I. Yankova.** Body Fat Distribution in Bulgarian Children and Adolescents Estimated by the Conicity Index. – *Acta morphol. anthropol.*, **17**, 2011, 175-181.
30. **Zhecheva, Y., I. Yankova.** Prevalence of Underweight and Overweight among Preschool Children from Sofia Assessed through Different International References. – *Acta morphol. anthropol.*, **24**(3-4), 2017, 53-62.

Eruption of the Permanent Teeth in Bulgarian Children: Preliminary Data

Boyan Kirilov

*Institute of Experimental Morphology, Pathology and Anthropology with Museum, Bulgarian Academy
of Sciences, 1113 Sofia, Bulgaria*

Corresponding author e-mail: drkirilov@yandex.com

The aim of the study is to evaluate the time of the eruption of permanent teeth in children aged 6 – 8 years. A total of 121 subjects aged 6 to 8 years, divided into three age groups were investigated. Height, body weight and cephalometric characteristics - bizygomatic breadth, bigonial breadth, physiognomical, morphological face height, etc. were measured. Dental status – type of bite, number of erupting teeth, carious activity, rotations were determined. The results are processed by the statistical program SPSS 16. The first molars (both upper and lower) and the central lower incisors erupt the earliest at the age of 80 months (6 years and 8 months). The eruption of these teeth is earlier in boys than in girls. Girls tend to have more erupted teeth in the all age groups and earlier eruption of teeth 14, 24, 25, 33, 43, 44. Results are similar compared to other studies.

Key words: eruption, permanent teeth, Bulgarian children

Introduction

The term *eruption* and in particular *tooth eruption* is the process of forming the dental germ, all dental structures and its movements inside the jaw, penetrating the mucosa, appearing inside the mouth and getting or not in contact with its antagonist tooth or teeth. The process of developing of the teeth begins intrauterine in the moment of forming the dental germ and finishes in the teenage years of life with forming of the root system of the last permanent teeth. The eruption of permanent teeth is influenced by various factors: genetics, sex, nutrition, preterm birth; socioeconomic factors; body height and weight; systemic diseases [1]. Tooth eruption is used in forensic medicine for determination of age in cases of identification of an individual; in criminal cases in connection with the offences of rape, kidnapping, and infanticide; in criminal cases involving children, to determine whether the child has reached an age at which the law holds him responsible for his actions [16]. Tooth eruption is also used in paleoanthropology to determine age and life expectancy [9].

The age of tooth eruption is one of the main indicators used to evaluate the biological maturity and morpho-functional status of children. The assessment of the time and sequence of eruption of the different groups of teeth in children allows to establish whether it is normal, retained, retarded or complicated and to take timely measures to optimize their oral health. The eruption of permanent teeth is used in the process of preparing a treatment plan in dentistry and orthodontics [15]. Understanding and knowledge of the processes of normal tooth eruption and its variation is required by each clinician for diagnosing and treatment [14].

The aim of the study is to estimate the time of the eruption of permanent teeth in Bulgarian children aged 6-8 years.

Materials and Methods

The present study includes 121 children – 53 boys and 63 girls, divided into three age groups – 6, 7 and 8 years. The distribution of the subjects by age and sex is presented in **Table 1**.

Table 1. *Distribution of the children by age and sex*

Sex	Count	Age			Total
		6	7	8	
boys	n	15	29	14	58
	% within Sex	25,9%	50,0%	24,1%	
	% within Age	60,0%	42,6%	50,0%	
girls	n	10	39	14	63
	% within Sex	15,9%	61,9%	22,2%	
	% within Age	40,0%	57,4%	50,0%	
Total	n	25	68	28	121

Before starting the examination children and their parents were informed about the purpose of the study. Written informed consent was obtained, in accordance with the ethical principles for medical research involving human subjects in the Helsinki Declaration of World Medical Association [19]. Only children in good general and clinical health were included in the study. The oral and dental status included number of erupted teeth, carious activity and lesions; type of bite, rotations and orthodontic pathology, oral lesions, hypoplasia, dysplasia of the teeth was taken with dental mirror and dental probe. Tooth was registered as erupted when any part of the clinical crown was presented inside the oral cavity. The degree of eruption (from early eruption – only part of the tuberculum or incisive edge presented in the oral cavity to in full occlusion) was also assessed. Some cephalometric characteristics, height and body weight, were also measured by Martin-

Saller's [12] classical method. The statistical analysis was done with the SPSS program 16.0. Frequencies analysis and Pearson Chi-square test were used for determining differences between the sex and age groups.

Results and Discussion

Eruption of teeth 12 (upper right lateral incisor), 11(upper right central incisor), 21 (upper left central incisor), 22 (upper left lateral incisor), 32 (lower left lateral incisor), 42 (lower right lateral incisor) is observed in the children aged 6, 7 and 8 years.

In **Fig. 1** is shown the differences in the eruption of upper right lateral incisor (tooth 12) between the children in the three studied age groups. In the group of 6-year-old boys and girls only 12% have eruptive tooth 12. In the group of 7-year-olds the percentage rises significantly with 26.8% and reaches 38.2%, and in the group of 8-year-olds more than half children (57.1%) have erupted upper right lateral incisor. The increment between the 7 and 8 years is significant too (18.9%).

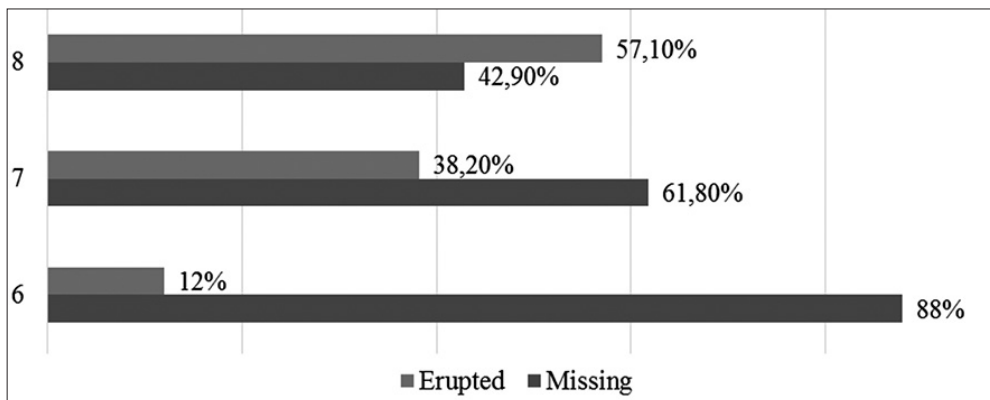


Fig. 1. Age difference in eruption of upper right lateral incisor (12)
 $(\chi^2_{(2, N = 121)} = 11.595, p = .003)$. The size effect is moderate (Cramer's $V = .310$)

In **Fig. 2** is shown the differences in the eruption of upper right central incisor (tooth 11). In the group of 6-year-old boys and girls almost half (48%) have eruptive tooth 11. In the group of 7-year-olds the percentage rises significantly with 29.9% and reaches 77.9%, and in the group of 8-year-olds almost 90 % of the children (89.3%) have erupted upper right central incisor. The increment between the 7 and 8 years is significant too (11.4%).

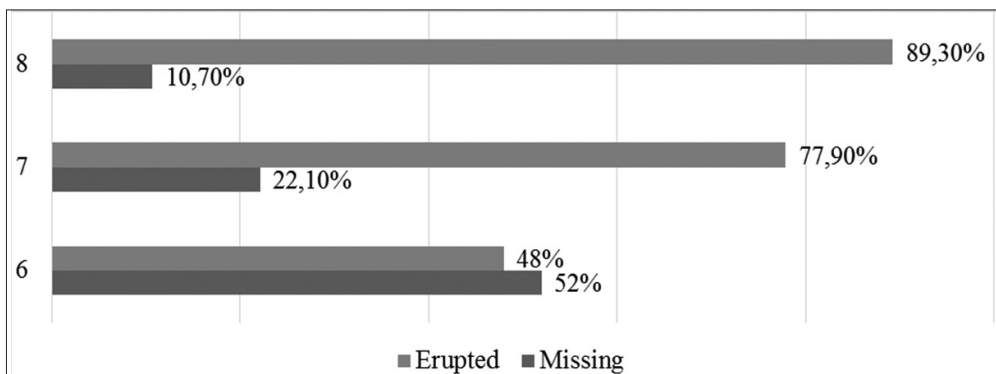


Fig. 2. Age difference in eruption of upper right central incisor (11)
($\chi^2_{(2, N=121)} = 12.847$, $p = .002$). The size effect is moderate (Cramer's $V = .326$)

In **Fig. 3** is shown the differences in the eruption of upper left central incisor (tooth 21). The results are similar with tooth 11. In the group of 6-year-old children half of them (48%) have eruptive tooth 21. In the group of 7-year-olds the percentage rises significantly with 31.4% and reaches 79.4%, and in the group of 8-year-olds 90 % of the children (89.3%) have erupted upper right central incisor. The increment between the 7 and 8 years is also significant (9.9%).



Fig. 3. Age difference in eruption of upper left central incisor (21)
($\chi^2_{(2, N=121)} = 13.546$, $p = .001$). The size effect is moderate (Cramer's $V = .335$)

In **Fig. 4** is shown the differences in the eruption of upper left lateral incisor (tooth 22) between the children in the three studied age groups. In the group of 6-year-old boys and girls only 8% have eruptive tooth 22. In the group of 7-year-olds the percentage rises significantly with 31.7% and reaches 39.7%, and in the group of 8-year-olds more than half children (53.6%) have erupted upper right lateral incisor. The increment between the 7 and 8 years is considerable too (13.9%).

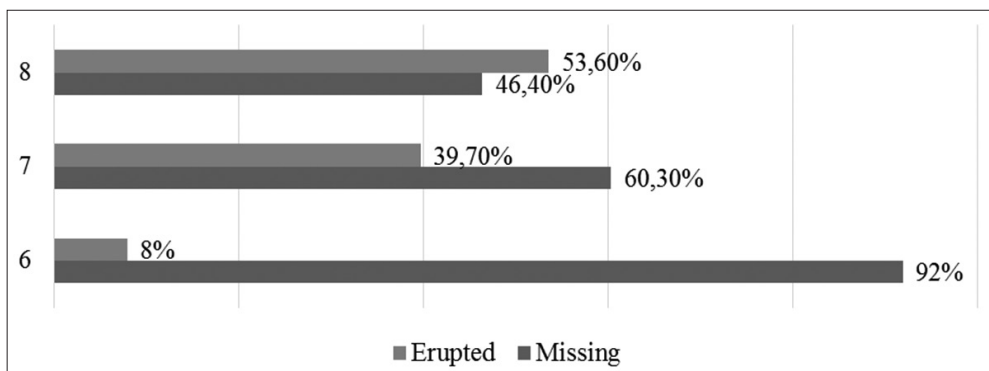


Fig. 4. Age difference in eruption of upper left lateral incisor (22)
($\chi^2_{(2, N=121)} = 12.603$, $p = .002$). The size effect is moderate (Cramer's $V = .323$)

In **Fig. 5** is shown the differences in the eruption of lower left lateral incisor (tooth 32). Twenty four percentages of 6 years old children have eruptive tooth 32. In the group of 7-year-olds the percentage increases significantly with 48.1% and reaches 72.1%, and in the group of 8-year-olds 78.6% of the children have erupted upper right lateral incisor. The increment between the 7 and 8 years is lower 6.5%.

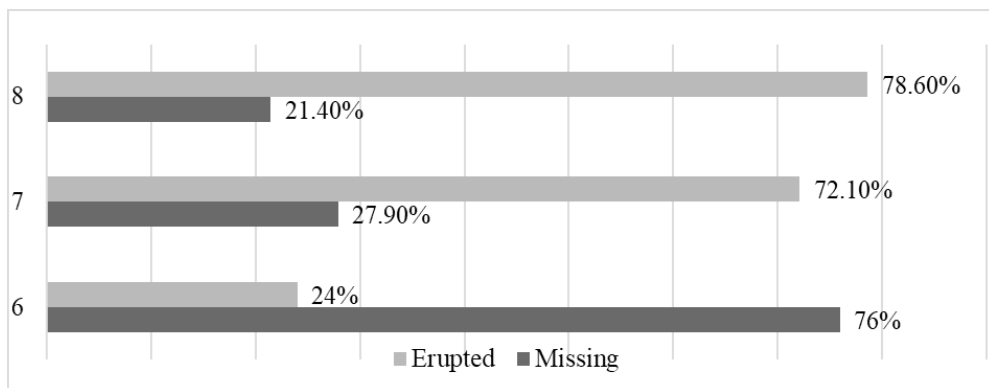


Fig. 5. Age difference in eruption of lower left lateral incisor (32)
($\chi^2_{(2, N=121)} = 21.756$, $p < .001$). The size effect is moderate (Cramer's $V = .424$)

Similar are the results for tooth 42 (lower right lateral incisor) which are presented in **Fig. 6**. Statistically significant differences ($p = .002$) in the eruption between the children in the examined age groups are established. In the group of 6-year-olds boys and girls 28% have eruptive tooth 42. In 7-year-old children the percentage achieves 64.7%, with an increase of 36.7%. In the group of 8-year-olds 71.4% of the boys and girls already have erupted upper right lateral incisor. The increment between the 7 and 8 years is 6.7%.

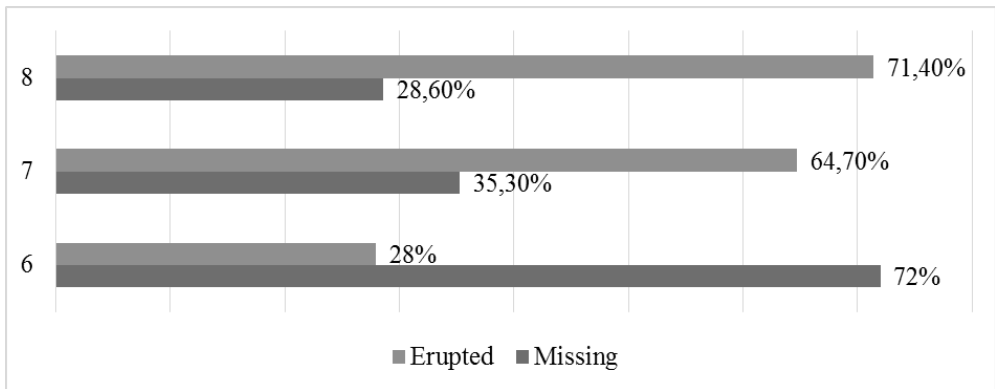


Fig. 6. Age difference in eruption of lower right lateral incisor (42)
 $(\chi^2_{(2, N=121)} = 12.600, p = .002)$. The size effect is moderate (Cramer's $V = .323$)

In **Table 2** are presented the data for percentage of erupted teeth in 6-, 7- and 8-year-olds children, divided by sex.

Table 2. Percentage of erupted teeth in the different age groups divided by sex

Age (years)	Sex	
	Boys	Girls
6	55.5%	60%
7	70.5%	73.9%
8	53.3%	60.5%

The girls have more erupted teeth than boys in all age groups, but the biggest differences is observed at the age of 8 – 7,2%. Similar results are obtained for children from other countries [2, 3, 4, 8, 11, 13, 14].

In the three age groups are presented different erupted permanent teeth (**Fig. 7**). At the age of six, all eight incisors (central and lateral of the two jaws) and the first four molars are erupted. At the age of seven another tooth erupts – the lower right first premolar. The most erupted permanent teeth are established at the age of eight – all incisors (central and lateral), all first premolars, all first molars, lower canines and the upper second left premolar.

The eruption of permanent teeth follows a certain sequence. The earliest permanent teeth to erupt are the central lower incisors and the first upper and lower molars. The age in which they are found to erupt is 80 months (6 years and 8 months). Those cases were in boys. The central lower incisor erupted in half of the children and the molars in all of them, which suggest that molars erupt earlier than the central lower incisors. Similar results are found in other studies performed in Greece [17], Turkey [18], Syria [8],

Fig. 7. Erupted permanent teeth at the different age groups.

6XXX21	12XXX6	6XXX21	12XXX6
6XXX21	12XXX6	6X4X21	12XXX6

Erupted permanent teeth at the age of 6.

Erupted permanent teeth at the age of 7.

6X4X21	12X456
6X4321	1234X6

Erupted permanent teeth at the age of 8.
With “X” are marked the missing teeth

Australia [4], USA [5], Great Britain [7], Lithuania [2], India [6], Spain [10], Uganda [11]. On the other hand at the age of eight years teeth 14, 24, 25, 33, 43, 44 erupt. All of the cases with the mentioned teeth were in girls. Girls tend to have more erupted teeth in all age groups. Dashash and Al-Jazar [8], Carr [4], Almonaitiene [2], Chhabra [6], Kutesa et al [11], Bayrak et al [3], Ogodescu et al [13], Peneva et al [14] present either earlier eruption or more erupted teeth in females.

Table 3 presents the percentage of erupted upper and lower teeth in all age groups in both sexes.

Table 3. Erupted teeth of upper and lower jaws in boys and girls from the three age groups

Teeth	Sex					
	6y		7y		8y	
	Boys	Girls	Boys	Girls	Boys	Girls
Upper molars	83%	95%	91%	95%	100%	100%
Lower molars	93%	100%	90%	97%	100%	100%
Upper central incisors	83%	62%	83%	62%	85%	92%
Lower central incisors	96%	97%	96%	97%	100%	100%
Upper lateral incisors	36%	41%	36%	41%	46%	64%
Lower lateral incisors	62%	73%	62%	73%	67%	67%

The highest percentage of eruptive teeth is observed in the mandible. Other authors obtained similar results - more erupted teeth in the mandible than in the maxilla [2,6,8,10,14].

Conclusion

Tooth eruption is one of the factors to be used when evaluating the process of physical development and it's used by every dental clinician, working with children. The present study shows tendencies for the time, sequence, sex differences in the process of tooth eruption.

The first molars (both upper and lower) and the central lower incisors are the earliest to erupt at the age of 80 months (6 years and 8 months). The eruption of these teeth is earlier in boys than in girls. Girls tend to have more erupted teeth in the all age groups and earlier eruption of teeth 14, 24, 25, 33, 43, 44.

References

1. **Almonaitiene, R., I. Balciuniene, J. Tutkuvienė.** Factors influencing permanent teeth eruption. Part one – general factors. – *Stomatologija*, **12**, 2010, 67-72.
2. **Almonaitiene, R., I. Balciuniene, J. Tutkuvienė.** Standards for permanent teeth emergence time and sequence in Lithuanian children, residents of Vilnius city. – *Stomatologija*, **14**, 2012, 93-100.
3. **Bayrak, S., E. Sen Tunc, N. Tuloglu, A. Acikgoz.** Timing of Permanent Teeth Eruption in Turkish Children – *Int. J. Clin. Pediatr. Dent.*, **37**, 2012, 207-212.
4. **Carr, L. M.** Eruption ages of permanent teeth. – *Aust. Dent. J.*, 1962, 367-373.
5. **Cattell, P.** The eruption and growth of the permanent teeth – *J. Dent. Res.*, **8**, 1928, 279-287.
6. **Chhabra, U., S. S. Sidhu, P. Singhal.** Sequence & eruption of permanent teeth in Punjabi boys & girls – *IAA*, **23**, 1993, 45-51.
7. **Clements, E. M. B., E. Davies-Thomas, K. G. Pickett.** Time of eruption of permanent teeth in british children at independent, rural and urban schools. – *BMJ*, 1957, 1511-1513.
8. **Dashash, M., N. Al-Jazar.** Timing and sequence of emergence of permanent teeth in Syrian schoolchildren. – *J. Invest. Clin. Dent.* 2017, 1-7.
9. **De Bonis, L., L. Viriot.** Teeth and paleoanthropology. – *Connect. Tissue Res.*, **43**, 2002, 87-93.
10. **Hernández, M., E. Espasa, J. R. Boj.** Eruption Chronology of the Permanent Dentition in Spanish Children – *J. Clin. Pediatr. Dent.*, **32**, 2008, 347-350.
11. **Kutesa, A., E. M. Nkamba, L. Muwazi, W. Buwembo, C. M. Rwenyonyi.** Weight, height and eruption times of permanent teeth of children aged 4–15 years in Kampala, Uganda. – *BMC Oral Health*, **13**, 2013, 1-8.
12. **Martin, R., K. Saller.** *Textbook of Anthropology*, Stuttgart, Gustav Fischer Verlag, Band 2, 1959. (Lehrbuch der Anthropologie) [in German].
13. **Ogodescu, A. E., A. Tudor, K. Szabo, C. Daescu, E. Bratu, A. Ogodescu.** Up-to-date standards of permanent tooth eruption in Romanian children. – *Jurnalul Pediatrului*, **14**, 2011, 10-16.
14. **Peneva, M., R. Kabaktchieva, M. Rashkova, E. Tsoleva.** Dynamics of tooth development – In: *Oral Embriology, Hystology and Biology, Book of pediatric dentistry*, Sofia, Iztok-Zapad publishing house, 2009, 141-151 [in Bulgarian].

15. **Sachan, K., V. P. Sharma, P. Tandon.** Reliability of Nolla's dental age assessment method for Lucknow population – *J. Pediatr. Dent.*, **1**, 2013, 8-13.
16. **Sajeev, S.** Permanent tooth eruption and its value in age assessment a study on 290 school children in Tamilnadu. *PhD Thesis*, Madurai medical college, 2008, 1-2 p.
17. **Wedl, J. S., S. Danias, R. Schmelzle, R. E. Friedrich.** Eruption times of permanent teeth in children and young adolescents in Athens (Greece). – *Clin Oral Invest*, **9**, 2005, 131–134.
18. **Wedl, J. S., V. Schoder, F. A. S. Blake, R. Schmelzle, R. E. Friedrich.** Eruption times of permanent teeth in teenage boys and girls in Izmir (Turkey). – *J. Clin. Forensic Med.*, **11**, 2004, 299-302.
19. World Medical Association, Declaration of Helsinki. Ethical principles for medical research involving human subjects. – *WMJ*, **54**(4), 2008, 122-125.

Morphometric Analysis of the Orbital Area in Young Bulgarians with 3D Laser Scanning

Tsvetanka Petleshkova^{1}, Stefan Sivkov¹, Atanas Baltadjiev¹, Hristo Manev², Ralitsa Raycheva³, Pavel Timonov⁴*

¹ Department of Anatomy, Histology and Embryology, Faculty of Medicine, Medical University of Plovdiv, 15A Vassil Aprilov Blvd., 4002, Bulgaria

² Department of Medical Informatics, Biostatistics and E-learning, Faculty of Public Health, Medical University of Plovdiv, 15A Vassil Aprilov Blvd., 4002, Bulgaria

³ Department of Social Medicine and Public Health, Faculty of Public Health, Medical University of Plovdiv, 15A Vassil Aprilov Blvd., 4002, Bulgaria

⁴ Department of Pathologic Anatomy and Forensic Medicine, Faculty of Medicine, Medical University of Plovdiv, 15A Vassil Aprilov Blvd., 4002, Bulgaria

*Corresponding author e-mail: Tsvetanka.Petleshkova@mu-plovdiv.bg

The present study aimed to make a 3D morphometric analysis of the orbital area in young Bulgarians. The study included 95 healthy individuals (46 males and 49 females) of Bulgarian origin aged 21-30 years. Three-dimensional coordinates of soft-tissue landmarks were determined in the orbital area using hand-held laser scanner. Using the landmarks outer canthal and intercanthal distances were measured. The individuals were categorized according to the measurements obtained for each distance. In the intercanthal distance most of the males were in the category middle and females in the category narrow. In the outer canthal distance most of the males were in categories wide and very wide and females in the category wide. Statistically significant differences between sexes were found in three categories of the outer canthal distance – middle, wide and very wide ($p < 0.05$). The method provides quantitative information for anatomical and anthropometric descriptions, medical evaluations, and forensic medicine.

Key words: orbital measurements, 3D laser scanning, categorization

Introduction

The age, gender, and ethnic characteristics of the various components of facial morphology have been the subject of numerous anthropometric studies aimed to create a database that will be useful for scientists or other medical professionals. Many of the studies are focused on the study of the orbital area. Orbitofacial anthropometry plays a key role in the assessment of dysmorphic syndromes, hypertelorism, facial injuries, in the diagnosis of abnormalities of the neural crest [11]. Deference values characterizing

this area have been established for different ethnic groups and races: Chinese men and women [5], Italian [3, 12], Sudanese, [13], Egyptian [1], Indian [11], Pakistani [4] and Turkish [2]. Data on the morphology of the orbital region in different age groups of the Bulgarian population were obtained by the methods of classical direct cephalometry [6, 7, 8,17]. In this method, the measurement in the orbital area is applied with the help of sliding calipers. Measurements with such sharp instruments near the orbital region may pose some risk, especially when interacting with examinations in very young or non-connecting patients [5]. With the advent of new computer technologies, it is possible to create three-dimensional digital images of the face, in which it is possible to make a quantitative analysis of the volume and area of individual facial structures – eyes, nose, mouth and lips, chin and ears. Digital cephalometry is a fast and non-invasive method that avoids the compression of soft tissues, the possibility of making mistakes when repeatedly collecting data from the subjects. [14]. Different methods for acquiring digital images are used in other areas of physical anthropology, such as craniometry [9, 10] and forensic medicine [16]. The **aim** of this study is to make a morphometric characteristic of the orbital region and to report the most common orbital categories among young Bulgarians using 3D laser scanning.

Material and Methods

Subjects: Ninety-five healthy Bulgarians (46 males and 49 females) aged 21-30 years were included in the study. Individuals with ethnicity different from Bulgarian, history of facial injury, craniofacial anomalies and mental disorders were excluded from the study. The participants were previously informed about all the procedures and gave their consent to participate in the study.

Collection of three-dimensional landmarks: Three-dimensional images were obtained using a hand-held laser scanner (FastSCAN Cobra, Polhemus Inc., Colchester VT). On each of the obtained images a set of 3D anthropometric landmarks were placed bilaterally: exocanthion – (ex_r, ex_l); endocanthion – (en_r, en_l) [15] (**Table 1**). The procedure was performed by a single operator (**Figure 1**).

Table 1. Description of the landmarks

Landmarks	Description
Endocanthion – (en _r , en _l)	The point located on the outer corner of the eye of each of the eye fissure.
Exocanthion – (ex _r , ex _l)	The point located on the inner corner of the eye of each of the eye fissure.

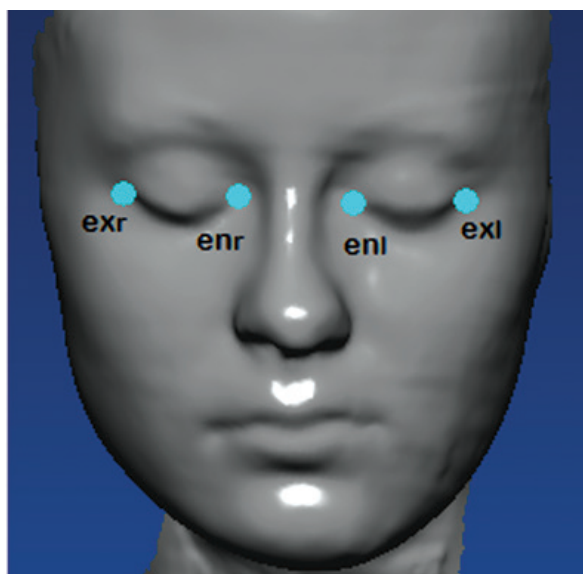


Fig. 1. Three-dimensional images.

Data analysis: Using these three-dimensional landmarks the intercanthal distance ($en_r - en_l$) and outer canthal distance ($ex_r - ex_l$) were measured (mm) (**Table 2**). Based on the measurements obtained for the intercanthal distance (en-en) the individuals were divided into five groups (after M. Popov)(cited by 17):

– very narrow	x-27 mm
– narrow	28-33 mm
– middle	34-39 mm
– wide	40-45 mm
– very wide	46-x mm

Based on the values obtained for the outer canthal distance (ex-ex) the individuals were divided into five groups (after M. Popov):

– very narrow	x-69 mm
– narrow	70-79 mm
– middle	80-89 mm
– wide	90-99 mm
– very wide	100-x mm

Statistics: Data were analyzed using descriptive statistics (mean±standard deviation / proportion±standard error), t-test (numeric variables) and z-test (categorical variables). Level of significance was set at $p < 0.05$.

Table 2. Description of the measurements

Measurements	Description
Intercanthal distance (en_r-en_l)	The linear distance between the two points endocanthion – right and left
Outer canthal distance (ex_r-ex_l)	The linear distance between the two points exocanthion – right and left

Results

The results of the categorization in the outer canthal and intercanthal distance for males and females are shown in **Tables 3-5**.

In the intercanthal distance most of the males fell in the categories middle and narrow (54.3% and 41.3%, respectively). In the category wide intercanthal distance males appeared in small percentage (4.3%). No individuals fell in the categories very narrow and very wide intercanthal distance. Most of the females were in the categories narrow (53.1%) and middle (44.9%). Only 2.0% of the females fell in the category wide and none in the categories very narrow and very wide. No statistically significant difference in the categories was found between males and females ($p > 0.05$).

The results from the categorization of the outer canthal distance in males showed that most of them fell into the categories wide and very wide (52.2% and 45.7%, respectively). The percentage of subjects in the category middle was small (2.0%), and no subjects were found in the categories narrow and very narrow.

In the females most of the subjects were in the category wide (75.5%). In the categories middle and very wide the females appeared in close percentages (14.3% and 10.2%, respectively). No subjects fell in the categories narrow and very narrow. Statistically significant differences between both sexes were found in three of the categories – middle, wide, and very wide ($p < 0.05$).

Table 3. Linear measurements in the orbital region

Variable (mm)	Sex	Mean	SD	Min	Max	Statistical significance
Intercanthal distance en_r-en_l	males	34,14	3,17	27,57	41,69	$p > 0,05$
	females	33,59	2,74	27,72	40,48	
Outer canthal distance ex_r-ex_l	males	98,85	5,00	89,05	113,72	$p < 0,001$
	females	94,59	4,04	84,32	103,54	

Table 4. Intercanthal distance (enr-enl). Distribution of the individuals into categories (after M. Popov)

Categories	Males %	Females %	p
very narrow	0	0	p> 0,05
narrow	41,3	53,1	p> 0,05
middle	54,3	44,9	p> 0,05
wide	4,3	2,0	p> 0,05
very wide	0	0	p> 0,05

Table 5. Outer canthal distance(exr-exl). Distribution of the individuals into categories (after M. Popov)

Categories	Males %	Females %	p
very narrow	0	0	p> 0,05
narrow	0	0	p> 0,05
middle	2,2	14,3	p< 0,05
wide	52,2	75,5	p< 0,05
very wide	45,7	10,2	p< 0,05

Discussion

The results obtained by us in the distribution by categories showed that most of the males were with middle intercanthal distance and females with narrow. In both sexes, the subjects did not fall into the extreme categories very wide and very narrow. Most of the females presented with wide outer canthal distance, while males presented with close values for the categories wide and very wide. Statistically significant difference in the distribution by categories between sexes was found in the outer canthal distance.

To validate the three-dimensional (3D) laser scanning system in recording the facial morphology, the results of our study were compared with the results of a national study (17) including adult individuals of Bulgarian origin, aged between 30 and 40 years. The validation was performed in three aspects including accuracy, precision and reliability.

In the intercanthal distance in both studies most of the males fall into the category middle, 54.3% and 56.7% respectively. In the category narrow males appear in close percentages (41.3% and 35.4%, respectively). The percentage of males in the category wide is low – 4.3% in our study and 5.7% in the control study. In both studies, no males fall into the category very wide. The highest percentage of males and females fell into the categories narrow and middle intercanthal distance. The females are in high percentage in the category narrow – 53.1% in our study and 49.0% in the control study. In the category middle intercanthal distance the percentages of the females were 44.9% and 44.7%, respectively. In the category wide intercanthal distance the percentage of females was very low in both studies (2.0% and 1.6%, respectively). In both studies, no females fell in the category very wide intercanthal distance and 4.7% of females from the previous study fell into the category very narrow.

In the outer canthal distance in both studies, the most of the males fall into two of the categories – wide and very wide. In the category very wide outer canthal distance the percentage of males in our study is 45.7%, and 43.4% in the control study. In the category wide outer canthal distance males appear equally in both studies – 52.2%. The percentage of males in the category middle outer canthal distance is very low -2.2% in our and 4% in the control study. In both studies no subjects are found in the categories very narrow and narrow. In the females most of subjects in both studies fall into the category wide outer canthal distance – 75.5% in our study and 65.4% in the control study. In the categories middle and very wide intercanthal distance, the percentages of females are lower in both studies. In the category of middle outer canthal distance the females appear in 14.3% in our study and in 18.1% in the control one, and in the category very wide in 10.2% and 16.2%, respectively. In both studies, no females fall into the category very narrow, while in the category narrow, no subjects are found in our study and only 0.2% of the subjects in the control study.

Conclusion

The categorization in the outer canthal distance shows that most of the males and females are with wide outer canthal distance. In terms of intercanthal distance most of the males fall in the category middle, and females in the category narrow. Sexual dimorphism is found only in the outer canthal distance. The results of the categorization are similar with the literature data for both sexes suggesting that the 3D laser scanning system is accurate, precise, and reliable to record the facial morphology for both clinic and research purposes.

References

1. **Abdel-Rahman, R. H., S. G. Amr, A. A. Khalil.** Sexual Dimorphism of Anthropometric Measurements of Periorbital Soft Tissues in a Sample of Egyptian Adults. – *Mansoura J. Forens. Med. Clin. Toxicol.*, **27**(1), 2019, 13-25.
2. **Bozkir, M. G., P. Karakaş, O. Oğuz.** Measurements of soft tissue orbits in Turkish young adults. – *Surg. Radiol. Anat.*, **25**(1), 2003, 54-57.
3. **Celebi, A. A., C. H. Kau, F. Femiano, L. Bucci, P. Perillo.** A three-dimensional anthropometric evaluation of facial morphology. – *J Craniofac. Surg.*, **29**(2), 2018, 304-308.
4. **Hayat, N., S. Alkhairy, A. Cheema, M. Ehsan, M. A. Khan.** Normal interpupillary, inner canthal distance and outer canthal distance in a normal population of Pakistan. – *Pak. J. Med. Sci.*, **35**(1), 2019, 50-54.
5. **Jayaratne, Y. S., C. K. Deutsch, R. A. Zwahlen.** Normative findings for periocular anthropometric measurements among Chinese young adults in Hong Kong. – *Biomed. Res. Int.*, 821428, 2013.
6. **Madjarova, L. M., M. M. Madzharov, L. G. Farkas, M. J. Katic.** Anthropometry of soft tissue orbits in Bulgarian newborns: norms for incanthal and bicular widths and length of palpebral fissures in 100 boys and 100 girls. – *Cleft Palate-Craniofac. J.* **36**, 1999, 123-126.
7. **Nacheva, A., J. Zhecheva, I. Yankova, Z. Filcheva, Z. Mitova, Y. Yordanov.** Physical development of Children and Youths in Bulgaria on the Borderline between 20th and 21st century. Sofia, Prof. Marin Drinov Academic Publishing House, 2012.[in Bulgarian]

8. **Nikolova, M., S. Mladenova.** Changes in head and face morphology of Plovdiv children and adolescents in three successive generations. – *Human Ecology*, **1**, 2003, 197-199.
9. **Nikolova, S., D. Toneva, I. Georgiev.** Cranial base angulation in metopic and non-metopic cranial series. – *Acta morphol. anthropol.*, **24**, 2017, 45-49.
10. **Nikolova, S., D. Toneva, A. Dandov.** Digital Morphometric Analysis and Comparison of Orbital Region in Metopic and Non-metopic Cranial Series. – *Acta morphol. anthropol.*, **27**, 2020, 53-60.
11. **Radha, K., K. R. Srinivasan.** Anthropometric Assessment of Canthal Distances and Canthal Index of South Indian Region: A Cross-Sectional Study. - *Medico-legal Update*, **21**, 2021, 794-797.
12. **Sforza, C., G. Grandi, F. Catti, D. G. Tommasi, A. Ugolini, V. F. Ferrario.** Age-and sexrelated changes in the soft tissues of the orbital region. – *Forensic Sci. Int.*, **185**(1-3), 2009, 115.
13. **Sforza, C., F. Elamin, D. G. Tommasi, C. Dolci, V. F. Ferrario.** Morphometry of the soft tissues of the orbital region in Northern Sudanese persons. – *Forensic Sci Int.*, **228**(1-3), 2013, 180.e1-11.
14. **Sforza, C., V. Ferrario.** Soft-tissue facial anthropometry in three dimensions: from anatomical landmarks to digital morphology in research, clinics and forensic anthropology. – *J. Anthropol. Sci.*, **84**, 2006, 97-124.
15. **Swennen, G. R. J., F. Schutyser, J. E. Hausamen.** Three-Dimensional Cephalometry: a Color Atlas and Manual. Heidelberg: Springer, 2006
16. **Timonov, P.** Determination of sex by femur in the Bulgarian population. *PhD thesis*, Medical University, Plovdiv, 2014, 115-117.
17. **Yordanov, Y., A. Nacheva, S. Tornjova-Randelova, N. Kondova, B. Dimitrova, D. Paskova-Topalova.** Anthropology of the Bulgarian Population at the end of the 20th century (30-40 years old persons). Sofia, Professor Marin Drinov Academic publishing house, 2006.

Intra and Inter-Sexual Variation in Second (2D) and Fourth (4D) Digit Length and Ratio (2D:4D) among the Bhantus of Andaman and Nicobar Islands, India: A Cross-sectional Study

Koel Mukherjee^{1*}, Kaustav Das²

¹ Anthropological Survey of India, Andaman and Nicobar Regional Centre, Port Blair, India

² Department of Anthropology, Bangabasi College, Kolkata, India

*Corresponding author e-mail: koelanthro@gmail.com

This study aimed to determine sex and bilateral variation from digit length and ratio among the Bantu people living in the Andaman and Nicobar Islands of India. Total of 305 adults aged 18-60 years were included. Required anthropometric measurements were taken following standard techniques. Based on digit ratio, hand pattern was classified into three types: A ($2D < 4D$), B ($2D = 4D$), and C ($2D > 4D$). Results revealed males have longer mean 2D and 4D lengths than females. Hand pattern A was the predominant characteristic in this population. Significant bilateral variation was found in 4D length ($p < 0.01$) and 2D:4D ($p < 0.05$) ratio of females, but not in males. Unlike other studies, the 2D:4D ratio did not show any sex variation, statistically significant sex differences ($p < 0.01$) were observed for only digit lengths in both hands but not in digit ratio. Further studies should be conducted on a larger sample and different populations.

Key words: 2D (index finger), 4D (ring finger), 2D:4D (digit ratio), Hand pattern, Bantu

Introduction

Biomarkers are emerging emphases in persistent disparities and global challenges in health that readily ally with human biology and anthropology. They have proven to be valuable tools for investigating biocultural pathways to health and disease and can be used to probe the causal matrix generated by cumulative socially determined circumstances, lifetime experience and exposures, and biodynamics that shape health over the life course [10, 48]. For a long time, several anthropologists put efforts to contemplate the substantial well-demarcated differences in ethnic groups by utilizing various biomarkers and perceive the full range of mechanisms through which ethnicity and their ancestry can correlate with numerical biological traits and health outcomes [7].

For the last couple of decades, researchers use the second (2D, index finger) to fourth (4D, ring finger) digit ratio (2D:4D) as a potential proxy marker showing variations in different ethnic and geographic groups [8, 17, 33, 42, 50, 55, 60, 83]. Existing literature proposed a relationship between prenatal androgen exposure and the length of the digit [38, 42, 65]. The 2D:4D ratio is assumed to be stable during the prenatal stage or after two years of age, which become constant throughout life [15, 38, 42, 51, 65]. It has been seen that the digit ratio is negatively correlated with testosterone but positively to estrogen exposure, which means males are expected to have a comparatively lower 2D:4D ratio than females [42, 60, 65]. Thus, it has been well established that the 2D:4D ratio is sexually dimorphic in humans [21, 42], but the developmental mechanism underlying sexually dimorphic digit development remains unknown [85].

In addition to the significant sexual dimorphism [3, 21, 22, 37, 42, 82], several studies revealed evidence of the relationship between 2D:4D ratio and various human phenotypic traits [6, 56]. The low 2D:4D is showing a correlation with left-handedness [44, 75], increased risk of anxiety [43], heterosexual preference [15], aggression in males [49, 75], and females [5], etc. On the other hand, studies also revealed high 2D:4D had been linked with increased risk of heart diseases [56], low sperm count [44], preference of homosexuality [15], risk of obesity [56], etc. Despite these findings, androgen-related outcomes like increased risk of autism [39], psychiatric disorder [14], facial asymmetry [11], enhanced athletic ability [46] have also been found associated with digit ratio. In recent years, researchers also explored the use of the 2D:4D ratio in the field of medical sciences to diagnose breast cancer risk, lung cancer, risk of severe osteoarthritis, and brain tumour [4, 20, 27, 29].

In India, the studies on digit lengths and ratios are mostly conducted to explore population variation in ethnicity and sex among different communities [8,28,33,69]. Further, numerous studies have also been done to find out the association of digit ratios with physical attributes [21,25], body composition indicators [41], coronary heart disease [84], dental carries [62], polycystic ovarian syndrome [67], myopia [34], preliminary infertility in males [35], depression [24], dyslexia [63], schizophrenia [77], effect on birth order [40], performance and ability of sportspersons [72], stature estimation [23,70], etc.

Andaman and Nicobar Islands have a long history of human occupation with remarkable ethnic and cultural diversity. It has three strands- several tribal groups, descendants of criminals under sentence of transportation for life from India and Burma, and immigrants after the 1947 partition of India [78]. Therefore, Andaman is home to people from different regions, religions, languages, castes, and cultures who migrated from different parts of the mainland during the 20th century [26]. Bantus are originally the inhabitants of Uttar Pradesh, India. But due to their criminal activities of theft and robbery like neighboring communities of Bauriyas, Karwals, Sansiyas, they were also declared as “*Criminal Tribe*” by the British Government [80], and many of them were sent to the Cellular Jail of Andaman for imprisonment during the 1920s [53,68]. After their punishment period, many were settled in the Andaman Islands [53]. However, to the best of our knowledge, no study has been conducted to investigate ethnic or sex variation among any community living in the Andaman or any other islands in India.

Therefore, given the present situation, this research work is the first attempt to: a) study bilateral variation as well as sex variation from digit lengths and their ratio and b) examine the association of age, anthropometric, and derived variables with the 2D:4D ratio among the Bantu community living in Andaman and Nicobar Islands, India.

Materials and Methods

This community-based cross-sectional study was conducted among 305 adult Bhanu individuals (males: 134; females: 171) aged 18-60 years residing in the rural areas of South Andaman district, Andaman and Nicobar Islands, India. The present study was carried out during July-August 2019. Necessary permissions had been obtained from local administration, and the community leaders were informed before initiating the study. Only those volunteers were considered having no physical disability, previous history of surgical episodes, and apparently healthy at the time of the investigation. They were explained about the objectives of this study, and consent was obtained from them. This work was carried out following the principles of the Declaration of Helsinki.

All the anthropometric measurements were taken following the standard protocol [81]. A sliding calliper was used to measure the length of the 2D and 4D of both hands. Before performing the hands' measurements, participants were asked to free their fingers for any rings or jewellery. The length was measured on 2D and 4D from the finger's tip to the base (most proximal to palm) on the ventral surface of the hand without putting any pressure on the fingers. Matrin's anthropometer rod and Omron Body composition Monitor (HBF-212) machine were used to measure the height (cm) and weight (kg) of the individuals. Hip (cm), waist (cm), and neck (cm) circumferences were measured by using calibrated, non-elastic fiber tape. Body mass index (BMI) was computed using the formula of $BMI = \text{weight (kg)} / \text{height (m)}^2$. The waist-to-hip ratio (WHR) and 2D:4D ratio of both hands were also calculated. Based on digit ratio, hand pattern was classified into three types: A ($2D < 4D$), B ($2D = 4D$), and C ($2D > 4D$).

The statistical analysis was performed in the Statistical Package for Social Sciences software (SPSS, IBM; version 26.0). Descriptive statistics of mean, standard deviation (SD), range, and standard error of the mean (SE) were generated for age and all anthropometric and derived variables. Chi-square test (χ^2) was applied to find out the significant difference in the prevalence of different hand patterns in both hands of all the participants. Paired *t*-test and independent-sample *t*-test have been performed to test mean differences in digit lengths and their ratios in both hands within and between sexes. Pearson correlation was also carried out to see the relationship between 2D:4D ratios, age, anthropometric, and derived variables. The *p* values of <0.01 and <0.05 were considered to be statistically significant.

Results

Table 1 depicted the descriptive statistics of age; anthropometric variables such as height (cm), weight (kg), waist circumference (cm), hip circumference (cm), neck circumference (cm); derived variables like BMI (kg/m^2) and WHR; and length of the 2D, 4D and their ratios (2D:4D) in both hands among the study population of either sex. The mean age of both males (40.17 ± 14.96 years) and females (40.05 ± 16.13 years) was similar. Except for hip circumference, all anthropometric variables had shown higher mean values in males than females. For BMI, females showed a comparatively higher mean value ($24.21 \pm 5.16 \text{ kg/m}^2$) than males ($23.30 \pm 4.10 \text{ kg/m}^2$). On the contrary, males

Table 1. Descriptive statistics of age, anthropometric variables, 2D and 4D length and their ratios of both hands of males and females among the Bantu community

Sex	Variables		Mean	SD	Minimum	Maximum	SE
Male (n= 134)	Age (years)		40.17	14.96	18.00	60.00	1.293
	Height (cm)		167.97	6.07	150.70	188.50	.524
	Weight (kg)		65.85	12.698	40.40	99.10	1.096
	Waist Circumference (cm)		85.39	12.965	53.50	116.60	1.128
	Hip Circumference (cm)		91.16	7.716	70.10	108.00	.671
	Neck Circumference (cm)		34.81	2.776	28.70	42.50	.244
	BMI (kg/m ²)		23.30	4.108	14.25	34.09	.354
	WHR		.933	.091	.63	1.15	.007
	Right hand	2D (cm)	6.72	.401	5.60	8.20	.034
		4D (cm)	6.84	.409	5.70	8.10	.035
	Left hand	2D (cm)	6.74	.409	5.60	8.20	.035
		4D (cm)	6.84	.386	6.00	8.20	.033
	Right hand	2D:4D	.983	.045	.87	1.12	.003
	Left hand	2D:4D	.985	.037	.86	1.08	.003
Female (n= 171)	Age (years)		40.05	16.13	18.00	60.00	1.233
	Height (cm)		153.76	6.95	133.50	172.00	.532
	Weight (kg)		57.16	12.33	33.00	96.50	.943
	Waist Circumference (cm)		81.13	12.57	51.00	112.00	.967
	Hip Circumference (cm)		92.14	10.30	66.40	123.00	.792
	Neck Circumference (cm)		30.62	2.45	25.50	39.80	.188
	BMI (kg/m ²)		24.21	5.16	13.58	43.94	.394
	WHR		.878	.076	.70	1.12	.005
	Right hand	2D (cm)	6.22	.391	5.50	7.30	.029
		4D (cm)	6.34	.379	5.50	7.40	.029
	Left hand	2D (cm)	6.21	.389	5.20	7.20	.029
		4D (cm)	6.29	.397	5.30	7.30	.030
	Right hand	2D:4D	.980	.046	.63	1.08	.003
	Left hand	2D:4D	.988	.037	.90	1.09	.002

demonstrated a higher mean value of WHR (0.933 ± 0.091) than females (0.878 ± 0.076). In case of digit lengths, males have longer mean 2D and 4D than females in both hands, and particularly, mean 4D was found greater than mean 2D in both males and females. Digit ratio was higher in the left hand (male: 0.985 ± 0.037 ; female: 0.988 ± 0.037) compared to the right hand (male: 0.982 ± 0.045 ; female: 0.980 ± 0.046) among both males and females.

According to the hand pattern based on sex, the distribution of the studied population has been represented in **Table 2**. For both hands, pattern A ($2D<4D$) showed the highest frequency in both sexes, followed by Pattern B ($2D=4D$). Interestingly, on the right hand, pattern C ($2D>4D$) showed a slightly higher frequency in males (27.6%) than females (22.2%) and a reverse trend in the left hand (females: 32.2%; males: 25.4%). The overall result of the hand pattern demonstrated statistically non-significant differences between sexes.

Table 2. Distribution of studied population according to the hand pattern based on sex

Sex	Hand Pattern [Right hand]			χ^2	Hand Pattern [Left hand]			χ^2
	A [2D<4D]	B [2D=4D]	C [2D>4D]		A [2D<4D]	B [2D=4D]	C [2D>4D]	
Male (n = 134)	77 (57.5)	20 (14.9)	37 (27.6)	1.415 ^{NS}	74 (55.2)	26 (19.4)	34 (25.4)	4.157 ^{NS}
Female (n = 171)	109 (63.7)	24 (14.0)	38 (22.2)		96 (56.1)	20 (11.7)	55 (32.2)	

Percentages are presented in the parentheses; NS= Statistically not significant

Table 3 presented the bilateral variation in 2D, 4D length and their ratios of the study participants. Paired *t*-test revealed no significant differences between right and left hands of males in 2D ($t = -1.012$, $p = .313$), 4D ($t = -0.309$, $p = .757$), and 2D:4D ($t = -0.341$, $p = .734$). On the other hand, in females, except 2D ($t = 0.444$, $p = .888$) comparison of both 4D ($t = 3.817$, $p = .000$) and 2D:4D ($t = -2.379$, $p = .018$) between right and left hand showed statistically significant differences.

Independent sample *t*-test revealed significant differences in digit lengths of both hands; right 2D ($t = 10.894$, $p = .000$) and 4D ($t = 10.941$, $p = .000$), as well as left 2D ($t = 11.360$, $p = .000$), and 4D ($t = 12.157$, $p = .000$) between the sexes. But 2D:4D ratios of both hands were found non-significant (**Table 4**).

Pearson correlation coefficient for the relationship between 2D:4D ratios, age, anthropometric, and derived variables was exhibited in **Table 5**. The right-hand 2D:4D ratio of females revealed a statistically significant positive correlation with height (0.205 , $p<0.01$). Other than that, no significant relationship was found between digit ratios and age and other anthropometric variables for both Bantu males and females. It has been observed that neck circumference was negatively correlated with the 2D:4D ratio for both males and females but in opposite hands (males: left hand; females: right hand). Except for neck circumference, other variables were found positively correlated with 2D:4D in both hands for males. For females, age and WHR were also negatively correlated with the 2D:4D ratio in both hands.

Table 3. Bilateral symmetry of 2D, 4D length and their ratios among the studied participants

Sex		2D	4D	2D:4D
Male (n = 134)	Mean	- 0.017	- 0.005	- 0.001
	SD	0.204	0.223	0.040
	<i>t</i>	- 1.012 ^{NS}	- 0.309 ^{NS}	- 0.341 ^{NS}
Female (n = 171)	Mean	0.006	0.044	- 0.008
	SD	0.191	0.152	0.044
	<i>t</i>	0.444 ^{NS}	3.817**	- 2.379*

NS= Statistically not significant; **p<0.01, *p<0.05

Table 4. Occurrence of sex variation in the studied population

2D		Right hand		Left hand		2D:4D	
		4D	2D	4D	Right hand	Left hand	
95% CI	Lower	0.407	0.410	0.431	0.461	-0.007	-0.120
	Upper	0.587	0.590	0.612	0.640	0.013	0.005
<i>t</i>		10.894*	10.941*	11.360*	12.157*	0.628 ^{NS}	-0.804 ^{NS}

NS= Statistically not significant; *p<0.05

Table 5. Pearson correlation coefficients for the relationship between 2D:4D ratios, age and anthropometric variables

Variables	Male (n= 134)		Female (n= 171)	
	Right hand	Left hand	Right hand	Left hand
	2D:4D	2D:4D	2D:4D	2D:4D
Age	.060	.059	-.085	-.093
Height	.033	.065	.205**	.059
Weight	.083	.051	.137	.079
Waist circumference	.089	.098	.030	.037
Hip circumference	.042	.028	.079	.089
Neck circumference	.032	-.073	-.115	.064
WHR	.090	.128	-.060	-.035
BMI	.068	.026	.046	.053

**p<0.01

Discussion

The digit length and ratio are complex and multifactorial traits resulting from an intriguing combination of ‘*nature*’ and ‘*nurture*’, the unique reciprocal interaction between environment, genetic, etc., each contributing to the overall phenotype. In this backdrop, it is of utmost necessity to explore the distinctive biological variations reflecting both the significance and complexity of genetic heritage among the various ethnic groups living in different environmental conditions. Therefore, the present study was conducted among Bhantu adult individuals of Andaman and Nicobar Islands of India to determine intra-sexual and inter-sexual variation from digit lengths and ratios. Besides that, the association between 2D:4D with age, anthropometric, and derived variables was also explored. Many studies from India and abroad have already established differences between sexes in the absolute length of 2D and 4D [28,33,37,69,82]. Generally, males have longer 2D and 4D than females [28,33,69], and the present study also exhibits similar trends. In case of hand pattern, pattern A ($2D < 4D$) was found dominant for both hands among the study population. The findings are similar to previous studies involving different populations from countries like Nigeria [17], China [83], Italy and Romania [74], India [69], and Malaysia [55]. Again, in India, among the females, an opposite trend ($2D > 4D$) has also been found from the north Indian [8] and the north-west Indian population [22]. On the other hand, Setiya et al. exhibited equal digit lengths ($2D = 4D$) among female medical college students in Madhya Pradesh [71]. However, fluctuations in 2D, 4D lengths, and ratios in females possibly due to changes in hormonal levels during the menstrual cycle was reported by Mayhew et al. [50]. On the contrary, a similar study from rural Poland failed to confirm the result and found no differences in digit lengths and ratios of both hands across the menstrual cycle [30]. Among males, the presence of longer 4D compare to 2D was in concurrence with the findings of Nayek et al. [55], Setiya et al. [71], and Sen et al. [69,70].

Furthermore, statistically significant bilateral variation was found in the 4D length and 2D:4D ratio among females corroborating with the earlier studies [8,32,50]. However, males did not show any bilateral variations in the digit lengths and ratio in this study, similar to the study of Paul et al. [58], Gillam et al. [64], and Robertson et al. [65]. In contrast, others have evidence of significant bilateral variation among males [62,76].

Typically, it has been seen that the 2D:4D ratio is lower in males than females [42,45,82]. The probable reason behind this phenomenon is the relationship between digit ratio and prenatal androgen exposure, specifically, a lower 2D:4D is correlated with the presence of a high level of testosterone, a characteristic feature of males, while a higher 2D:4D ratio correlates with a low level of testosterone, a distinctive feature of female [22,42]. While the exact reason is unclear, it was argued that Hox gene might influence the differences in both the digits and genitals in mammals [16,38,42]. Several hormones like estradiol, progesterone, testosterone, etc., and their cognate receptors have been seen to regulate Hox gene expression [36,61]. Nevertheless, no significant sexual dimorphism was observed in 2D:4D ratios in this study which contradicts many previous studies. Similar findings were also observed among the Zulus [45], Dutch [64], Austrians [79], Hadza hunter-gatherers [2], and Yali of Papua [47]. A probable reason

behind no sexual differences in digit ratio among these populations may be due to the harsh environmental conditions that lead to more competition irrespective of sexes [47]. Even other studies at the molecular level did not support the hypothesis that digit ratio is related to prenatal androgen exposure [18,52] or adult testosterone levels [19,31]. Thus, there is scope for future studies focussing on comprehensive historical perspective as well as gene-environment interaction in studying digit ratios.

Additionally, the present study also investigated the relationships between digit ratios and anthropometric variables in the studied population. Only right-hand 2D:4D of females have shown a positively significant (0.205, $p < 0.01$) correlation with height among all the anthropometric and derived variables. This finding is similar to the work of Lippa where a positive significant correlation was observed between height and digit ratio in both hands of females, not males [37]. Previous literature showed variations in results, where no significant correlation of height with 2D:4D has also been reported by many researchers [13,21,42,54]. While some other researchers reported a significant negative association between height and digit ratios [3,73]. Except for height, there was no significant correlation between digit ratio and other anthropometric variables in the present study. In accordance with the findings of Barut et al. [3], Muller et al. [54], and Jacob et al. [21], it was found that the 2D:4D ratio had no relationship with weight. Again, in this study, waist and hip circumferences were found non significantly associated with 2D:4D for both males and females, same as the findings of Muller et al. [54]. On the other hand, Fink et al. found a negative association between 2D:4D (both hands) and waist and hip circumferences in females [13]. However, other studies also produced similar trends in males [9,12]. Previous studies showed inconsistent results for BMI, where no significant association between digit ratio and BMI has been reported like the present study [21,25,41,54]. However, Fink et al. noted a significant positive relationship between BMI and digit ratio in the left hand of males [13]. In accord with the study of Jeevanandam and Prathibha [25], neck circumference did not reveal any statistically significant correlation with digit ratio. This was contradictory to previous works where a significant positive correlation was found between the digit ratio and neck circumference of males only [1,12]. In case of WHR, earlier works [13,41] did not show any significant relation with digit ratio, as in the present study. As studies revealed an independent association of WHR and neck circumference with obesity and risk of heart disease so the use of digit ratio may be indicative for being overweight in females and suggests a predisposition toward cardiovascular disease [1,57,59].

Conclusion

The present study was unique as it was probably the first presentation of information on sexual dimorphism, intraindividual variation from digit length, and their ratio of both sexes in Bhantus of Andaman. Sexual dimorphism was only seen in digit lengths, not in the digit ratio, indicating no consensus on the intra-sexual and inter-sexual variations in digit ratios and traits across various ethnic groups. Nevertheless, significant bilateral variation was observed for the 4D and 2D:4D ratio in the case of females only. Among different anthropometric variables, only height was found significantly correlated with

the right-hand 2D:4D ratio of females. Further research is required on large samples considering the ethnic and sex differences for exploring the meaningful associations between digit ratios, hormonal influence, and behavioural traits.

Acknowledgements: The authors gratefully acknowledge all the participants for their cooperation and help during data collection. Furthermore, special thanks to the Director, Anthropological Survey of India, Ministry of Culture, Government of India, for providing all sorts of logistic support for the successful accomplishment of this research work.

References

1. Aksu, F., H. Topacoglu, C. Arman, A. Atac, S. Tetik. Neck circumference and 2:4 digit ratio in patients with acute myocardial infarction. – *Turkiye Klin. Cardiovsc. Sci.*, **21**, 2009, 147152.
2. Apicella, C. L., V. A. Tobolsky, F. W. Marlowe, K. W. Miller. Hadza hunter-gatherer men do not have more masculine digit ratios (2D: 4D). – *Am. J. Phys. Anthropol.*, **15**, 2016, 223-232.
3. Barut, C., U. Tan, A. Dogan. Association of height and weight with second to fourth digit ratio (2D:4D) and sex differences. – *Percept. Mot. Skills*, **106**, 2008, 627-632.
4. Bunevicius, A. The Association of Digit Ratio (2D:4D) with cancer: a systematic review and meta-analysis. – *Dis. Markers*, **2018**, 2018, 7698193.
5. Carré, J. M, T. L. Ortiz, B. Labine, B. J. Moreau, E. Viding, C. S. Neumann, G. Bernard. Digit ratio (2D:4D) and psychopathic traits moderate the effect of exogenous testosterone on socio-cognitive processes in men. – *Psychoneuroendocrinology*, **62**, 2015, 319-326.
6. Ciumas, C., A. Lindén Hirschberg, I. Savic. High fetal testosterone and sexually dimorphic cerebral networks in females. – *Cereb. Cortex*, **19**, 2009, 1167-1174.
7. Crews, D. Biological Anthropology and Human Aging: Some Current Directions in Aging Research. – *Annu. Rev. Anthropol.*, **22**, 1993, 395-423.
8. Dey, S., A. K. Kapoor. Digit ratio (2D:4D) – A forensic marker for sexual dimorphism in North Indian population. – *Egypt J. Forensic Sci.*, **6**, 2016, 422-428.
9. Ergul, E. O. Relationships between the 2D:4D digit ratio, waist circumference, hand preferences, weight, height, waist-to-height ratio and BMI in a Turkish population. – *Int. J. Morphol.*, **37**, 2019, 1299-1304.
10. Finch, C. E., J. W. Vaupel, K. Kinsella. *Cells and surveys: Should biological measures be included in social science research?* Washington, DC: National Academy Press, 2000.
11. Fink, B., J. T. Manning, N. Neave, U. Tan. Second to fourth digit ratio and hand skill in Austrian children. – *Biol. Psychol.*, **67**, 2004, 375-384.
12. Fink, B., J. T. Manning, N. Neave. The 2nd-4th digit ratio (2D:4D) and neck circumference: Implications for risk factors in coronary heart disease. – *Int. J. Obes.*, **30**, 2006, 711-714.
13. Fink, B., N. Neave, J. T. Manning. Second to fourth digit ratio, body mass index, waisttohip ratio, and waisttochest ratio: Their relationships in heterosexual men and women. – *Ann. Hum. Biol.*, **30**, 2003, 728738.
14. Fusar-Poli, L., A. Rodolico, S. Sturiale, B. Carotenuto, A. Natale, D. Arillotta, S. Spyridon, S. S. Maria, A. Eugenio. Second-to-Fourth Digit Ratio (2D:4D) in Psychiatric Disorders: A Systematic Review of Case-control Studies. – *Clin. Psychopharmacol. Neurosci.*, **19**, 2021, 26-45.
15. Galis, F., C. M. Ten Broek, S. Van Dongen, L. C. Wijnaendts. Sexual dimorphism in the prenatal digit ratio (2D: 4D). – *Arch. Sex Behav.*, **39**, 2010, 57-62.
16. Gillam, L., R. McDonald, F. J. Ebling, T. M. Mayhew. Human 2D (index) and 4D (ring) finger lengths and ratios: cross-sectional data on linear growth patterns, sexual dimorphism and lateral asymmetry from 4 to 60 years of age. – *J. Anat.*, **213**, 2008, 325-335.
17. Gwunireama, I. U., E. C. Ihemelandu. Geographical influence on digit ratio (2D: 4D): a case study of Andoni and Ikwerre ethnic groups in Niger Delta, Nigeria. – *J. Appl. Biosci.*, **27**, 2010, 1736-1741.

18. **Hollier, L. P., J. A. Keelan, E. S. Jamnadass, M. T. Maybery, M. Hickey, A. J. Whitehouse.** Adult digit ratio (2D:4D) is not related to umbilical cord androgen or estrogen concentrations, their ratios or net bioactivity. – *Early Hum. Dev.*, **91**, 2015, 111-117.
19. **Hönekopp, J., L. Bartholdt, L. Beier, A. Liebert.** Second to fourth digit length ratio (2D:4D) and adult sex hormone levels: New data and a meta-analytic review. – *Psychoneuroendocrinology*, **32**, 2007, 313-321.
20. **Hong, L., M. Zhan-Bing, S. Zhi-Yun, S. Xiao-Xia, Z. Jun-Li, H. Zheng-Hao.** Digit ratio (2D:4D) in Chinese women with breast cancer. – *Am. J. Hum. Biol.*, **26**, 2014, 562-564.
21. **Jacob, M., R. Avadhani, B. Nair, R. Nallathamby, M. A. Soman.** Cross sectional study of second and fourth digit ratio with physical attributes in South Indian population. – *Int. J. Anat. Res.*, **3**, 2015, 1133-1137.
22. **Jain, M., U. Dhall, S. Pandey, S. Jain.** Second to Fourth Digit Ratio(2D:4D) in North-West Indians: Sexual Dimorphism. – *J. Anat. Soc. India*, **61**, 2012, 242-245.
23. **Jasuja, O.P., G. Singh.** Estimation of stature from hand and phalange length. – *J. Indian Acad. Forensic Med.*, **26**, 2004, 100-105.
24. **Jeevanandam, S., K. M. Prathibha, K. Raman.** Relevance of 2D:4D Ratio as a Marker of Depression in Adolescents of a South Indian Medical College – A Cross Sectional Study. – *Int. J. Physiology*, **7**, 2019, 80-85.
25. **Jeevanandam, S., K. M. Prathibha.** Measurement of 2D:4D Ratio and Neck Circumference in Adolescents: Sexual Dimorphism and its Implications in Obesity – A Cross Sectional Study. – *Indian J. Endocr. Metab.*, **22**, 2018, 724-727.
26. **Kailash.** Peaceful Coexistence: Lessons from Andamans. – *Econ. Polit. Wkly.*, **35**, 2000, 2859-2865.
27. **Kalichman, L., V. Batsevich, E. Kobylansky.** 2D:4D finger length ratio and radiographic hand osteoarthritis. – *Rheumatol. Int.*, **38**, 2018, 865-870.
28. **Kanchan, T., G. P. Kumar, R. G. Menezes, P. Rastogi, P. P. Rao, A. Menon, B. S. K. Shetty, Y. P. R. Babu, F. N. P. Monterio, P. Bhagavath, V. C. Nayak.** Sexual dimorphism of the index to ring finger ratio in South Indian adolescents. – *J. Forensic Leg. Med.*, **17**, 2010, 243-246.
29. **Kasielska-Trojan, A., J. T. Manning, A. Antczak, A. Dutkowska, W. Kuczynski, A. Sitek, B. Antoszewski.** Digit ratio (2D:4D) in women and men with lung cancer. – *Sci. Rep.*, **10**, 2020, 11369.
30. **Klimek, M., U. M. Marcinkowska, G. Jasienska.** Value of digit ratio 2D:4D, a biomarker of prenatal hormone exposure, is stable across the menstrual cycle. – *Early Hum. Dev.* **110**, 2017, 21-24.
31. **Kowal, M., P. Sorokowski, A. Żelaźniewicz, J. Nowak, S. Orzechowski, G. Żurek, A. Zurek, A. Juskiewicz, L. Wojtycka, W. Sieniuc, M. Poniatowska, K. Tarnowska, K. Kowalska, K. Drabik, P. Łukaszek, K. Krawczyk, T. Stefaniak, N. Danek.** No relationship between the digit ratios (2D:4D) and salivary testosterone change: Study on men under an acute exercise. – *Sci. Rep.*, **10**, 2020, 10068.
32. **Králík, M., P. Ingrová, S. Koziel, A. Hupková, O. Klíma.** Overall trends vs. individual trajectories in the second-to-fourth digit (2D:4D) and metacarpal (2M:4M) ratios during puberty and adolescence. – *Am. J. Phys. Anthropol.*, **162**, 2017, 641-656.
33. **Krishan, K., T. Kanchan, N. Asha, S. Kaur, P.M. Chatterjee, B. Singh.** Estimation of sex from index and ring finger in a North Indian population. – *J. Forensic Leg. Med.*, **20**, 2013, 471-479.
34. **Krishnakumar, M., S. Atheeshwar, M. D. Chandrasekar.** Myopia and digit ratio in medical college students. – *PLoS One*, **9**, 2014, e89800.
35. **Krishnamoorthi, N., N. Shetty, N. Shenoy, A. Shenoy, C. C. Pais, M. Yadiyal.** Does Right Hand Second Digit to Fourth Digit Ratio Correlate with Primary Infertility in Males? – *Indian J. Public Health Res. Dev.*, **10**, 2019, 444-447.
36. **Laurent, M., L. Antonio, M. Sinnesael, V. Dubois, E. Gielen, F. Classens, D. Vanderschueren.** Androgens and estrogens in skeletal sexual dimorphism. – *Asian J. Androl.*, **16**, 2014, 213-222.

37. **Lippa, R. A.** Are 2D:4D finger-length ratios related to sexual orientation? Yes for men, no for women. – *J. Pers. Soc. Psychol.*, **85**, 2003, 179-188.
38. **Lutchmaya, S., S. Baron-Cohen, P. Raggatt, R. Knickmeyer, J. T. Manning.** 2nd to 4th digit ratios, fetal testosterone and estradiol. – *Early Hum. Dev.*, **77**, 2004, 23-28.
39. **Mackus, M., D. de Kruijff, L. S. Otten, A. D. Kraneveld, J. Garssen, J. C. Verster.** The 2D:4D Digit Ratio as a Biomarker for Autism Spectrum Disorder. – *Autism Res. Treat.*, **2017**, 2017, 1048302.
40. **Maitra, A., C. Maitra, D. K. Jha, R. Biswas.** Finger Length Ratio (2D:4D) in Central India and an Attempt to Verify Fraternal Birth Order Effect: A Population Based Cross-Sectional Study. – *J. Clin. Diagn. Res.*, **10**, 2016, CC09-CC12.
41. **Majumder, J., B. Bagepally.** The right hand second to fourth digit ratio (2D:4D) and its relationship with body composition indicators among young population. – *Asian J. Med. Sci.*, **6**, 2015, 78-84.
42. **Manning, J. T., D. Scutt, J. Wilson, D. I. Lewis-Jones.** The ratio of 2nd to 4th digit length: a predictor of sperm numbers and concentrations of testosterone, luteinizing hormone and oestrogen. – *Hum. Reprod.*, **13**, 1998, 3000-3004.
43. **Manning, J. T., L. P. Kilduff, R. Trivers.** Digit ratio (2D:4D) in Klinefelter's syndrome. – *Andrology*, **1**, 2013, 94-99.
44. **Manning, J. T., M. Peters.** Digit ratio (2D:4D) and hand preference for writing in the BBC Internet Study. – *Laterality*, **14**, 2009, 528-540.
45. **Manning, J. T., P. Henzi, P. Venkatramana, S. Martin, D. Singh.** Second to fourth digit ratio: ethnic differences and family size in English, Indian and South African populations. – *Ann. Hum. Biol.*, **30**, 2003, 579-588.
46. **Manning, J. T., R. P. Taylor.** Second to fourth digit ratio and male ability in sport: implications for sexual selection in humans. – *Evol. Hum. Behav.*, **22**, 2001, 61-69.
47. **Marczak, M., M. Misiak, A. Sorokowska, P. Sorokowski.** No sex difference in digit ratios (2D:4D) in the traditional Yali of Papua and its meaning for the previous hypotheses on the inter-population variability in 2D:4D. – *Am. J. Hum. Biol.*, **30**, 2018, e23078.
48. **Marmot, M. G., G. D. Smith, S. Stansfeld, C. Patel, F. North, J. Head, I. White, E. Brunner, A. Feeney.** Health inequalities among British civil servants: the Whitehall II study. – *Lancet*, **337**, 1991, 1387-1393.
49. **Martel, M. M., K. Klump, J. T. Nigg, S. M. Breedlove, C. L. Sisk.** Potential hormonal mechanisms of attention-deficit/hyperactivity disorder and major depressive disorder: a new perspective. – *Horm. Behav.*, **55**, 2009, 465-479.
50. **Mayhew, T. M., L. Gillam, R. McDonald, F. J. P. Ebling.** Human 2D (index) and 4D (ring) digit lengths: their variation and relationships during the menstrual cycle. – *J. Anat.*, **211**, 2007, 630-638.
51. **McIntyre, M. H., P. T. Ellison, D. E. Lieberman, E. Demerath, B. Towne.** The development of sex differences in digital formula from infancy in the Fels Longitudinal Study. – *Proc. Biol. Sci.*, **272**, 2005, 1473-1479.
52. **Medland, S. E., J. C. Loehlin, N. G. Martin.** No effects of prenatal hormone transfer on digit ratio in a large sample of same- and opposite-sex dizygotic twins. – *Personal Individ. Differ.*, **44**, 2008, 1225-1234.
53. **Mukherjee, K., M. Pandi, K. V. Rao.** Socio-Demographic Factors Associated with Health Condition among Adult Bantu Population of Andaman: A Cross-Sectional Study. – *Journal of the Anthropological Survey of India*, **70**, 2021, 126-138.
54. **Muller, D. C., J. T. Manning, J. L. Hopper, D. R. English, G. G. Giles, G. Severi.** No strong association between second to fourth digit ratio (2D:4D) and adult anthropometric measures with emphasis on adiposity. – *Ann. Hum. Biol.*, **40**, 2013, 201-204.
55. **Nayak, S. B., D. Nair, V. Ravi, A. P. Aithal.** A comparative study on digit ratio and hand patterns of three ethnic races of Malaysia. – *Egypt J. Forensic Sci.*, **8**, 2018, 56.

56. Oyeyemi, B. F., O. A. Iyiola, A. W. Oyeyemi, K. A. Oricha, A. T. Anifowoshe, N. A. Alamukii. Sexual dimorphism in ratio of second and fourth digits and its relationship with metabolic syndrome indices and cardiovascular risk factors. – *J. Res. Med. Sci.*, **19**, 2014, 234.
57. Ozakaya, I., A. Tunckale. Neck circumference positively related with central obesity and overweight in Turkish university students: a preliminary study. – *Cent. Eur. J. Public Health*, **24**, 2016, 91-94.
58. Paul, S. N., B. S. Kato, J. L. Hunkin, S. Vivekanandan, T.D. Spector. The big finger: the second to fourth digit ratio is a predictor of sporting ability in women. – *Br. J. Sports Med.*, **40**, 2006, 981-983.
59. Pei, X., L. Liu, M. U. Imam, M. Lu, Y. Chen, P. Sun, Y. Guo, Y. Xu, Z. Ping, X. Fu. Neck circumference may be a valuable tool for screening individuals with obesity: findings from a young Chinese population and a meta-analysis. – *BMC Public Health*, **18**, 2018, 529.
60. Peters, M., K. Mackenzie, P. Bryden. Finger length and distal finger extent patterns in humans. – *Am. J. Phys. Anthropol.*, **117**, 2002, 209-217.
61. Purves, D., G. J. Augustine, D. Fitzpatrick, L. C. Katz, A. S. LaMantia, J. O. McNamara, S. M. Williams. Neuroscience. 2nd edition. Sunderland (MA): Sinauer Associates, 2001. Available from: <https://www.ncbi.nlm.nih.gov/books/NBK11161/>
62. Rajawat, A., C. Majeti, U. K. Podugu, M. Kaushik, X. Nagamaheshwari, N. Mehra. Association of Hormonal Fingerprints and Dental Caries: A Pilot Study. – *J. Conserv. Dent.*, **23**, 2020, 337-340.
63. Ramasamy, S., R. R. Thaj, S. U. Ibrahim. 2nd to 4th Digit Ratio (2D:4D) – Is It a Marker for Dyslexia? – *Indian Journal of Mental Health*, **6**, 2019, 340-346.
64. Rammsayer, T. H., S. J. Troche. Sexual dimorphism in second-to-fourth digit ratio and its relation to gender-role orientation in males and females. – *Pers. Individ. Differ.*, **42**, 2007, 911-920.
65. Rebecca, B., P. J. Benson. Digit ratio (2D: 4D) and the spatial representation of magnitude. – *Horm. Behav.*, **50**, 2006, 194-199.
66. Robertson, J., W. Zhang, J. J. Liu, K. R. Muir, R. A. Maciewicz, M. Dohert. Radiographic assessment of the index to ring finger ratio (2D:4D) in adults. – *J. Anat.*, **212**, 2008, 42-48.
67. Roy, R., R. Kundu, M. Sengupta, P. Som. Association between digit length ratio (2D:4D) and polycystic ovarian syndrome (PCOS)—A study among eastern Indian population. – *J. Anat. Soc. India*, **67**, 2018, S14-19.
68. Roychowdhury, R. *The untold Andaman and Nicobar Islands*. New Delhi: Manas Publications, 2011.
69. Sen, J., T. Kanchan, A. Ghosh, N. Mondal, K. Krishan. Estimation of sex from index and ring finger lengths in an indigenous population of Eastern India. – *J. Clin. Diagn. Res.*, **9**, 2015, HC01-5.
70. Sen, J., T. Kanchan, A. Ghosh, N. Mondal, K. Krishan. Estimation of stature from lengths of index and ring fingers in a North-eastern Indian population. – *J. Forensic Leg. Med.*, **22**, 2014, 10-15.
71. Setiya, M., M. Jehan, R. Godwin, A. Sastya. Sexual dimorphism of digit ratio (2D:4D) in Madhya Pradesh – *Int. J. Sci. Stud.*, **4**, 2017, 155-159.
72. Sudhakar, H. H., P. Majumdar, V. Umesh, K. Panda. Second to fourth digit ratio is a predictor of sporting ability in elite Indian male kabaddi players. – *Asian J. Sports Med.*, **5**, 2014, e23073.
73. Tester, N., A. Campbell. Sporting Achievement: What Is the Contribution of Digit Ratio? – *J. Pers.*, **75**, 2007, 663-678.
74. Tomulescu, I. M., G. L. Nicoras. Comparative study of finger lengths and digit ratio in men of Ancona, Italy and Oradea, Romania. – *Studia Univ. VG. SSV.*, **25**, 2015, 151-155.
75. Trabert, B., B. J. Graubard, R. L. Erickson, Y. Zhang, K. A. McGlynn. Second to fourth digit ratio, handedness and testicular germ cell tumors. – *Early Hum. Dev.*, **89**, 2013, 463-466.
76. Unal, M. Digit ratio 2D:4D is a possible indicator for androgenetic alopecia in males. – *J. Cosmet. Dermatol.*, **17**, 2018, 545-548.
77. Venkatasubramanian, G., R. Arasappa, N. P. Rao, B. N. Gangadhar. Digit ratio (2D:4D) asymmetry and Schneiderian first rank symptoms: implications for cerebral lateralisation theories of schizophrenia. – *Laterality*, **16**, 2011, 499-512.
78. Vidyarthi, L. Cultural diversities in the Andaman and Nicobar Islands: a preliminary report. – *Indian Anthropologist*, **1**, 1971, 80-92.

79. **Voracek, M., J. Pietschnig, I. W. Nader, S. Stieger.** Digit ratio (2D: 4D) and sex-role orientation: Further evidence and metaanalysis. – *Pers. Individ. Differ.*, **51**, 2011, 417-422.
80. **Wahi, L. N.** The Bhatu – A criminal tribe of the United Provinces. – *Man India.*, **29**, 1949, 84-91.
81. **Weiner, J. S., J. A. Lourie.** *Practical human Biology*. London, NY: Academic Press, 1981.
82. **Williams, T. J., M. E. Pepitone, S. E. Christensen, B. M. Cooke, A. D. Huberman, N. J. Breedlove, T. J. Breedlove, C. L. Jordan, S. M. Breedlove.** Finger-length ratios and sexual orientation. – *Nature*, **404**, 2000, 455-456.
83. **Xu, Y., Y. Zheng.** The digit ratio (2D:4D) in China: a meta-analysis. – *Am. J. Hum. Biol.*, **27**, 2015, 304-309.
84. **Yadav, R., M. Bala.** A study of 2nd to 4th digit ratio (2D: 4D) in relation to hypertension in north Indian males and its implications for risk factors in coronary heart disease. – *Indian Journal Clin. Anat. Physiol.*, **3**, 2016, 24.
85. **Zheng, Z., M. J. Cohn.** Developmental basis of sexually dimorphic digit ratios. – *Proc. Natl. Acad. Sci.*, **108**, 2011, 16289-16294.

Analysis of bilateral asymmetry of some anthropometric measurements of humerus used in Forensic practice

Antoaneta Fasova¹, Atanas Baltadjiev¹, Ivan Tsranchev², Pavel Timonov², Ferihan Popova¹, Mohammad Eisa Ali³*

¹ Department of Anatomy, Histology and Embryology, Faculty of Medicine, Medical University of Plovdiv, 15a Vassil Aprilov blv, Plovdiv, Bulgaria

² Department of Forensic medicine and Deontology, Faculty of Medicine, Medical University of Plovdiv, 15a Vassil Aprilov blv, Plovdiv, Bulgaria

³ Student, Faculty of Medicine, Medical University of Plovdiv, 15a Vassil Aprilov blv, Plovdiv, Bulgaria

* Corresponding author e-mail: antoaneta_ioan@yahoo.com

The aim of the present study is to evaluate the manifestation of bilateral asymmetry in the proximal and distal end of humerus among the contemporary Bulgarian population. A total of 113 pairs of complete humeri from 54 females and 59 males were studied. Measurements of humerus include circumference of head, vertical diameter of head, transverse diameter of head and epicondylar breadth analyzed with SPSS 23.0. The Paired Sample T test was used to compare the right and the left sides. For each side the values of the bones were tested for normality of distribution by the Kolmogorov-Smirnov test. No statistical difference was found between right and left side for the mean values computed for both genders. We concluded that the bilateral asymmetry is not present in the humeral dimensions, thus, allowed the bones of both sides to be grouped together for further analysis, especially in forensic medicine, anthropology, normal morphology, and archeology.

Key words: bilateral asymmetry, humerus, Bulgarian population

Introduction

The sex differences in the quantitative and qualitative features of the human humerus and femur are a good and reliable indicator for sex, age and stature determination from skeletal remains in Forensic anthropology. In addition, due to their structure, size, location, strength, they or their fragments are common objects of study in Forensic anthropological practice, especially in cases of mass disasters or murders in which the corpses are often decapitated or dismembered. Some authors emphasize the need of anthropometric studies on fragmented bones, as in anthropology it is much more often necessary to determine sex by fragments than by structurally preserved bones.

Symmetry is defined as correspondence in size, shape, and relative position of parts on opposite sides of a dividing line or median plane while asymmetry is described as a lack or absence of symmetry. Although bilateral symmetry in paired morphological traits is evident in humans, significant deviation from this is observed in internal organs, human brain, and especially upper limb [23].

In their anthropological studies of humerus, Pavlov and Matev, Sato and Noriyasu, Charisi et al., Atamturk et al., Ross and Manneschi, Shehri and Siloman, Reddy and Doshi [1,3,12,14,15,17,19] did not establish statistically significant lateralization in both sexes.

The examination of the upper and lower limb asymmetry can be useful to medical scientists, archeologists, anthropologists [6,7,11] and forensic experts for medicolegal studies [9,20,24].

The **aim** of the present study is to determine the presence or lack of symmetry between some parameters of pairs of left and right human humerus.

Materials and Methods

The present study included 59 pairs of complete dry male humeri and 54 pairs of complete dry female humeri of Bulgarian origin. The bones were collected from the Department of General and Clinical Pathology and Forensic Medicine, Medical University of Plovdiv and the Department of General and Clinical Pathology and Forensic Medicine, Medical University of Varna, Bulgaria. The bones included in this study fulfill the following criteria: show no anomalies, deformations or abrasions; have sustained no fractures previously; have reached skeletal maturity. They belong to Bulgarians born after 1920. The mean age of the male bones is 56,8 years, and of the female ones 64.3 years. The bones were the subject of forensic examinations in cases of identification of dead bodies with late postmortem changes or in stage of skeletonization. The study has been carried out in accordance with The Code of Ethics of the World Medical Association (Declaration of Helsinki). A total of four humeral dimensions were taken using sliding caliper and steel tape. Measurements include **circumference of the head (M8)**, **vertical diameter of the head (M10)**, **transverse diameter of the head (M9)** and **epicondylar breadth (M4)** and were taken according the standard technique of Martin and Saller [10]. We have chosen these measurements of the humerus because these are the most frequently studied parameters in Forensic practice and in most anthropological studies, and this will allow us to compare our results. Statistical analysis was performed using SPSS 23.0. Means and standard deviations of the results of individual factors were calculated and statistically analyzed to identify any significant differences. We defined the protocol as follows: for each pair, the humeral parameters were measured on both left and right humeri to assess if a statistically significant difference between the two sides could be recorded. To minimize measurement error, we completed five measurements for each variable of each side. Then we excluded the least measurement and the greatest measurement. Finally, we computed the mean of the three other values and used it to characterize a bone. Basic descriptive statistics were computed.

Results

For each side, the values of the bones were tested for normality of the distribution by the Kolmogorov-Smirnov test. The Independent Samples test for equality of means of male and female independent samples was performed for all measured variables. The Kolmogorov-Smirnov test found that all variables have a normal empirical distribution ($p > 0.05$). The data obtained from the anthropometric humeral measurements were subjected to Paired Sample T test to compare the right and the left sides. The results show lack of significant difference between the mean values of the left and right sides calculated for both sexes ($p > 0.05$).

The min and max values of the measurements are shown in **Table 1** and **Table 2**.

Table 1. Min and max values of the measurements (mm) of the male humeral bones.

Variables	Left			Right			Indicators of asymmetry		
	N	Min	Max	N	Min	Max	Absolute difference	t	P
Circumference of the head	59	123.58	171.82	59	120.79	174.37	0.12	0.191	0.850
Vertical diameter of the head	59	38.41	57.43	59	38.59	56.83	0.21	0.756	0.458
Transverse diameter of the head	59	35.66	51.98	59	34.70	51.80	0.57	2.373	0.162
Epicondylar breadth	59	49.82	78.62	59	49.88	78.20	0.18	1.476	0.153

Table 2. Min and max values of the measurements (mm) of the female humeral bones.

Variables	Left			Right			Indicators of asymmetry		
	N	Min	Max	N	Min	Max	Absolute difference	t	P
Circumference of the head	54	99.01	154.27	54	101.52	153.18	-0.71	-1.461	0.163
Vertical diameter of the head	54	30.59	51.17	54	30.50	51.02	0.12	1.725	0.104
Transverse diameter of the head	54	29.32	46.78	54	29.42	46.34	0.17	1.852	0.083
Epicondylar breadth	54	41.42	67.22	54	40.01	68.51	0.06	0.107	0.916

Circumference of humeral head

The circumference of the humeral head in the male skeletons is greater by 0.12 mm in the left humerus. In female skeletons, the difference between the mean values on the right and left is 0.71 mm, respectively, in favor of the right humerus. No significant bilateral differences between the examined parameters for both sexes were detected (males: $p = 0.850$; females: $p = 0.163$).

Vertical diameter of humeral head

The vertical diameter of the male humeral head in the left is 0.21 mm larger than the right one. In female skeletons, this size is also larger in the left humeri, with a difference of 0.12 mm. Bilateral differences were not statistically significant for both sexes (males: $p = 0.458$; females: $p = 0.104$).

Transverse diameter of humeral head

This measurement in males and females shows higher values in the left humerus than the right. The absolute differences between their mean values are 0.57 mm and 0.17 mm, respectively, but without statistical significance (males: $p = 0.162$; females: $p = 0.083$).

Humeral distal epicondylar breadth

The data of the humeral distal epicondylar breadth show that in both sexes the left humerus has higher values than the right one by 0.18 mm in the male skeletons and 0.06 mm in the female skeletons. Bilateral differences were not statistically significant (males: $p = 0.153$; females: $p = 0.916$).

The comparative assessment of the direction of the manifested asymmetry in the anthropometric measurements of humerus shows that both sexes have left-handed asymmetry. In one of the parameters, a discrepancy of the direction for both sexes is found – this is the circumference of the head of the humerus. Regardless of directions of lateralization, all humeral variables show statistically insignificant bilateral variation ($p > 0.05$) in both males and females.

Discussion

The anthropometric characteristic of the paired humeri allows considering the manifestations of bilateral asymmetry. The lack of such will ensure us to create a “mixed” sample in the intersex plan, which will be subjected to mathematical and statistical processing. This in turn is not a methodological error. Similar studies on bilateral samples are often found in the literature, especially in forensic studies.

More recent population studies show diminishing of the directionality and magnitude of asymmetry, probably reflecting changes in external factors, such as division of labor. An osteometric study of the long bones of the upper limb in the modern Greek population of the second half of the 20th century was conducted by Charisi et al.

[3] in 204 individuals (111 men and 93 women) from the skeletal collection of the University of Athens. The authors examined the humerus, radius and ulna by comparing the maximum bone length, width of the proximal and distal end on the left and right side. In most cases, the measurements on the right are slightly larger than those on the left in absolute values, but no bilateral asymmetry was found. This is confirmed by the results of the t-test, in which all the mean values of the studied parameters between the two sides are not statistically significant.

According to Trinkaus et al. [22] bilateral asymmetry is best observed in the diaphyses and especially in their circumference or other cross sections. The analysis of humeral asymmetry in recent human skeletal samples and an extant tennis-player sample documents minimal asymmetry in bone length, little asymmetry in distal humeral articular breadth, but pronounced and variable asymmetry in mid- and distal diaphyseal crosssectional geometric parameters [22].

Studies on other skeletal parts have shown that the preferential use of one arm is best reflected on other bones, such as the scapula [4,5,18]. The mechanical load caused by the movements of the upper limb leads to differences in the morphology of the glenoid fossa. Other studies have found that bilateral asymmetry is more common in metacarpal bones than in other skeletal elements of the arm because they are used more frequently in daily activities [8,13,16].

Sato and Noriyasu [17] investigate the morphological and functional relationships between the head of the humerus and the glenoid cavity. They examined a total of 173 sets of humeri and their corresponding scapulae. The dimensions of the head in the right humerus in both sexes are generally larger than in the left, but no significant bilateral differences have been found. The size of the glenoid cavity is also larger in the right scapula. The authors explain the larger dimensions on the right with greater range of motion in the right shoulder, due to the more frequent use of the dominant arm.

Stirland [21] in his study of the attachment points of muscles on the humerus based on radiographic studies proved that there is no statistical significance in the lateralization of these points.

In 2010 Atamtyrk et al. [1] present a retrospective study of 84 X-ray radiographs of 46 women and 38 men aged between 20 and 79 years from Istanbul. The collected sample contains both left and right humeri belonging to different patients. The authors did not establish statistical significance between bilateral osteometric parameters. The studied parameters of the humerus are: maximum length, vertical diameter of the head, maximum breadth in the middle of the body, distal epicondylar breadth.

In Bulgaria Pavlov and Matev in 1975 [12] investigated the morphometric characteristic of humerus in Bulgarian men. The authors examined 143 pairs of humeri that belong to men who died in the Serbian, Balkan, and First World War with a mean age of 29.6 years. The examined parameters are maximum length of the humerus, the largest and smallest width in the middle of the body, midshaft circumference, head circumference, epicondylar breadth, maximum diameter of the head, vertical diameter of the head. Although the authors found that the right humerus was longer and more massive than the left one, they confirmed a statistically insignificant bilateral difference. These data confirmed our results.

Behavioral evidence for sex differences in upper limb preference are mixed, and potentially confounded by cultural factors. Benjamin et al. [2] found evidence for decreasing sexual dimorphism in upper limb lateralization in industrial versus pre-industrial European samples, which could indicate more strongly defined sex-related differences in limb lateralized behavior in the earlier group.

Conclusions

No statistical difference was found between the right and left side for the mean values computed for both sexes. More recent populations show reduction of the directionality and magnitude in asymmetry, probably reflecting changes in exogenous factors, such as division of labor.

We concluded that the bilateral asymmetry is not present in the examined humeral dimensions, thus, allowed the bones of both sides to be grouped together for further analysis. The bones could be subjected to statistical analysis to determine important anthropometric indicators in the Forensic practice such as age, sex, and stature. Their estimation plays a key role for the forensic analysis of human skeletal remains. On the other hand, when fragmentary and incomplete bones are all that are available to the forensic anthropologist for use in sex, age and stature determination, non-metric and metric discriminating parameters that have been derived from complete bones may be of little use. In such circumstances, the discriminating metric methods in the proximal and distal end of the humerus are of specific application to fragmentary bones and could be more useful.

References

1. **Atamtürk, D., M. Akçal, I. Duyar, N. Mas.** Sex estimation from the radiographic measurements of the humerus. – *Eurasian J. Anthropol.*, **1**(2), 2010, 99-108.
2. **Auerbach, B. M., C. B. Ruff.** Limb bone bilateral asymmetry: variability and commonality among modern humans. – *J. Hum. Evol.*, **50**, 2006, 203-218.
3. **Charisi, D., C. Eliopoulos, V. Vanna, C. Koiliias, S. Manolis.** Sexual dimorphism of the arm bones in a modern Greek population. – *J. Forensic Sci.*, **56**(1), 2011, 10-18.
4. **Glassman, D. M., W. M. Bass.** Bilateral asymmetry of long arm bones and jugular foramen: implications for handedness. – *J. Forensic Sci.*, **31**, 1986, 589-635.
5. **Glassman, D. M., S. E. Dana.** Handedness and the bilateral asymmetry of the jugular foramen. – *J. Forensic Sci.*, **37**, 1992, 140-146.
6. **Iscan, M., D. Shihai.** Sexual dimorphism in the Chinese femur. – *Forensic Sci. Int.*, **74**(1-2), 1995, 79-87.
7. **King C. A., M. Y. Iscan, S. R. Loth.** Metric and comparative analysis of sexual dimorphism in the thai femur. – *J. Forensic Sci.*, **43**(5), 1998, 954-958.
8. **Lazenby, R. A.** Identification of sex from metacarpals: effect of side asymmetry. – *J. Forensic Sci.*, **39**, 1994, 1188-94.
9. **Mall, G., M. Hubig, A. Buttner, J. Kuznik, R. Penning, M. Graw.** Sex determination and estimation of stature from long bones of the arm. – *Forensic Sci. Int.*, **117**(1-2), 2001, 23-30.
10. **Martin, R., K. Saller.** *Lehrbuch der Anthropologie in systematischer Darstellung, Band I.* Stuttgart, Gustav Fischer, Stuttgart, 1957, 532-535.

11. **Nikolova, M., I. Petrov.** Age-related changes in non-collagen proteins in the long bones in man. – *Folia Morphologica*, **29**(1), 1981, 52-55.
12. **Pavlov, P., T. Matev.** Morphometric characteristics of humerus in contemporary Bulgarians. – *Medicobiological problems*, **3**, 1975, 21-30. [in Bulgarian]
13. **Plato, C. C., J. L. Wood, A. H. Norris.** Bilateral asymmetry in bone measurements of the hand and lateral hand dominance. – *Am. J. Phys. Anthropol.*, **52**, 1980, 27-31.
14. **Reddy, B., M. Doshi.** Sex determination from adult human humerus by discriminant function analysis. – *Int. J. Res. Med. Sci.*, **5**(9), 2017, 3891-3897.
15. **Ross, A., M. Manneschi.** New identification criteria for the Chilean population: Estimation of sex and stature. – *Forensic Sci. Int.*, 2011, 204:206.e1–206.e3.
16. **Roy, T. A., C. B. Ruff, C. C. Plato.** Hand dominance and bilateral asymmetry in the structure of the second metacarpal. – *Am. J. Phys. Anthropol.*, **94**, 1994, 203–211.
17. **Sato, T., S. Noriyasu.** The morphological relationship between the humerus head and scapular glenoid region. – *Anthropol. Sci.*, **102**(4), 1994, 379-394.
18. **Schulter-Ellis, F. P.** Evidence of handedness on documented skeletons. – *J. Forensic Sci.*, **25**, 1980, 624-630.
19. **Shehri, F. A., K. E. Soliman.** Determination of sex from radiographic measurements of the humerus by discriminant function analysis in Saudi population, Qassim region, KSA. -*Forensic Sci. Int.*, **253**, 2015, 138.e1-6.
20. **Steyn, M., M. Y. Iscan.** Osteometric variation in the humerus: sexual dimorphism in South Africans. – *Forensic Sci. Int.*, **106**(2), 1999, 77-85.
21. **Stirland, A.** Musculoskeletal Evidence for Activity: Problems of Evaluation. - *Int. J. Osteoarchaeol.*, **8**, 1998, 354-362.
22. **Trinkaus, E., S. E. Churchill, C. B. Ruff.** Postcranial robusticity in Homo II: humeral bilateral asymmetry and bone plasticity. – *Am. J. Phys. Anthropol.*, **93**, 1994, 1-34.
23. **Zaidi, Z. E.** Body asymmetries: incidence, etiology, and clinical implications. – *Aust. J. Basic & Appl. Sci.*, **5**(9), 2011, 2157-2191.
24. **Zlatev, S., M. Nikolova.** Mathematical models of growth in stature and weight of children and young. – *J. of Anthropology /BAS/*, **3**, 2000, 50-61.

Repositioning Gross Anatomy Practical for Future Pandemics: A Paradigm Shift from Traditional to Effective Alternatives

Terkuma Chia^{1}, Abayomi Oyeyemi Ajagbe¹, Oluwanisola Akanji Onigbinde¹, Oluwatosin Imoleayo Oyeniran², Begümhan Turhan³*

¹ Department of Anatomy, Faculty of Basic Medical Sciences, College of Health Sciences, Nile University of Nigeria, Abuja, Nigeria

² Department of Physiology, Faculty of Basic Medical Sciences, College of Health Sciences, Nile University of Nigeria, Abuja, Nigeria

³ Department of Physiotherapy and Rehabilitation, Faculty of Health Sciences, Hasan Kalyoncu University, Gaziantep, Turkey

* Corresponding author e-mail: terkumachia@hotmail.com

Background: The education sector around the world has been seriously affected by the pandemic including anatomy education which largely depends on cadaveric dissection. The COVID-19 pandemic has brought about new standards which cut across different spheres of life, including teaching and learning.

Results: Following the challenges experienced in conducting face-face teaching and practical; especially gross anatomy practical alongside online teaching during the COVID-19 school closures, it is imperative to adopt alternative models of conducting and teaching gross anatomy practical. These methods may not be entirely new; however, their use in some climes is almost non-existent while on a low scale in others. In this study, we explored the effective alternative approaches of teaching gross anatomy practical that may be used towards future pandemics.

Conclusions: These alternatives if adopted will bring much ease in switching between different modes in case of any future occurrences, such as the lockdowns experienced through the COVID-19 pandemic.

Key words: Anatomy education and practical; COVID-19; Cadaveric dissection; Pandemics; Gross anatomy

Introduction

The consequences of the COVID-19 outbreak on medical education entirely and anatomy education continually unfold as the virus is still spreading [2, 32]. These effects were even more heightened due to the lack of a vaccine against the virus until recently. Even with the advent of vaccines, the complete elimination of the virus may still be a long way off especially in low and middle-income countries that lack production capacity or logistics infrastructure to rapidly inoculate their citizens. Therefore, continued closures

of institutions may persist and practically oriented subjects like human anatomy that have been unable to undertake the traditional cadaveric practical teaching following the transition to online learning platforms may further be affected globally [29].

Even though there is a proposition that practical teaching may still be undertaken alongside online teaching [30], this is largely unrealistic in many climes that depend largely on cadaver dissection as the dominant means of gross anatomy practical teaching [9, 10, 28, 30, 34]. More so, teaching with human bodies has proven to be irreplaceable even in universities with the best technological resources. Thus, as long as doctors treat human beings, knowledge by contact with human beings will be essential.

Furthermore, with the frequent outbreaks of viral diseases in the last decades, it is pertinent to reposition anatomy education and particularly its practical aspects to be able to cope through periods of prolonged online learning. This paper explores alternative approaches of teaching gross anatomy practical that may be used side by side with the traditional cadaver dissection. These alternatives if adopted will bring much ease in switching between different modes in case of any future occurrence such as the lockdowns experienced during the COVID-19 pandemic.

Materials and Methods

A non-systematic search strategy was utilized in popular research repositories and databases, such as Google Scholar, Research Gate, Web of Science, Science Direct, and PubMed using selected keywords between January to May 2021. The keywords used to identify and extract articles relating and peculiar to the teaching of Anatomy include COVID-19, anatomy education and practical, cadaveric dissection; pandemic, gross anatomy, and anatomy teaching. This literature search yielded 70 publications and abstracts of the results were reviewed for relevance and inclusion in the study. A total of 50 articles highlighting different modalities for teaching anatomy practical met our quality and inclusion requirements and were identified, selected, and discussed. All articles were reviewed critically and included as appropriate to provide readers sufficient evidence for use of the highlighted methods.

Evolution of anatomy education

Human anatomy as a discipline has been regarded as being multifaceted, in which surface learning approach and rote learning of anatomical terms and catalog of structures has been espoused by most students [16]. The teaching of anatomy has been through a sequence of pedagogic lectures and laboratory practical concatenations which entails cadaveric dissection, observing prosected cadavers, and anatomical models [9,16]. The application of resources such as plastic models and computer-assisted simulator technologies in anatomy has been recommended as a way of dignity to seclusion in medical ethics [21].

The study of human anatomy is now a practical skill required by most medical practitioners, unlike its prior imaginative, humanist, and descriptive approach [12]. Learning anatomy using cadavers is a conventional technique for teaching anatomy.

Also, several kinds of research indicated that medical (anatomy) education will be ineffective without cadavers. Yet, certain researchers believe that a well-structured anatomy curriculum without cadavers may be equivalent or enhanced to one with cadavers for learning gross anatomy [48].

Cadaver dissection in anatomy education

Anatomy originates from the contraction of two Greek words, “Ana” (remove) and “Tomy” (cut). The record showed that the first dissection of the human cadaver was done by Herophilus and Erasistratus in the early 3rd century [44]. Over the years, anatomical studies have advanced and became recognized as a creative and spiritual study of life, travail, and death [35]. This gave rise to the “Anatomical Theatres” in Padua and Bologna in the year 1490 and 1637 respectively [35]. However, the quest for cadavers arose leading to shortages of cadavers. Bodies of executed convicts became the sole lawfully accessible cadavers that were available under the law [6].

What’s more, the growth of medical schools and the concomitant surge in the request for cadavers at the beginning of the 19th century led to the prevalence of grave robbing despite its prohibition [49]. This surge in demand for cadavers necessitated legislation to make unclaimed bodies available to anatomists for dissection [49]. However, in recent years, voluntary donations of bodies have become a valid resource and standard for obtaining bodies for anatomy teaching and research in medical schools and universities globally.

Today, cadaver dissection is the fundamental approach in the teaching of anatomy which assists in learning the relations and macroscopic structures of anatomy formation [21]. Besides, anatomy laboratory particularly cadaver dissection is considered as the initial place for tutelage in the application of affective response among several others [43].

Consequences of COVID-19 pandemic on Gross Anatomy Practical

Towards the end of the year 2019, the novel coronavirus disease 2019 (COVID-19) emerged in China and by January 2020, quickly became an international public health emergency [22, 33]. Over 177 million individuals have contracted the virus and the death of over 3.8 million has been estimated in 221 countries/regions as of June 2021 [20]. The rapid transmission rate of the virus occasioned widespread lockdowns globally to interrupt its transmission [22, 33]. These have directly affected anatomy education as it largely depends on cadaveric dissection and the probability of being infected with the virus during dissection is high [22].

Additionally, the present COVID-19 pandemic has made accessibility to the human specimen for dissection difficult. Before this pandemic, the impetus for innovative teaching and learning approaches of anatomy as obtainable in various medical schools across the globe has been insufficient or inaccessible cadavers. This situation is even more acute due to this pandemic. Precisely one of the main problems of the pandemic was the reduction of voluntary donations and, therefore, lack of access and unavailability to those bodies.

Teaching and learning are now online, while the uses of 3D applications, simulators, virtual atlases, and several other digital resources have now become common

place [22]. Though technology has provided facilities for teaching and learning during the pandemic, if they are in a situation of lockdown, students will still not be able to access simulators, plastinated materials, and other digital resources that are in the same departments as the cadavers. For universities in low-income countries, most of the practical classes are on hold as the majority could not afford the resources for high-cost technology. In addition, the economic crisis posed by the pandemic and the failure of teachers to prepare teaching materials in normal times disrupted gross anatomy teaching especially in resource-limited settings where such high-tech platforms are not available, unaffordable and internet connection is poor [29].

Evaluation and validation of anatomical knowledge and examinations during the COVID-19 pandemic

Though novel pedagogical skills such as creative teaching, learning, and evaluation have been strongly emphasized for medical education in recent times, the process of memorization, visual memory, and auditory recall of anatomy knowledge (contents) by students can play a vital role in learning and understanding of anatomy [14, 24]. The process of memorization by students, and the online training sessions conducted for learners and educators by several medical schools have been so important during the pandemic, thus affirming the possibilities of recall memory via rote memorization.

As the teaching of anatomy and other medical-allied courses have resumed in the majority of medical schools and universities around the globe, it is essential to evaluate and validate the level and depth of anatomical knowledge derived by learners during the pandemic [37, 39]. The mode of assessment and examination of students' knowledge of the subject matter is also paramount to monitor learning outcomes and performances [39]. Though the universal experience with virtual examinations shows reasonable success with benefits to learners, alongside financial and logistical gain to the examiner, more improvements in virtual examination software and remote surveillance are required to overcome real cautions such as candidate verification, cheating inhibition, cybersecurity, and IT letdown [37].

Online examinations offer profits to both students and teachers in medical and anatomical examinations and may also save cost. Online examinations are expected to be progressively used in the post-COVID era, nevertheless, they cannot substitute the conventional assessment of students' anatomical knowledge [37].

Teaching gross anatomy practical beyond the COVID-19 pandemic era

The change in the world education sector due to the pandemic has also contributed to the teaching of anatomy. The quality of anatomy education can be enhanced by taking the opportunities of this situation, and the most efficient online anatomy education can be decided by learning from negative experiences during pandemics [47]. The new standards occasioned by the COVID-19 pandemic have cut across different spheres of life, including teaching and learning.

Following the challenges experienced in conducting practical; especially gross anatomy practical alongside online teaching during the COVID-19 school closures, it

is imperative to adopt alternative models of conducting and teaching gross anatomy practical. These methods may not be entirely new; however, their use in some climes is almost non-existent while on a low scale in others [29]. Although, developing education methods on the online education system would make them suitable for use even after the pandemic [47].

Effective Alternative Methods to Traditional (Cadaveric) Teaching of Gross Anatomy Practical

Virtual dissection platforms

Virtual dissection is among some of the commonly employed teaching platforms following the COVID-19 pandemic and lockdown measures. Most often, disease outbreaks result in restricted access to cadavers especially in settings that depend largely on them. Still, virtual dissection programs via personal computers (PCs) offer its users easy and stress-free contact to cadaver dissection [29]. The advantages of virtual dissection relative to conventional cadaveric dissection cannot be overemphasized especially during disease outbreaks [29].

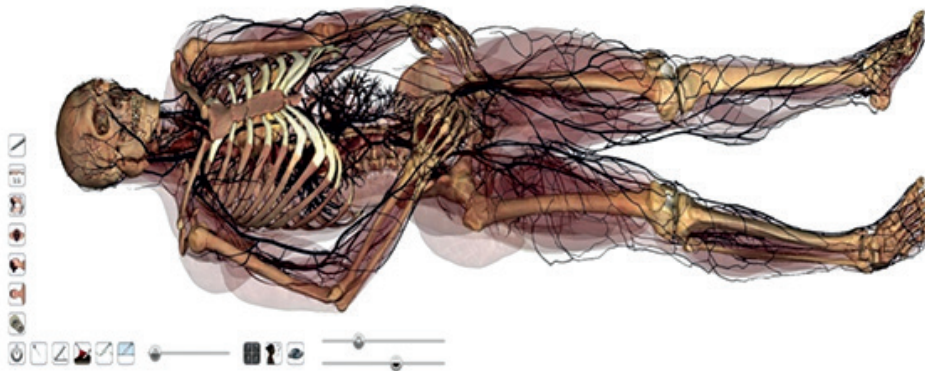


Fig. 1. Virtual dissection (Anatomage, Retrieved from <https://www.anatomage.com/imagelibrary/>)

Three-dimensional (3D) anatomy models

Three-dimensional (3D) anatomy models consist of both digital and non-digital resources. They include 3D computer, mobile- and web-based models, 3D plastic models amongst others. These models can be rotated or oriented into various positions to enhance learning. This way, the interrelation between separate anatomical structures in space and mental maneuverer can be appreciated. Gross anatomy and related knowledge of radiology are learned by some of the 3D digital anatomy models [4].

Nicholson et al. [27], reported that 3D anatomical ear models have a positive impact on students learning. A study on the use of 3D neuroanatomy tools conducted by Estevez et al. [13], revealed that 3D physical modeling is a prolific technique of learning the anatomy of the brain and assists students for visualization of 3D neuroanatomy.

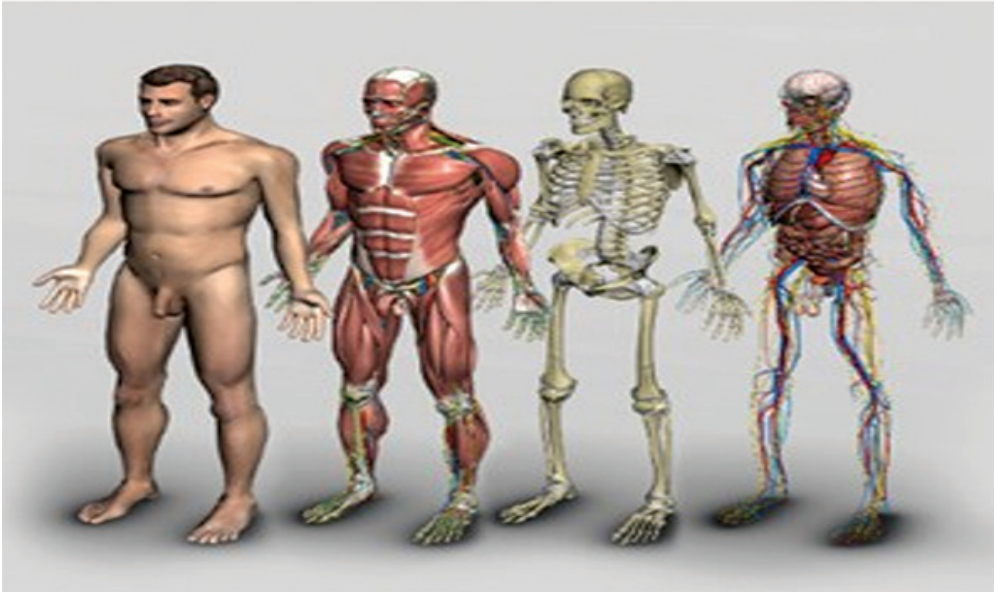


Fig. 2. 3-D Human Anatomy models (Norecopa, Retrieved from <https://norecopa.no/norina/3d-human-anatomy>)

Anatomy gaming

The idea of gamification in education is for learning rather than competition or entertainment. Generally, games are often designed and structured according to guiding rules for play which aims primarily to entertain; besides the competition inherent in them [38]. However, gamification in education aims to facilitate the achievement of curriculum goals using existing learning activities incorporated into games. The idea of gaming excludes engaging learners with a game within the classroom context [38]. It encompasses the use of game design features inconventionally non-game settings. The use of games is now increasingly employed as an attachment to customary teaching approaches in recent times [38].

In anatomy, gamification is employed in various forms comprising digital (web-based simulations, virtual and augmented reality) and non-digital forms (board and card games) [41]. Gamification allows participants the chance to relax and catch fun during learning [3]. This is essential and recommended for learning, as the art of teaching and sincere medical care demands energy and might be self-detrimental, thus causing burnout [3]. Gamification has been beneficial and a source of motivation to students and tutors as demonstrated by its ability to enhance study, retention, and knowledge application among students [3].

Worthy of note is that only the process can be gamified not the outcome. Since engagement rarely equates to real learning, hence, gamification should not be performed in ways that interrupt the learning course [3]. Therefore, some behavioral changes such as motivation for self-learning must be adopted. Academic rigor should be sustained,

despite students' need for a relaxed environment [3]. According to Mackenzie et al., gamification helps students develop mental models through playing the game to give accurate anatomical knowledge [23].

Plastination

Plastination was invented by Dr. Gunter VonHagens in the late 1970s. It entails the preservation of tissue of entire organs using polymers (resin and silicone) to simulate life-like specimens. This permits visualization of intractable anatomical concepts in a human body [35,11]. The use of plastinated prosections for teaching was first done in 2009 by the University of Warwick Medical School. This was followed by St George's and Nottingham Universities all in the United Kingdom [35].

Plastinated specimens pose no risk to human health since they are non-toxic, and can be moved freely from the laboratory to the classroom for learning. Congenital anomalies and pathology can also be displayed in plastinated specimens. Plastinated specimens could also be pinned easily for examination purposes and students' learning and 3D anatomical models can be developed from ultra-thin dissections of plastinated organs [7].

Three-Dimensional (3D) printing

The inception of rapid prototyping or additive manufacturing better known as 3D printing dates back to the late 1980s [50]. Nylon, metal, styrene, polyacetic acid, carbon fiber filament, acrylonitrile, and wood can be employed as materials to design three-dimensional printing digital models [18]. Based on the classification, the operation of 3D printing in medical education can be grouped into three treatments which are; modeling prototypes for surgical design, training, and education; natural tissue engineering, and designing implantable prosthetics [50].

3D printing technology can be employed to comprehend the anatomy of lesions and their related structures such as cerebral structures, vessels, and cranial nerves that are not well understood on radiographic two-dimensional images [50]. The manufacturing of various forms of anatomy specimen (bones, ligaments, tendons) of the same archetype as a real specimen with different strength materials can be performed via 3D printing [5].

Body painting

Body painting is an innovative approach in anatomy education that involves painting of the visceral organs (internal structures), muscles, vessels, bones, nerves on living human body surface which enhance better understanding of proportions and positions of anatomical structures [1, 14, 16, 19]. The practice of body painting by numerous tribes and cultures is an ancient form of art commonly used for ceremonial purposes, fashion, and entertainment [19]. This practice has been reinvented and applied to anatomical learning. Its earliest comprehensive practice for teaching can be dated to the year 1999 by Op Den Akker et al [31]. They developed a course that involved surface markings and tinting complete organs at the point of its prominence on the body performed by the learners [19, 26, 31].

Moreover, it was reported that this activity boosts the student's confidence for peer physical examination and assists in the acquisition of other clinical skills [1]. Body painting proffers the solution for the pertinence of gross anatomy in clinical practice through its knowledge of surface anatomy [14]. Among others, body painting has vastly assisted clinical skills teaching such as palpation, auscultation, and faster recollection of anatomical information especially surface markings of muscles and touchable bony landmarks.



Fig. 3. Body painting (The University of Melbourne, Retrieved from https://biomedicalsciences.unimelb.edu.au/departments/archived-departments/anatomy-and_neuroscience/news-and-events/archive-news/grin-and-bare-it-for-science)

Photogrammetry

This entails the application of photographs of an object which integrates the use of photographs, videos, and computerized prototypes. At different angles, 2D photographs of an object are captured and later veneer via computer software to produce a 3D renovation [43]. Identical points between images captured at varying angles are recognized by the software, and it is also employed to glaze the images by harmonizing their common points [36].

Photogrammetry as a teaching tool is inexpensive, making use of common equipment like digital cameras, lighting tools, and some image processing software [36]. Application of photogrammetry has been applied in neuroanatomical morphometric studies where sequential sections of the brain have been made to study the structural network of cerebellar white matter [36]; examinations of tracheostomy in patients whom laryngectomies were performed, among others [36]. In anatomy education, photogrammetry could be used for the manufacturing of detailed, connected, and approachable digital 3D prosection models [36].

Medical imaging

The usage of imaging in teaching anatomy is necessitated by the need to elucidate radiology. Pathological organs and in vivo visualization of structures can be learned through imaging. However, radiological models cannot replace traditional dissection but will enhance better understanding [45]. Faculty and students in countries like the United Kingdom, Germany, United States of America have already adopted ultrasound imaging courses [45].

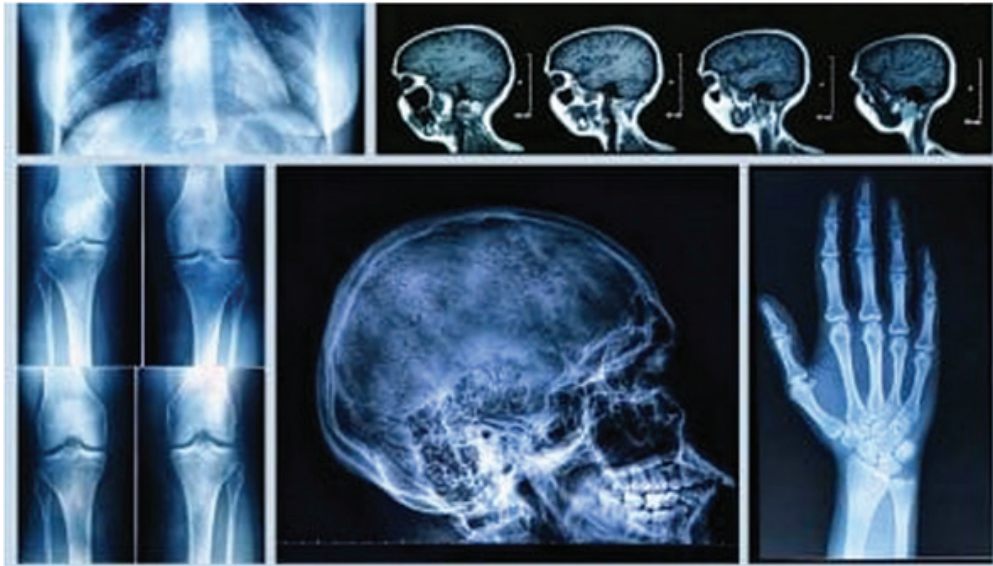


Fig. 4. Medical Imaging (Open MedScience, Retrieved from <https://openmedscience.com/medical-imaging/>)

Simulation

This is the act of juxtaposing the real and mimicking the natures of reality [21]. Medical simulators span from modest duplications of bodily structures for job-based learning to more advanced high patient simulators [46]. Anesthetists in the 20th century manufactured Resusci-Anne which is regarded as the first medical simulator [21]. Resusci Anne which also goes by numerous names (Rescue Anne, Resusci Annie, Resuscitation Annie, or CPR Doll) is commonly used in teaching cardiopulmonary resuscitation (CPR) [40]. Similarly, Laerdal SimMan is another moderate-accuracy patient simulator that is globally used [40]. This is a human simulator that can be used to perform heartbeat, carotid pulse, mouth moves, winking, measurement of blood pressure, duplication of human acts amongst others [21].

Medical simulation helps to harmonize the lacuna between the classroom and the clinical environment [40]. With the use of simulation, learners thrive in clinical skills and grow from being a novice to professional [40]. It also surges retentiveness and

accuracy [40]. However, simulation should be simply to complement but not serve as a substitute for clinical education [21].

Spatial visualization

The ability to think and maneuver two- and three-dimensional objects mentally is referred to as spatial visualization. Research reveals students with developed spatial visualization abilities are more successful in science, technology, engineering, and mathematics (STEM) courses [42]. Spatial visualization can be applied in learning anatomical structures as it is best learned through interconnection to related structures. Anatomy atlases and texts permit only two-dimensional (2D) static anatomical representations and limited visualization of the functional anatomy of distinct dynamic areas [4]. Visual-spatial skills hold much promise for medical students, surgical trainees, and surgeons in the knowledge of anatomical structures [4].

Virtual and Augmented Reality

The constant demand for novel and efficient tools to teach anatomy has led to the rapid development of virtual (VR) and augmented reality (AR) technologies [8, 17]. The development and application of VR and AR devices, software, and application have made learning and studying of gross anatomy happen via hands-on immersive experiences. The learning of structural and gross anatomy through virtual and augmented reality is as effective and efficient as tablet-based (TB) applications [25]. The introduction of these novel modes of study has given rise to enhanced learning, engagement, and performances of students [8, 25].

The adoption and utilization of virtual and augmented reality have proven to be valuable and indispensable for teaching and learning anatomy as obtainable with other



Fig. 5. Virtual Reality (Bond University, Retrieved from <https://bond.edu.au/news/48456/bond-science-students-get-lesson-%E2%80%98virtual-reality%E2%80%99-human-anatomy>)

alternative modes [8,25]. More so, they encourage essential aids including enhanced immersion and engagement of learners. These consequences indicate boundless possibilities for the effective use of virtual and augmented reality as resources to complement lesson and curricular contents in anatomical education.

Conclusion

Conclusively, if these novel and innovative modalities are embraced and in place, the disruptions in gross anatomy practical teaching will not arise in the event of schools shutdown arising from future pandemics as realized during the COVID-19 outbreak. More so, it will allow for an easy transition in times of non-access to cadavers or dissection laboratories, thus ensuring that the learning of gross anatomy practical is sustained during such times.

Recommendation

Firstly, the application of emerging technology tools and integration of different modalities in teaching gross anatomy practical will hold much promise for students' learning. Secondly, the adoption of these innovative tools will enhance the assimilation and knowledge retention of medical students and learners in the anatomical learning process. Thus, the undue pressure posed on the sourcing and availability of cadavers will be drastically reduced, as alternative methods to teaching gross anatomy practical simultaneously with cadaveric dissection are now readily available.

References

1. Aka, J. J., N. E. Cookson, F. W. Hafferty, G. M. Finn. Teaching by stealth: utilising the hidden curriculum through body painting within anatomy education. – *Eur. J. Anat.*, **22**, 2018, 173-182.
2. Alsoufi, A., A. Alsuyihili, A. Msherghi, A. Elhadi, H. Atiyah, A. Ashini. Impact of the COVID-19 pandemic on medical education: Medical students' knowledge, attitudes, and practices regarding electronic learning. – *PLoS One*, **15**, 2020, e0242905.
3. Ang, E. T., J. M. Chan, V. Gopal, N. Li Shia. Gamifying anatomy education. – *Clin. Anat.*, **31**, 2018, 997-1005.
4. Azer, S. A., S. Azer. 3D anatomy models and impact on learning: a review of the quality of the literature. – *Health. Prof. Educ.*, **2**, 2016, 80-98.
5. Baskaran, V., G. Štrkalj, M. Štrkalj, A. Di Ieva. Current Applications and Future Perspectives of the Use of 3D Printing in Anatomical Training and Neurosurgery. – *Front. Neuroanat.*, **10**, 2016, 69.
6. Bennett, R. E. Capital Punishment and the Criminal Corpse in Scotland. – *Nature*, **3**, 2017, 1740-1834.
7. Bin P., A. Conti, C. Buccelli, G. Addeo, E. Capasso, M. Piras. Plastination: ethical and medico-legal considerations. – *Open. Med.*, **11**, 2016, 584-586.
8. Bölek, K., A. M. van Walsum, G. De Jong, D. Henssen. The Effectiveness of the use of augmented reality in anatomy education: A systematic review and meta-analysis. Research Square (2021) (preprint), <http://dx.doi.org/10.21203/rs.3.rs-154748/v1>.
9. Chia, T., O. I. Oyeniran. Anatomy education in Nigeria: challenges and prospects. – *J. Contemp. Med. Edu.*, **9**, 2019, 61-65.

10. **Chia, T., O. I. Oyeniran.** Ethical Considerations in the Use of Unclaimed Bodies for Anatomical Dissection: A Call for Action. – *Ulutas. Med. J.*, **6**, 2020, 5-8.
11. **Douglass, C., R. Glover.** Plastination: Preservation technology enhances biology teaching. – *Am. Biol. Teach.*, **7**, 2003, 503-510.
12. **Dyer, G. S., M. E. Thorndike.** Quidne mortui vivos docent? The evolving purpose of human dissection in medical education. – *Acad. Med.*, **10**, 2000, 969-979.
13. **Estevez, M. E., K. A. Lindgren, P. R. Bergethon.** A novel three-dimensional tool for teaching human neuroanatomy. – *Anat. Sci. Educ.*, **6**, 2010, 309-317.
14. **Finn, G. M.** Current perspectives on the role of body painting in medical education. – *Adv. Med. Educ. Pract.*, **9**, 2018, 701-706.
15. **Folan, J. C., M. D. Supple.** Visual memory and auditory recall in anatomy students. – *Med. Educ.*, **20**, 1986, 516-520.
16. **Green, H., M. R. Dayal.** A qualitative assessment of student attitudes to the use of body painting as a learning tool in first year human anatomy: a pilot study. – *Int. J. Anat. Res.*, **2**, 2018, 5134-5144.
17. **Heather, A., T. Chinnah, V. Devaraj.** The use of virtual and augmented reality in anatomy teaching. – *MedEdPublish*.82019.
18. **Iwanaga, J., M. Loukas, A. S. Dumont, R. S. Tubbs.** A review of anatomy education during and after the COVID-19 pandemic: Revisiting traditional and modern methods to achieve future innovation. – *Clin. Anat.*, **34**, 2021, 108-114.
19. **Jariyapong, P., C. Punsawad, S. Bunratsami, P. Kongthong.** Body painting to promote self-active learning of hand anatomy for preclinical medical students. – *Med. Educ. Online.*, **21**, 2016, 30833.
20. **John Hopkins University and Medicine.** Coronavirus resource center; 2020 [Accessed on 17th June 2021. Available from: <https://coronavirus.jhu.edu/map.html>].
21. **Kurt, E., S. E.Yurdakul, A. Ataç.** An overview of the technologies used for anatomy education in terms of medical history. – *Procedia. Soc. Behav. Sci.*, **103**, 2013, 109-115.
22. **Lemos, G. A., D. N. Araújo, F. J. de Lima, R. F. Bispo.** Human anatomy education and management of anatomic specimens during and after COVID-19 pandemic: Ethical, legal and biosafety aspects. – *Ann. Anat.*, **233**, 2021, 151608.
23. **Mackenzie, J., G. Bailly, M. Nitsche, J. Rashbass.** Gaming Technologies for Anatomy Education'. In unpublished conference presentation. – *7th International Conference on Information Visualisation IV*, **3**, 2003, 16-18.
24. **Miller, S. A., W. Perrotti, D. U. Silverthorn, A. F. Dalley, K. E. Rarey.** From college to clinic: reasoning over memorization is key for understanding anatomy. – *Anat. Rec.*, **269**, 2002, 69-80.
25. **Moro, C., Z. Štromberga, A. Raikos, A. Stirling.** The effectiveness of virtual and augmented reality in health sciences and medical anatomy. – *Anat. Sci. Educ.*, **10**, 2017, 549-559.
26. **Nanjundaiah, K., S. Chowdapurkar.** Body-painting: a tool which can be used to teach surface anatomy. – *J. Clin. Diagn. Res.*, **8**, 2012, 1405-1408.
27. **Nicholson, D. T., C. Chalk, W. R. Funnell, S. J. Daniel.** Can virtual reality improve anatomy education? A randomised controlled study of a computer-generated three-dimensional anatomical ear model. – *Med. Educ.*, **40**, 2006, 1081-1087.
28. **Okafor, I. A., T. Chia.** Covid-19: Emerging Considerations for Body Sourcing and Handling. A Perspective View from Nigeria. – *Anat. Sci. Educ.*, **14**, 2021, 154-162.
29. **Onigbinde, O. A., T. Chia, O. I.Oyeniran, A. O.Ajagbe.** The place of cadaveric dissection in post-COVID-19 anatomy education. – *Morphologie*, **15**, 2020 <http://dx.doi.org/10.1016/j.morpho.2020.12.004>.
30. **Onigbinde, O. A.** COVID-19 pandemic era: How risky is the continuous usage of cadavers for teaching and research. – *Morphologie*, **20**, 2021 <http://dx.doi.org/10.1016/j.morpho.2021.02.005>.
31. **Op Den Akker, J. W., A.Bohnen, W. J.Oudegeest, B.Hillen.** Giving color to a new curriculum: bodypaint as a tool in medical education. – *Clin. Anat.*, **15**, 2002, 356-362.
32. **Ossai, E. N.** Impact of COVID-19 on medical education and the challenges: how prepared is Nigeria. – *Pan. Afr. Med. J.*, **14**, 2020, 45.

33. **Oyeniran, O., T. Chia, O. Onigbinde, A. Ajagbe.** Avoiding an imminent catastrophe from COVID-19 pandemic in Africa: The need to urgently prohibit mass gatherings. – *Cumhuriyet Tıp Dergisi*, **42**, 2020, 203-207.
34. **Oyeniran, O. I.** Sourcing and Availability of Cadavers for Anatomical Dissection amid Covid-19 Pandemic: Safety Challenges and Possible Solutions. – *Ulutas. Med. J.*, **6**, 2020, 188-192.
35. **Papa V., M. Vaccarezza.** Teaching anatomy in the XXI century: new aspects and pitfalls. – *Sci. World. J.*, 2013, 310-348.
36. **Petriceks, A. H., A. S. Peterson, M. Angeles, W. P. Brown.** Photogrammetry of Human Specimens: An Innovation in Anatomy Education. – *J. Med. Educ. Curric. Dev.*, **5**, 2018, 2382120518799356.
37. **Pettit, M., S. Shukla, J. Zhang, K. H. Sunil Kumar, V. Khanduja.** Virtual exams: has COVID-19 provided the impetus to change assessment methods in medicine. – *Bone & Joint Open*, **2**, 2021, 111-118.
38. **Rutledge, C., C. M. Walsh, N. Swinger, M. Auerbach, D. Castro, M. Dewan, et al.** Gamification in action: theoretical and practical considerations for medical educators. – *Acad. Med.*, **93**, 2018, 1014-1020.
39. **Sagoo, M. G., M. A. Vorstenbosch, P. J. Bazira, H. Ellis, M. Kambouri, C. Owen.** Online assessment of applied anatomy knowledge: the effect of images on medical students' performance. – *Anat. Sci. Educ.*, **14**, 2021, 342-351.
40. **Sahu, S., I. Lata.** Simulation in resuscitation teaching and training, evidence based practice review. – *J. Emerg. Trauma. Shock.*, **4**, 2010, 378-384.
41. **See, C.** Gamification in Anatomy Education. In *Teaching Anatomy*, Springer, Cham, 2020, 63-71.
42. **Sorby, S., N. Veurink, S. Streiner.** Does spatial skills instruction improve STEM outcomes? The answer is 'yes'. – *Learn. Individ. Differ.*, **67**, 2018, 209-222.
43. **Stewart, S., R. Charon.** Art, anatomy, learning, and living. – *JAMA*, **9**, 2002, 1182.
44. **Strkalj, G., D. Chorn.** Herophilus of Chalcedon and the practice of dissection in Hellenistic Alexandria. – *S. Afr. Med. J.*, **2**, 2008, 86-89.
45. **Sugand, K., P. Abrahams, A. Khurana.** The anatomy of anatomy: a review for its modernization. – *Anat. Sci. Educ.*, **2**, 2010, 83-93.
46. **Swamy, M., T. C. Bloomfield, R. H. Thomas, H. Singh, R. F. Searle.** Role of SimMan in teaching clinical skills to preclinical medical students. – *BMC. Med. Educ.*, **13**, 2013, 1-6.
47. **Turhan, B., Y. Yakut.** The opinions of physiotherapy students on online anatomy education during Covid-19 pandemic. – *Anatomy*, **2**, 2020, 134-138.
48. **Turhan, B.** Physiotherapy and rehabilitation students' opinions on anatomy education: a cross-sectional survey study. – *Physiother.Q.*, **2**, 2020, 46-51.
49. **Tward, A. D., H. A. Patterson.** From grave robbing to gifting: cadaver supply in the United States. – *JAMA*, **287**, 2002, 1183.
50. **Vaccarezza, M., V. Papa.** 3D printing: a valuable resource in human anatomy education. – *Anat. Sci. Int.*, **1**, 2015, 64-65.

Applying Anthropological Methods for Establishing the Sex, Age and Stature in a Case of Dismembered Corpse

Deyana Velkova, Emilia Kaisheva, Diana Gospodinova, William Dokov*

Clinic of Forensic Medicine at the University Hospital St. Marina – Varna, Bulgaria

* Corresponding author e-mail: deqna.velkova@gmail.com

One of the basic steps in resolving a criminal case is the identification of the victim. This part of the investigation might be difficult in cases with an advanced stage of decomposition or when there are missing parts of the body. Establishing sex, age and stature can provide important information to start the criminal investigation. This forensic case is used to show the accuracy and the informational value of the anthropological methods used in the clinic of forensic medicine at the University Hospital St. Marina - Varna. In the following case study, a number of methods were applied for estimating sex, age and stature to determine their accuracy. The anthropological methods described in this work show good precision: using them, a correct determination of the person's sex, age range and stature was achieved. All these biological characteristics were used in the later stages of the criminal investigation and the person's identification.

Key words: identification, anthropological methods, dismembered corpse

Introduction

One of the basic steps in resolving a criminal case is the identification of the victim. This part of the investigation might be difficult in cases with an advanced stage of decomposition/skeletonization or when there are missing parts of the body (in case of dismemberment). Establishing sex, age and stature can provide information, invaluable for the criminal investigation.

The following forensic case is used to show the accuracy and the informational value of the anthropological methods used in the clinic of forensic medicine at the University Hospital St. Marina - Varna.

A dismembered corpse in advanced stage of decomposition was found in a forested area near an intercity road. The main methods for establishing the time of death were applied, and it was determined that it occurred between the last ten to fourteen days [14]. There were seven body parts (belonging to a single person) which were found in plastic bags:

Part 1 – thorax – from the seventh cervical vertebra to the fifth lumbar vertebra, including all of the ribs, sternum, left and right clavicle and left and right scapula.

Part 2 – pelvis and the hips to the knees, including all pelvic bones and left and right femur.

Part 3 – right upper limb from the shoulder to the elbow, including only the right humerus.

Part 4 – right upper limb from the elbow to the hand, including radius, ulna and all of the hand bones.

Part 5 – left upper limb from the shoulder to the wrist, including the left humerus, radius and ulna.

Part 6 – right lower limb from the knee to the foot, including the right tibia, fibula and all of the foot bones.

Part 7 – left lower limb from the knee to the foot, including the left tibia, fibula and all of the foot bones.

Missing were, the head with the neck and the left hand. A month later, the police found a skull and three cervical vertebrae with some preserved soft tissue on them, belonging to the same person. The left hand and a part of the neck were never found. The identity of this corpse was later confirmed by DNA analysis.

In a case like this, one of the questions that we have to answer what is the identity of the person. DNA analysis is the most well-known and precise method for confirming identity, but its downside is that it is necessary to have comparative material from a supposed person of interest or his/hers blood relative. Acquiring such material can be a time-consuming process, and the police need information about the body, from the initial examination, to narrow the circle of potential subjects and continue the investigation. Forensic medicine experts focus on establishing the biological profile (sex, age and stature) and, if it is possible, some individual features of the person. Determining these characteristics is rarely problematic when the body is whole and well preserved. However, in the cases when the body is severely decomposed or dismembered or when only partial remains are found, the anthropological methods become invaluable for establishing the sex, age, and stature of the person.

Materials and Methods

In this specific forensic case, during the autopsy, an external and internal examination of the body was performed. A detailed description of the traumatic injuries was made and the time of death was determined. The identification features were examined by applying a set of anthropological methods for estimation of sex, age and stature, also blood and tissue samples were set aside for subsequent DNA analysis. These methods are the standard techniques used at the clinic of forensic medicine at the University Hospital St. Marina – Varna, when determining identity and also examining skeletal remains.

1. Sex – When performing a forensic anthropological analysis, sex estimation is one of the first and most important steps [18]. We usually use metric and non-metric methods to determine sex. The non-metric method is based on the presence or degree

of expression of sexually dimorphic traits. Nonmetric techniques for estimating sex are largely focused on the pelvis and cranium as bone conglomerates with well-defined signs of sexual dimorphism [7]. In our practice, we apply Walker's logistics regression equations for sex estimation of the skull and Khaled's method for estimating the sex from the pelvis based on Phenice's nonmetric traits and statistical methods [6, 21, 22]. The metric analysis is based on accurate measurements between specific landmarks of the bones. In our practice, we use a software called "Anthropolog" based on the anthropometric research of V. I. Pashkova and B. D. Reznikov [13,16]. This program analyzes 25 dimensions of the skull and classifies each of them as "definitely male/female", "probably male/female" and "unidentified". At the end, the software classifies the sex of the examined skull as "male", "female" or "unidentified". The software "Anthropolog" contains other options not only for estimation of sex but for determining age and stature. The program can be accessed openly on the Internet [13, 16].

2. Age – In the case study of the dismembered corpse, age-at-death was identified based on cranial sutures closure, changes of the pubic symphyseal surface and the degenerative processes of the bones [4, 11, 13, 16, 17]. The cranial suture assessment requires an observation of the stage of adhesion between the bones on the ectocranial and endocranial surface of the skull. The sutures on the ectocranial surface are rated on a scale between 0 and 4 and those on the endocranial surface between 0 and 3. Those findings were applied into the software "Anthropolog", which then yields separate results for the ectocranial and endocranial condition of the sutures [3, 4, 11, 13, 15, 16, 23]. The pubic symphyseal ageing is analysed using the Suchey-Brooks method with six stages of changes [2, 4, 17]. We always thoroughly check the condition of the bone tissue to search for degenerative processes, like osteoarthritis [4, 15].

3. Stature – We usually apply the method of Trotter and Gleser to estimate stature from long bones, but the software "Anthropolog" has an option to combine different methods for estimation the stature from the same bones. The program's output shows a mean value of stature from every examined long bone [1, 5, 8, 9, 12, 19, 20, 23].

Results

The identity of the person was confirmed using comparative DNA analysis, consequently the actual biological characteristics were compared to the results gained using the above mentioned anthropological methods. The body belonged to a 66 years old, 178 cm tall male. The results are presented in **Table 1**.

The sex estimation methods show a perfect match. All methods, used separately and together, identify the person as male.

The suture adhesion on the ectocranial surface is indicative of a 59 years old person and the same suture on the endocranial surface shows full obliteration, which indicates a person over 65 years. The endocranial condition of the sutures is the only characteristic that roughly matches the person's actual age. The ectocranial condition is 6 years lower than the actual age. However, the adhesion on both surfaces shows a range between 59 and over 65 years, which roughly matches the actual age. The Suchey-Brooks method

shows the 6th phase of symphyseal surface change, which corresponds to a mean age of 61.2 years and a range of 34-86 years old. The mean value is nearly 5 years lower than the actual age. Despite being very wide, the 34-86 years range does include the person’s actual age.

Table 1. Comparison between the true biological characteristics, and the ones estimated using anthropological methods.

Body parts	Used Anthropological method	Result gained using the anthropological method	Actual biological characteristics
Skull	Non-metric method for sex estimation – 3 to 5 score for the different features	male	male
	Metric method for sex estimation – definitely male – 3; probably male – 15; definitely female – 0; probably female – 3; unidentified - 4	male	
Pelvis	Non-metric method for sex estimation – 2 to 5 score for the different features	male	
Skull	Suture closure – score for ectocranial surface – 3 and 4; score for endocranial surface – 3;	59 years based on ectocranial adhesion; >65 years based on endocranial adhesion;	66 years
Pelvis	Pubic symphyseal surface changing – phase 6	Range 34-86, mean 61.2years	
Long bones	Stature from long bones – combined method: Humerus – 359mm Ulna – 281mm Radius – 265mm Femur – 475mm Tibia – 393mm Fibula – 386mm	Average value between 173.83 cm. and 179.04 cm. Humerus – 178.75cm Ulna – 178.22cm Radius – 179.04cm Femur – 173.83cm Tibia – 175.45cm Fibula – 174.6cm	178cm

The combined method for stature estimation returns an average value between 173.83 cm and 179.04 cm, which includes the person’s actual stature (178cm.). In our practice we have noticed that the stature, determined based on the dimensions of the lower limb bones, is more accurate than the one determined based on the upper limb. In the present case however, the values from the humerus, ulna and radius are closer to the actual stature than the others long bones.

Conclusion

In this case study a set of anthropological methods for estimating sex, age and stature was applied with the aim to show their accuracy and informational value. Although this was a case of dismemberment, almost all bones of the human body were found, yet our focus was only on those parts, which showed a high degree of expression of the traits for sex, age and stature. In our practice we also use these anthropological methods in cases where only skeletal remains are found. These types of analyses are usually limited to the few available bones, such as the skull, some of the long bones, and parts of the pelvis, among others.

The methods for sex estimation yield accurate results, individually and when combined. In our usual practice, we always combine the results from the different methods for sex determination. Age estimation is the most challenging task when examining remains. The results of this study are indicative of the difficulty because neither method used here established the exact age. However, both methods helped determine the person's age range.

All long bones of the skeleton were used to determine the person's stature and compare the accuracy of each estimation. The results show that the estimations based on the upper limb are closest to the actual stature.

Overall, the anthropological methods described in this work show good precision: they correctly determined the person's sex, age range and stature. All these biological characteristics were used in the criminal investigation and the person's identification.

References

1. **Alekseev, V. P.** Executive editor I. I. Gokhman – Osteometry. Anthropological Research Methodology-Science, 1966, 44-50. [in Russian]
2. **Brooks, S., J. M. Suchey.** Skeletal age determination based on the os pubis: a comparison of the Acsfidi – Nemeskőri and Suchey-Brooks methods. *Human Evolution*; 1990; 5(3), 227-238.
3. **Byers, S. N.** Introduction to Forensic Anthropology. Taylor & Francis; 2016, p.232-236.
4. **Christensen, A. M., N. V. Passalacqua, E. J. Bartelink.** Forensic Anthropology: Current Methods and Practice. Oxford ; San Diego, California: Academic Press; 2014, 199-222.
5. **Dupertuis, C. W., J. A. Hadden.** On the reconstruction of stature from long bones. – *Am. J. Phys. Anthropol.*, 9, 1951, 15-54.
6. **Klales, A. R., S. D. Ousley, J. M. Vollner.** A revised method of sexing the human innominate using Phenice's nonmetric traits and statistical methods. – *Am. J. Phys. Anthropol.*, 149, 2012, 104-114.
7. **Lewis, C. J., H. M. Garvin.** Reliability of the Walker Cranial Nonmetric Method and Implications for Sex Estimation. – *J. Forensic Sci.*, 61, 2016, 743-751.
8. **Lorke, D., H. Munzener, E. Walter.** Reconstruction of the body size of a person from the long limb bones. – *Dtschz. total judicial Med.*, 1953, 42. [in German]
9. **Manouvrier, L.** Determination of size from the large bones of the limbs. – *Mem Soc. Anthropol. Paris*, 1893; 4: 347-402. [in French]
10. **Martin, R.** A short guide to anthropometric measurements. State Medical Institute, 1929, 74-78. [in Russian]
11. **Meindl, R., C. Lovejoy.** Ectocranial suture closure: A revised method for the determination of skeletal age at death based on the lateral-anterior sutures. – *Am. J. Phys. Anthropol.*, 68, 1985, 57-66.

12. **Nainis, Y.** Forensic-osteological methods of personality identification by the proximal bones of the extremities: Author's abstract. dis. Dr. med. sciences. Tartu, 1966.49 p. [in Russian]
13. **Pashkova, V. I., B. D. Reznikov.** Forensic identification of a person based on bone remains. Saratov University Press 1978, 43-79. [in Russian]
14. **Radanov, S., I. Doychinov, P. Lisaev.** Forensic medicine and medical deontology, Siela 2006, 387-401. [in Bulgarian]
15. **Priya, E.** Methods of Skeletal Age Estimation used by Forensic Anthropologists in Adults: A Review. – FRCIJ, **4**, 2017, 41-51.
16. Program “Anthropolog”, Available at <http://antropol.narod.ru/programs.html>. [in Russian]
17. **Sakaue, K.** Application of the Suchey–Brooks system of pubic age estimation to recent Japanese skeletal material. – AS, **114**, 2006, 59-64.
18. **Spradley, M. K., R. L. Jantz.** Sex estimation in forensic anthropology: skull versus postcranial elements. – J. Forensic Sci., **56**, 2011, 289-96.
19. **Telkka, A.** On the prediction of human stature from the long bones. – Cells Tissues Organs, **9**, 1950, 103-117.
20. **Trotter, M., G. C. Gleser.** Estimation of stature from long bones of American Whites and Negroes. – Am. J. Phys. Anthropol., **10**, 1952, 463-514.
21. **Walker, P. L.** Greater sciatic notch morphology: Sex, age, and population differences. – Am. J. Phys. Anthropol., **127**, 2005, 385-391.
22. **Walker, P. L.** Sexing skulls using discriminant function analysis of visually assessed traits. – Am. J. Phys. Anthropol., **138**, 2008, 39-50.
23. **Yordanov, Y.** Anthropology. 2nd ed. Sofia: Classic and Style Ltd .; 2017, 146-259. [in Bulgarian]

Review Articles

Application of Dermatoglyphics traits of population variation study

Gazmend Temaj

College UBT, Faculty of Medicine and Pharmacy, Kalabriann, Pristina, Kosovo

Corresponding author e-mail: gazmend.temaj@ubt-uni.net

Scientific study of the epidermal ridges in hands, finger, feet, and toes is called dermatoglyphics. The word Dermatoglyphics derives from the Greek word derma = “skin”, and glyph = “carving”, and was used for first time in 1892 by Sir Francis Galton. Dr. Harold Cummins an American scientist is considered the father of fingerprint analysis.

This field has a lot of applications in modern day population and medical research. The present review is focused on the different aspects of dermatoglyphics and also its applications. A brief account about the development of dermatoglyphic studies in Kosovo and some countries in the southeast of Europe has also been discussed.

Key words: Dermatoglyphic analysis, dermatoglyphs and diseases, qualitative analysis, quantitative analysis, Monozygotic and Dizygotic twins

Introduction

Brief History of Dermatoglyphics

Fingerprint traits have been noticed since the ancient times. In China for example, the people have used their fingerprints to stamp the validity of documents. The use of fingerprint as signature in Japan, India and some countries in Europe were well documented. C. A. Mayer a German doctor wrote: “Although the arrangement of skin ridge is never duplicated in two persons, nevertheless the similarities are evident among some individuals” [5].

The first scientist who started to explain dermatoglyphics was Galton [7, 9, 12]; he searched on fingerprints of people and primates. The work of Galton, Herschel and

Faulds [7, 9, 12] has been essential to establishing the individuality and uniqueness of the images, and by this it is possible to identify humans using finger-palm prints as well [8].

A few years later, it has been possible to make a dermatoglyphic description of a foot. After that, a series of scientists continued to study the foot dermatoglyphics [11]. The first monographs are published by Cummins and Middel [5, 6]: the first monograph was about the skin relief in primates [5] and the second about general dermatoglyphics [6].

We know that Bansal (1965) [1], is the first author who wrote a report about bilateral symmetry, he has done measurements of the distance between the triradii of the third and the fourth finger.

Geographical distribution of palmar dermatoglyphic traits in inhabitants of Kosovo

Dermatoglyphic prints were collected from 800 inhabitants of south west Kosovo (Dukagjin valley). The sample consisted of Albanians (N=400) and Turks (N=400). The qualitative traits of dermatoglyphs which are analyzed during this study are: arch, ulnar and radial loop, whorl, accidental whorl and on palms (I, II, III, IV interdigital areas, thenar, hypothenar, main line index, and the axial »t« triradius position). During this study a significant difference in most of qualitative traits between Albanian and Turkish inhabitants was observed. This finding is a good indication of reproductive isolation between Albanian and Turkish inhabitants, despite the fact that both populations lived very close to each other for several centuries [36].

Dermatoglyphic study in the Albanian population from three Kosovo district regions was conducted to analyze qualitative traits. During this study microevolutionary changes were tried to be obtained.

The number of participants in this research was 641 people of Albanian nationality of both sexes. The analysis included arch, ulnar and radial loop, whorl, and accidental whorl on fingers; and on the palm it included the main line, Thenar, I, II, III, IV and hypothenar area.

The significant differences are found on several types between distinct groups in most of the cases. The results from the study by Temaj *et al.* show that inhabitants of the Albanian nationality from South Morava and Kosovo plain are genetically closer; the inhabitants from Dukagjini valley of Albanian nationality are less close to any of them. Temaj *et al.* show that analysis of qualitative dermatoglyphic traits is possible to utilize effectively to track the microevolutionary changes [37].

In order to compare two geographically and culturally isolated ethnic groups of Slavic Muslims from Zhupa and Gora regions in Kosovo, Petranović *et al.* analyzed their quantitative dermatoglyphic traits, compared them with each other and with the Albanian majority population. The ANOVA analysis showed more differences between the Albanians and both minority populations, i.e. between Zhupa and Gora populations. Petranović *et al.*, 2020, also detected selective inertia in Slavic Muslim women. The canonical discriminant analysis grouped the Gora and the Zhupa women together, and at the same time closer to the Gora men than to the Kosovo Plain women. The Gora and Zhupa men were much closer to each other than to the men from the Kosovo Plain. To conclude, the Gora and Zhupa populations differ less from each other, than from the Kosovo Albanians [27].

Geographical distribution of palmar dermatoglyphic traits in inhabitants of other countries in Europe

The qualitative dermatoglyphic traits are analyzed in 22 populations of Romania. These analyses are made by geographical and historical relationship [34].

A study by Karev shows that radial arch in males has a frequency 2.82% and in females 2.82%, among 2,130 Bulgarians [14].

The study by Karev in 264 right-, 246 mixed- and 360 left-handers in Bulgaria, shows that hypothenar radial arch, has a higher frequency on the right palm rather than on the left one [15].

Results from the study by Paraskova and Mitova show that in the studied population of Central Western Bulgaria: 1) an increased incidence of t; 2) decreased occurrence of images of Hy and a frequency of AIT and 3) the mean values for some of the dermatoglyphic traits analyzed are in the upper limits of the Eurasian scale, characteristic of the European population with Eastern characteristics [25].

The study by Kavgazova and Stoev in the region Gotse Delchev (villages of Kornitsa, Breznitsa and Lazhnitsa) have been studied aiming at the distinction of a dermatoglyphic complex specific of this population. The results from this study show that, the whole investigated sample belongs to the Europoid sphere and it is with well-pronounced South-Europoid features [16]. In the study by Kavgazova et al., during the study of population from Central Rhodopes (South Bulgaria) show similarity between the examination population and a number of populations from Volga region, Northern Caucasus, Middle Asia and Siberia. These similarities can explain by preservation of the genetic inheritance of the proto-Bulgarians, one of the three main components of the modern Bulgarians [17].

In the study of different groups from the region of Stradwa (Bulgaria), the bimanual asymmetry in some dermatoglyphic traits as whorls, DL10, accessorial interdigital triradili, index of Cummins and carpal axial triradial-t, from both sexes of the studied population was established [22].

Dermatoglyphic analysis in 279 Maltesians was carried out also for qualitative and quantitative traits. The data from Malta people are compared with 17 other groups of the Mediterranean region; the results show that people from Malta are from the same cluster as the people from Greece, Sardinia and Spain [2].

In Croatia, many studies for qualitative and quantitative dermatoglyphic traits among Croatian inhabitants have been carried out. The study from the Island of Olib for finger and palm traits are compared with dermatoglyphic traits from the Silba island. The finding supports the hypothesis about selective inertia of digital and palm dermatoglyphic traits [32].

Miličić, 2002, conducted a study for latent structure of quantitative dermatoglyphic traits in the population of Middle Dalmatia region especially of the inhabitants of the Brač, Hvar and Korcula islands, the peninsula of Peljesac and Makarska coastal region. She analyzed 18 variables of fingers and palms. The analysis from this study gives information about similarities and differences between the inhabitants who live in these islands and inter – individual variabilities in females compared to males [21].

Nagy and Pap have carried out examinations of dermatoglyphic traits in 11 Hungarian and 5 Gypsy population members for finger and also palm samples. In most of dermatoglyphic traits they found statistical significance, and they came to conclusion that both populations have a different origin and an admixture exists between Hungarians and Gypsies [23].

Association of Dermatoglyphics with Disease

Clinical study conducted in 1936 [6]; Cummins, 1936 [6], at the time pointed dermatoglyphic traits in patients with Down syndrome. Since then a number of studies have been conducted among individuals with different syndromes and chromosomal aberration. Results from different publications revealed smaller or greater deviations from normal finger prints and palm findings. The same was reported by many researchers in numerous genetically determined states.

Huge progress to understanding association of dermatoglyphs with medical disorders was made in the last years.

Many researchers have identified an association of chromosomal aberration with Down syndrome, such as decrease of frequency of whorl on fingertips. Many publications by different authors [13, 30, 31] have shown different frequencies of dermatoglyphic traits in a finger and a palm.

In Edwards's syndrome six or more arches in all fingertips are found. Radial loop on the thumb was found also in many patients compared with normal population [18, 39].

In trisomy 13 or Patau syndrome a radial loop with higher frequency was found, and atd angle for females is 186° and for males 196° [26].

Statistical significance for frequencies of dermatoglyphic traits and gonadal dysgenesis are found also, the report by Skrinjaric et al. [35].

Rudan et al. 1980, suggest that indication dermatoglyphic traits could be applied in the early detection of breast cancer, for the selection of the "high risk group" of diseases [33].

Some authors from India suggest that dermatoglyphic patterns can help effectively to study the genetic basis of breast cancer. Dermatoglyphic traits might prove to be an anatomical, non-invasive, inexpensive and effective tool for screening and studying the patterns in the high-risk population [4].

In the study by Raizada et al., 2013 [28] a significant increase in the arch pattern and a decrease in the radial loops in the right thumb, the left thumb, the left index finger and the left middle finger ($p < 0.001$) is shown. A comparison for all fingers of both hands (left and right) in patients with breast cancer shows higher frequencies compared with control group. The lower values of the TFRC (total finger right count (below 50) is shown to be associated with carcinoma breast. Also it shows lower values of the AFRC (absolute finger right count) (below 100) to be associated with the cancer patients.

Dermatoglyphic traits are a facilitated marker for detection of predisposition of pituitary tumor development, and can help in early treatment of the patients [10].

The results of the study of Novak-Laus et al., 2005 [24] reveal that patients with glaucoma have genetic predisposition to develop primary open-angle glaucoma, thus emphasizing the relevance of hereditary factors in the etiopathogenesis of this disease.

Statistical significance is found also between patients with psoriasis and control group for loop, arch and composite patterns, but statistical significance for whorl pattern is not observed. Similarly, statistical significance is found between patients with diseases alopecia areata and control group for loop and arch patterns, but no significant difference regarding the whorl pattern. There was no significant difference regarding any of the dermatoglyphic traits between vitiligo and pemphigus vulgaris patients and controls [29].

Dermatoglyphic trait analysis in twin diagnosis

Twins study appeared to be a good method for genetic predisposition and environment influence. This is shown by Galton 1875 [9]; he has made several experiments to explain environmental influence and genetic inheritance. Galton 1875 [9], has prepared different question test to achieve his aim and to explain manner of genetic inheritance. Today different studies from different disciplines such as psychology, morphology and genetics are used to explain influence of environment factors and genetic inheritance in twins.

Dermatoglyphic traits such as qualitative and quantitative traits are an important element of the twin method study. Dermatoglyphic traits in twin method study lead to the advance of discipline such as medicine (used to establish relationship between change in skin and to explain inheritance of chromosomal disorders as well as to determine the zygotic twins); anthropology (used to explain the origin of different population); criminology (used to solve different questions, rejection or identification of an individual).

Polish twins show a higher value of genetic parameters in hypothenar region [19].

Genetic factors appear to play a pivotal role in the determination of dermatoglyphic traits in monozygotic and dizygotic twins; it appears that genetic effect determines the distribution of traits with intermediate value in hypothenar and thenar region [3].

Twins examination in Albanian population of Kosovo for qualitative traits in hypothenar appears to have a sharply higher heritability in thenar and weak genetic component in hypothenar [38].

In Bulgarian twins for qualitative traits it appears that radial loop is higher in hypothenar in monozygotic twins and dizygotic twins; while ulnar arch is higher in the left hand of dizygotic twins and the right hand of monozygotic twins [20].

Conclusion

The present review briefly explains application of dermatoglyphic traits in genetic population study, identification, inheritance, and twins study, association of different diseases and chromosomal aberration with dermatoglyphics. Dermatoglyphic traits study gives higher contribution to explaining the human variation in genetic population, genetic inheritance and diagnosis for different diseases.

“Dermatoglyphics” in the future might play a significant role not only for the purpose of screening but also for studying and behavior of breast and other cancer diseases.

In conclusion, it is noteworthy that comprehensive dermatoglyphic traits research in genetic population and twins is needed to further elucidate the intimate relationships between heritability and environment in human pathology.

References

1. **Bansal, I. J. S.** Palmar dermatoglyphics in maharashtrians in India. – *Acta geneticae medicae et gemellologiae*, **14**(4), 1965, 431-437.
2. **Bozicevic, D., J. Milicic, J. Ndhlowu, D. Pavicevic, P. Rudan, A. Vassalo.** Dermatoglyphic Traits in the Malta Population. – *Coll. Antropol.*, **17**(1), 1993, 137-146.
3. **Callegari-Jacques, S. M., F. M. Salzano, H. F. Pena.** Palmar dermatoglyphic patterns in twins. – *Hum. Hered.*, **27**, 1977, 437-443.
4. **Chintamani Khandelwal, R., A. Mittal, S. Saijanani, A. Tuteja, A. Bansal, D. Bhatnagar, S. Saxena.** Qualitative and quantitative dermatoglyphic traits in patients with breast cancer: a prospective clinical study. – *BMC Cancer*, **13**, 2007, 7, 44.
5. **Cummins, H.** The topographic history of volar pads (walking pads, Tastballen) in the human embryo. – *Contrib. Embryol. Carnegie. Inst. Wash.*, **20**, 1929, 103-126.
6. **Cummins, H., C. Midlo.** *Fingerprints, Palms, and Soles. An Introduction to Dermatoglyphics.* New York, USA, Dover Publications, 1961.
7. **Faulds, H.** *Guide to Finger-print Identification.* Hanley, Wood, Mitchell & Co Ltd, 1905.
8. **Fournier, N., H. Ross.** Sex, ancestral, and pattern type variation of fingerprint minutiae: A forensic perspective on anthropological dermatoglyphics. – *J. Am. Phys. Anthropol.*, **158**(3), 2015, 78-84.
9. **Galton, F.** The history of twins, as a criterion of the relative powers of nature and nurture. – *Fraser's Magazine*, **12**, 1875, 566-576.
10. **Gradiser, M., M. Matovinovic Osvatic, D. Dilber, I. Bilic-Curcic.** Assessment of Environmental and Hereditary Influence on Development of Pituitary Tumors Using Dermatoglyphic Traits and Their Potential as Screening Markers. – *Int. J. Environ. Res. Public Health*, **13**(3), 2016, 330.
11. **Hepburn, D.** *The Papillary Ridges of the Hands and Feet of Monkeys and Men.* – Royal Dublin Society, **538**, 1895.
12. **Herschel, W. J.** *The Origin of Finger-Printing.* Oxford University Press, London, 1916
13. **Holt, S. B., J. Lindsten.** Dermatoglyphic anomalies in Turner's syndrome. – *Ann. Hum. Genet. Lond.*, **28**, 1964, 87-100.
14. **Karev, G. B.** Hypothenar radial arch in man: observations on its distribution, morphology, symmetry, and inheritance. – *Am. J. Phys. Anthropol.*, **84**(4), 1991, 479-487.
15. **Karev, G. B.** Three palmar dermatoglyphic traits and their asymmetry in Bulgarian right-, mixed- and left-handers. – *Anthropol. Anz.*, **68**(3), 2011, 291-307.
16. **Kavgazova, L., R. Stoev.** Dermatoglyphic characteristics of a population from Gotse Delchev region (South-Western Bulgaria). – *Acta morphol. anthropol.*, **5**, 2000, 115-120.
17. **Kavgazova, L., R. Stoev, Z. Mitova.** Dermatoglyphic characteristics of a population from the Central Rhodopes (South Bulgaria). – *Anthr. Anzeiger*, **57**(4), 2000, 349-360.
18. **Loeffler, L.** Papillary ridges and cutaneous furrows (Papillarleisten-und Hautfurchensystem). In Becker, P. E. (Ed.): *Humangenetik.* Stuttgart, Georg ThiemeVerlag, **Vol. I/2**, 1969, pp. 205-408.
19. **Loesch, D.** Genetical studies of the palmar and sole patterns and some dermnatoglyphic measurements in twins. – *Ann. Hum. Genet.*, **43**(1), 1979, 37-53.
20. **Maslarski, I. I., L. F. Belenska.** Qualitative analysis of prints of palms and fingers of twins. – *J. Global Biosci.*, **4**, 2015, 2833-2841.
21. **Miličić, J.** Latent structure of quantitative dermatoglyphic traits of middle Dalmatia (Croatia). – *Coll. Antropol.*, **26**, 2002, 39-45.
22. **Minkov, Tsv., V. Dimitrova, S. Maximova.** Anthropological characterization of Bulgarian population from the region of Strandja according to dermatoglyphic data. – *Glasnik ADJ*, **36**, 2001, 123-130.

23. **Nagy, A. S., M. Pap.** Comparative analysis of dermatoglyphic traits in Hungarian and Gypsy populations. – *Hum. Biol.*, **76**(3), 2004, 383-400.
24. **Novak-Laus, K., J. Milicić, E. Tedeschi-Reiner, R. Iveković, V. Mijić, S. Masnec-Paskvalin, O. Zrinsćak, Z. Mandić.** Analysis of the quantitative dermatoglyphic traits of the digito-palmar complex in patients with primary open angle glaucoma. – *Coll. Antropol.*, **29**(2), 2005, 637-642.
25. **Paraskova, N., Z. Mitova.** Southeuropoid Speciphics in the Dermatoglyphic Characteristics of the Bulgarian Population from Central Western Bulgaria. – *Acta morphol. anthropol.*, **26**(1-2), 2019, 71-78.
26. **Penrose, L. S., S. B. Holt.** Note on dermatoglyphic data in a brachydactylous family. – *Ann. Hum. Genet.*, **29**, 1966, 383.
27. **Petranović, M. Z., Ž. Tomas, T. Škarić-Jurić, A. Moder, S. Xharra, K. Sopi, R. Hadžiselimović, H. Nefić, G. Temaj.** Palmar and Finger Ridge Count in Two Isolated Slavic Muslim Populations (Zhupa and Gora) from Kosovo in Comparison with Kosovo Albanians. – *Acta morphol. anthropol.*, **27**(3-4), 2020, 82-93.
28. **Raizada, A., V. Johri, T. Ramnath, D. Chowdhary, R. Garg.** A cross-sectional study on the palmar dermatoglyphics in relation to carcinoma breast patients. – *J. Clin. Diagn. Res.*, **7**(4), 2013, 609-612.
29. **Rather, A. P., I. Hassan, S. Naaz, R. Khan, F. Rasool.** Dermatoglyphic Patterns in Various Dermatoses among Kashmiri Population: A Case Control Study. – *Egyptian Dermatology Online Journal*, **10**(1), 2014, 1-11.
30. **Reed, T.** Dermatoglyphics in Down's syndrome. – *Clinical Genetics.*, **(6)**, 1974, 236.
31. **Reed, T. E., D. S. Borgaonkar, P. M. Conneally, P. Yu, W. E. Nance, J. C. Christian.** Dermatoglyphic nomogram for the diagnosis of Down's syndrome. – *J. Pediatr.*, **77**, 1970, 1024-1032.
32. **Rudan, P., D. Letinic, A. Chaventre.** Digital and Palm Dermatoglyphs of the Population of the Island of Olib (Yugoslavia)-Analysis of Microevolutionary Patterns. – *Coll. Antropol.*, **8**(2), 1984, 201-212.
33. **Rudan, P., Z. Pisl, B. Basek, I. Skrinjaric, F. Budiman, P. Nola, N. Rudan, Z. Maricic, I. Prodan.** Quantitative dermatoglyphic traits in patients with breast cancer-preliminary report. – *Acta med. Iug.*, **34**, 1980, 73-79.
34. **Scheil, H. G., H. D. Schmidt, C. Vulpe, A. Tarcă.** Dermatoglyphic studies in Romania. – *Anthropol. Anz.*, **66**(3), 2008, 273-279.
35. **Skrinjaric, I., Z. Kaic, Z. Poje, M. Dumic, Lj. Zergollern.** Dermatoglyphic in gonadal dysgenesis: analysis of palmar patterns. – *Acta med. Iug.*, **40**, 1986, 39-48.
36. **Temaj, G., J. Milicić, T. Skarić-Jurić, I. Behluli, N. Smolej-Narancić, R. Hadžiselimović, H. Nefić.** Comparative analysis of dermatoglyphic traits in Albanian and Turkish population living in Kosovo. – *Coll. Antropol.*, **33**(4), 2009, 1001-1005.
37. **Temaj, G., M. Z. Petranović, T. Skarić-Jurić, I. Behluli, N. S. Narancić, S. Xharra, R. Sopi, J. Milicić.** A detection of microevolutionary changes by the analysis of qualitative dermatoglyphic traits: an example of Albanians from Kosovo. – *Anthropol. Anz.*, **69**(4), 2012, 461-472.
38. **Temaj, G., T. Škarić-Jurić, Ž. Tomas, I. Behluli, N. Smolej-Narancić, R. Sopi, M. Jakupi, J. Miličić.** Qualitative dermatoglyphic traits in monozygotic and dizygotic twins of Albanian population in Kosovo. – *Homo*, **63**(6), 2012, 459-467.
39. **Uchida, I. A., H. C. Soltan.** Evaluation of dermatoglyphics in medical genetics. – *Pediatr. Clin. North Am.*, **10**, 1963, 409.

Role of dermatoglyphics for breast cancer prevention and prognosis

Tsonka Dimitrova

Department of Biology, Faculty of Pharmacy, Medical University of Varna, Varna, Bulgaria

* Corresponding author e-mail: tsonka72@abv.bg

Breast cancer in women is an oncological disease with a great medico-social importance because of its wide dissemination, ineffective mass prevention, difficult early diagnosis and unsuccessful delayed treatment. Recently, the armamentarium of preventive methods has been enriched by dermatoglyphics. In the present concise survey, some recent publications by foreign and Bulgarian authors devoted to the role of the dermatoglyphics for the prevention and prognosis of female breast cancer are presented. A special attention is paid to the significant differences between breast cancer females and healthy controls in terms of the qualitative and quantitative dactyloscopic and palmoscopic traits as well as the fluctuation asymmetry findings which could serve as cost-effective and trustworthy analytical tools for effective breast cancer prevention and prognosis.

Key words: female breast cancer, dermatoglyphics, prevention, prognosis

Introduction

Breast cancer in women represents a very serious medical and social problem in the whole world and engages united efforts of scientists and clinicians who uninterruptedly aim at achieving effective prophylaxis, early diagnosis and timely adequate treatment of this malignant disease. Numerous methods for screening and prevention have been developed and applied in many countries. During the recent decades, dermatoglyphics has been successfully introduced for breast cancer prevention and diagnosis in several countries in Asia, Africa and Europe as well.

The purpose of this concise review is to summarize some recent publications devoted to the role of the dermatoglyphics for the prevention and prognosis of female breast cancer.

Challenges of female breast cancer epidemiology

Nowadays breast cancer is the most common malignant neoplasm in women worldwide and in Bulgaria as well. Its incidence rate in Bulgaria and, especially in Northeast

Bulgaria, is permanently high [31,35]. There is an increasing overall trend of newly-diagnosed breast cancer in 53 African countries during the period between 1990 and 2016 [20]. The interest in modern prevention of this socially significant disease continuously increases [21,30,36,39].

The updated estimates on the global cancer burden using the GLOBOCAN 2020 of cancer incidence and mortality produced by the International Agency for Research on Cancer show that female breast cancer is the most frequent malignant neoplasm in women [28]. In 2020, there are a total of 2 261 419 new breast cancer cases (or 1.7%) and 684996 new breast cancer deaths (or 6.9% of all cancer cases) worldwide [9,28]. According to 2018 GLOBOCAN data, breast cancer age-standardized incidence rates are strongly and positively associated with the human development index [24].

The results from the application of mortality and population figures from the WHO and Eurostat databases during the period 1989-2021 demonstrate that progress in cancer epidemiology as well as in primary and secondary cancer prevention because of optimal adoption of breast cancer screening is a key determinant of the decreasing cancer mortality in Europe [6].

Palmar dermatoglyphics is simple, inexpensive, anatomical and non-invasive method [26] that is applied in a variety of medical fields. Several papers describe the peculiarities of the dermatoglyphic examinations in breast cancer patients [22,25,36]. They may be used as a reliable indicator for screening of high-risk population in terms of breast cancer. Usually, two basic classic dermatoglyphic methods are made use of: i) dactyloscopy of finger ridge count and finger indices and ii) palmoscopy assessing the palmar ridge count, palmar maximal atd, adt and dat angles, and palmar main lines A, B, C, and D [4].

In the present survey, the qualitative and quantitative dermatoglyphic traits as well as the fluctuation asymmetry findings are compared between female breast cancer patients and healthy women and the role of their significant differences in terms of disease prevention and prognosis are outlined.

Qualitative palmar dermatoglyphic traits

There are statistically significant differences between 82 breast cancer females and 60 healthy ones in the region of Varna, Bulgaria, in terms of the mean value of palmar thenar fields ($p=0.006$) as well as of the number and frequency of the palmar patterns in the II-IV interdigital fields of the hypothenar of the left hand ($\chi^2=4.220$; $p=0.040$) and right hand ($\chi^2=5.691$; $p=0.017$) [33]. The frequencies of the arches in left-hand ($t=2.025$; $p<0.05$) and in right-hand hypothenar ($t=2.700$; $p<0.01$) are significantly less while the frequency of the loops in left-hand hypothenar is reliably higher ($t=2.028$; $p<0.05$) in breast cancer females than in healthy ones. The sum frequencies of the arches, loops, whorls and image traces in right-hand hypothenar differ significantly between patients and controls ($\chi^2=3.228$; $p=0.006$).

The sum frequencies of left thumb, left and right index finger papillary traits differ significantly between breast cancer patients and healthy controls ($\chi^2=3.872$; $p=0.049$; $\chi^2=49.532$; $p=0.0001$ and $\chi^2=16.153$; $p=0.0001$; respectively) [37]. The frequencies of arches ($p<0.001$), ulnar loop ($p<0.001$) and whorls ($p<0.0001$) of index finger, of arches

of the left-hand fourth finger ($p<0.05$) and little finger ($p<0.05$) as well as of whorls of right-hand index finger, third finger and little finger are significantly different from those of healthy females ($p<0.001$; $p<0.05$ and $p<0.05$, respectively). The frequencies of whorls of patients' right index, middle and little fingers are significantly different from those of healthy females ($p<0.001$; $p<0.05$ and $p<0.05$, respectively). The total frequencies of left and right finger papillary traits differ significantly between breast cancer patients and healthy controls ($\chi^2=18.708$; $p=0.0001$ and $\chi^2=24.594$; $p=0.0001$, respectively). The total frequency of the finger papillary traits of the left and right hand as well as of both hands differs significantly between breast cancer patients and healthy controls ($\chi^2=79.345$; $p=0.0001$) [37].

The sum frequency distributions of the papillary traits of left-hand, right-hand and both-hands' fingerprints differ significantly between patients and controls ($p=0.0001$ each) in the region of Varna, Bulgaria [31]. The frequencies of palmar patterns in left-hand and right-hand c-d IV differ significantly between both groups ($\chi^2=28.828$; $p=0.0001$ and $\chi^2=18.517$; $p=0.0001$, respectively).

In left-hand fourth and little fingers, there are less ulnar loops and arches but more whorls in 50 breast cancer women aged between 30 and 70 years than in 50 age-matched healthy women in India [2]. There are significantly higher frequencies of fingerprint whorls and of fingerprints with ≥ 6 whorls in 122 breast cancer women than in 22 healthy controls in China ($p<0.001$ and $p<0.01$, respectively) [11]. The frequency of ≥ 6 whorls is statistically reliably higher in 60 breast cancer females than in 60 healthy ones ($\chi^2=5.71$; $p<0.02$) [3]. The sum frequency of whorls of right-hand index finger and little finger is higher in these patients than in control subjects, too ($\chi^2=5.67$; $p<0.02$ and $\chi^2=7.67$; $p<0.01$, respectively).

There is a reliably higher frequency of fingerprints with ≥ 6 whorls in 154 breast cancer females (in 48.7%; $\chi^2=27.452$; $p<0.05$) and in 154 ones with increased breast cancer risk (in 47.4%; $\chi^2=61.821$; $p<0.05$) than in 308 healthy controls (in 27.5% of the cases) in Tehran, Iran [1]. The frequency of fingerprints with ≥ 6 loops is significantly higher in 100 breast cancer women than in 100 healthy ones ($p<0.01$) [16]. The presence of either of radial or ulnar whorls, or of arches in ≥ 6 fingers in combination with the absence or radial loops and central whorls is significantly associated with breast cancer in 100 females as compared with 100 healthy controls in India [18].

In 50 breast cancer women aged between 25 and 60 years in India, there is a significantly higher frequency of left-hand and both-hands' arches (each $p<0.05$), of left-hand and both-hands' whorls (each $p<0.05$) and of right-hand whorls ($p<0.01$) than in 50 age-matched healthy women [27]. The number of ulnar loops of the right-hand third and fourth fingers as well as of the left-hand index finger is reliably greater in 100 breast cancer women aged between 30 and 60 years than in 100 age-matched healthy ones in India ($p<0.028$, $p=0.030$ and $p<0.048$, respectively) [26]. The number of right-hand and left-hand ulnar loops is significantly smaller (34.4% versus 76.8% and 34.6% versus 77.0%, respectively), while the number of whorls of these hands is statistically reliably greater (53.2% versus 15.8% and 56.0% versus 16.2%) in 100 breast cancer females than in 100 healthy ones in India [12].

Quantitative dactyloscopic findings

There are significant differences between 82 breast cancer women and 60 healthy ones in the region of Varna, Bulgaria, concerning the finger ridge counts of left-hand index finger ($p=0.043$) and third finger ($p=0.049$) as well as of right-hand thumb ($p=0.0001$) and index finger ($p=0.032$) (38). Total mean ridge counts of all the fingers of the right hand and both hands are significantly greater in patients than in controls ($p=0.027$ and $p=0.039$, respectively). The values of the correlation coefficients of the ridge counts of the first, second and fifth homologous fingers of both hands are smaller while those of the third and fourth homologous fingers of both hands are greater in breast cancer patients than in healthy females. There is a statistically significant difference concerning the third fingers only ($p<0.05$).

By using one-way ANOVA of the ridge counts of a-b, b-c and c-d, the presence of a significant difference between intergroup variation, on the one hand, and residual (not explained) variation, on the other hand, concerning the ridge count of b-c ($F=77,134$; $p=0,0001$) is proved [31].

The values of two specific finger indexes, i.e. Dankmeijer index and Poll index of the left hand, right hand and both hands are considerably smaller while those of the P. I. I. Cummins index, Geipel index and Furuhashi index of the left hand, right hand and both hands are considerably greater in breast cancer patients than in healthy females [38].

Quantitative palmoscopic findings

The results from independent t -test demonstrate that mean values of left-hand palmar ridge counts b-c III ($t=7.07$; $p=0.0001$) and a-d ($t=2.53$; $p=0.012$) as well as of right-hand ones ($p=0.0001$ and $p=0.0001$, respectively) are significantly higher in 82 breast cancer females than in 60 healthy ones in the region of Varna, Bulgaria [31]. Mean values of palmar ridge counts of both hands b-c III ($t=9.21$; $p=0,0001$) and a-d ($p=0.001$) are significantly greater in patients than in healthy women.

The frequencies of left-hand palmar main line A ($\chi^2=14.96$; $p=0.0001$), A 3(+4) ($p<0.001$) and A 5(5'+5''+6) ($p<0.001$) and of palmar main line D ($\chi^2=32.86$; $p=0.0001$), D 9(+10) ($p<0.0001$) and D 11(+12+13) ($p<0.0001$) are reliably different between the patients and controls [32].

There are statistically significantly different frequencies in terms of the palmar main line A ($\chi^2=22.51$; $p=0.0001$), A 3(+4) ($p<0.001$), A 5(5'+5''+6) ($p<0.001$), palmar main line D ($\chi^2=15.65$; $p=0.0001$), D 9(+10) ($p<0.001$), D 11(+12+13) ($p<0.001$), palmar main line B (absence) ($p<0.05$) as well as of palmar main line C (absence) ($p<0.02$) of the right hand between both groups [32].

In three equal groups of 50 women each, there are reliable differences in terms of total and absolute finger ridge counts between breast cancer females and high-breast cancer risk ones, on the one hand, and healthy women, on the other hand ($p<0.05$) (8). Mean finger ridge counts of the left hand and right hand are smaller in 60 women

with pathohistologically proved breast cancer than in 60 age-matched healthy women (12.4 ± 2.33 versus 18.4 ± 4.58 ; $p < 0.05$ and 12.4 ± 1.62 versus 19.64 ± 4.67 ; $p < 0.03$, respectively) [3]. Finger ridge counts in each digit of both hands are greater ($p < 0.001$) in 100 breast cancer women aged 30-60 years than in 100 age-matched controls in India [26]. There are reliable differences concerning the total right-hand finger ridge count (60.97 ± 14.09 versus 47.41 ± 14.11 ; $p = 0.001$) and the left-hand one (59.36 ± 14.54 versus 47.48 ± 14.01 ; $p = 0.001$) between these patients and controls.

The mean total finger ridge count is smaller in 40 breast cancer women than in 40 healthy ones in India (89.88 ± 13.26 versus 119 ± 10.4 ; $p < 0.001$) [5]. The total finger ridge count is greater ($p \leq 0.001$) in 100 women with pathohistologically proved breast cancer women aged 30-50 years than in 100 age-matched controls in India [12] while it is smaller in 20 women aged 20-60 years with malignant breast diseases than in 25 age-matched controls in Nigeria (12.76 ± 0.21 versus 15.51 ± 0.68) ($p < 0.05$) [17]. The mean values of the absolute finger ridge count are significantly greater in 100 breast cancer females aged 30-60 years than in 100 age-matched controls in India ($p < 0.003$) [26]. The absolute finger ridge count in 100 breast cancer women at a mean age of 45.6 ± 11.0 years differs significantly from that in 100 healthy women at a mean age of 33.3 ± 14.96 years ($\chi^2 = 12.22$; $p < 0.002$) [19].

The mean right-hand a-b ridge counts are 36.79 ± 7.51 in 100 breast cancer patients and 31.40 ± 4.91 in 100 age-matched controls while the mean left-hand a-b ridge counts are 35.18 ± 5.94 and 29.74 ± 5.53 , respectively ($p < 0.001$) [26]. There is a smaller mean right-hand a-b ridge count (30.83 versus 36.53 ; $p \leq 0.0015$) and left-hand one (32.70 versus 39.16 ; $p \leq 0.0003$) in 30 breast cancer females than in 30 healthy females [7] as well as right-hand and left-hand a-b ridge count ($p \leq 0.001$) in other 100 patients aged 30-50 years against other 100 age-matched controls in India [12]. The mean right-hand a-b ridge count (37.08 ± 2.58 versus 33.63 ± 1.97 ; $p < 0.001$) and the mean left-hand one (37.05 ± 2.93 versus 34.45 ± 2.98 ; $p < 0.001$) are greater in 40 breast cancer women than in 40 healthy ones in India [5]. In 150 Indian women divided in three equal groups of 50 women each, there are statistically significant differences concerning the a-b ridge count between breast cancer women and high-breast cancer risk ones, on the one hand, and healthy women, on the other hand ($p < 0.05$) [8]. There is a higher mean intensity index of the finger papillary traits in 60 breast cancer females than in 60 age-matched healthy women (12.91 versus 11.33 ; $t = 2.10$; $p < 0.03$) (3) as well as of PII Cummins finger index in 30 patients than in 30 age-matched controls (13.73 ± 4.9 versus 11.26 ± 4.45 ; $p \leq 0.0046$) [7].

The examination of the palmar dermatoglyphic traits of three equal groups of 50 women each indicates statistically significant differences in terms of atd angle between breast cancer females and high-breast cancer risk ones, on the one hand, and healthy women, on the other hand ($p < 0.05$) [8]. There is a higher incidence of an increased atd angle and b-c ridge count in breast cancer patients in Bosna and Herzegovina [14]. The mean value of right-hand atd angle is significantly smaller ($38.78^\circ \pm 2.08^\circ$ versus $42.44^\circ \pm 2.18^\circ$; $p < 0.05$) while that of dat angle is greater ($62.90^\circ \pm 2.85^\circ$ versus $58.20^\circ \pm 2.60^\circ$; $p < 0.05$) in 20 women aged 20-60 years with malignant breast diseases than in 25 healthy women in Nigeria [17]. The significant quantitative palmoscopic differences between 50 breast cancer females and 50 healthy ones aged 25-60 years in India present with significantly

greater atd angle values of the left hand ($p<0.05$) and of both hands ($p<0.05$) as well [27]. The mean atd angle values of the left and the right hand is smaller (41.5° versus 44.43° ; $p\leq 0.021$ and 41.6° versus 44.56° ; $p\leq 0.036$, respectively) among 30 breast cancer females than among 30 healthy women in India [7].

The mean right-hand atd-angle value (42.65 ± 4.14 versus 37.18 ± 2.58 ; $p<0.001$) and left-hand one (42.93 ± 3.93 versus 38.15 ± 2.68 ; $p<0.001$) are significantly greater in 40 breast cancer women than in 40 healthy ones in India [5]. There are statistically reliably smaller left-hand and right-hand atd angle values in 100 females with pathohistologically confirmed breast cancer ($p\leq 0.005$) than in 100 healthy females in India [12]. There are reliable differences in terms of the right-hand atd angle (77.75 ± 4.75 versus 79.30 ± 5.43 ; $p=0.028$) and left-hand one (77.61 ± 3.89 versus 79.41 ± 4.72 ; $p=0.004$) as well as concerning the dat angle (58.34 ± 4.99 versus 56.14 ± 4.97 ; $p=0.002$) between 100 breast cancer females and 100 controls in India [26]. The patterns of atd angle demonstrate a significant difference between the left and right palms of breast cancer patients in Bosna and Herzegovina and this palmar parameter identifies women with increased breast cancer risk [13].

The existence of genetic predisposition for breast cancer development is confirmed by the quantitative digital dermatoglyphic analysis in Bosna and Herzegovina [15].

Fluctuating asymmetry

Breast fluctuating asymmetry is higher in healthy women who are free of breast disease but subsequently develop breast cancer than in women who remain disease-free in the same period and both absolute and relative breast volume asymmetries are higher in women who develop cancer than in the control group [23].

The regression analysis of the fluctuating asymmetry in 82 breast cancer women and 60 healthy ones in the region of Varna, Bulgaria, reveals statistically significantly higher correlation coefficient values of the fourth fingers of both hands in breast cancer females than in healthy controls ($p<0.05$) [34]. There are considerably greater fluctuating asymmetry values of a-b II, c-d IV, and a-d palmar ridge counts concerning the fluctuating asymmetry in breast cancer females than in healthy ones. There are higher correlation coefficient values of the fluctuating asymmetry ($1-r^2$) in the ridge count of the homologous thumbs, forefingers and little fingers of both hands.

There is certain evidence that dermatoglyphic fluctuating asymmetry patterns could add some essential diagnostic and prognostic information in breast cancer patients and thus contribute to more effective screening and prevention [29].

There are significant differences between 112 breast cancer women and 112 healthy controls in Han ethnic from Ningxia, China, in terms of the fluctuating asymmetry of the right thumb finger ridge count and atd angle ($p<0.05$), the little finger and atd angle ($p<0.01$) as well as of the little finger and the ridge count of the fourth finger ($p<0.05$) [10]. Fluctuation asymmetry values of both hands derived from quantitative parameters such as finger ridge counts, a-b ridge counts and palmar angles are significantly greater in 100 breast cancer females than in 100 healthy controls for the thumb (by 2.01 times), subtotal ridge count (by 2.10 times) and palmar atd angle (by 2.01 times) in India [16].

Conclusion

These data convincingly prove that qualitative and quantitative dermatoglyphics has been used in different countries as a valuable cost-effective, non-invasive diagnostic and prognostic tool in the socially significant field of breast cancer. The purposeful application of these modern examinations among risk groups could undoubtedly contribute to the further enrichment of the screening and prognostic armamentarium of dermatoglyphics in terms of effective breast cancer prevention and prognosis. The analytical dermatoglyphic approach should be more widely applied in our country.

References

1. Abbasi, S., N. Einollahi, N. Dashti, F. Vaez-Zadeh. Study of dermatoglyphic patterns of hands in women with breast cancer. – *Pakistan J. Med. Sci.*, **22**(1), 2006, 18-22.
2. Abilasha, S., R. Harisudha, C. S. Janaki. Dermatoglyphics: A predictor tool to analyze the occurrence of breast cancer. – *Int. J. Med. Res. Health Sci.*, **3**(1), 2014, 28-31.
3. Chintamani, K. R., A. Mittal, S. Saijanani, A. Tuteja, A. Bansal, D. Bhatnagar, S. Saxena. Qualitative and quantitative dermatoglyphic traits in patients with breast cancer: a prospective clinical study. – *BMC Cancer*, **7**, 2007, 44.
4. Cummins, H., C. Midlo. Finger prints palms and soles. An introduction in dermatoglyphics. Blakinston, Philadelphia, New York: Reprinted Dower, 1961. 319 p.
5. Gul, S., N. Jabeen, S. Gupta, S. Raina. Palmar dermatoglyphic and breast cancer: A possible correlation. – *Int. J. Med. Health Res.*, **4**(2), 2018, 53-55.
6. La Vecchia, C., E. Negri, G. Carioli. Progress in cancer epidemiology: avoided deaths in Europe over the last three decades. – *Eur. J. Cancer Prev.*, 2021 Aug 26. doi: 10.1097/CEJ.0000000000000714.
7. Lavanya, J., P. Saraswathi, J. Vijayakumar, S. Prathap. Analysis of dermatoglyphic traits in patients with breast cancer. – *J. Pharm. Biomed. Sci.*, **23**(24), 2012, 1-5.
8. Lavanya, J., J. Vijayakumar, S. Prathap, J. Alagesan. Digital and palmar dermal ridge patterns in population with breast carcinoma. – *Biomedicine (India)*, **34**(3), 2014, 315-321.
9. Lei, S., R. Zheng, S. Zhang, S. Wang, R. Chen, K. Sun, H. Zeng, J. Zhou, W. Wei. Global patterns of breast cancer incidence and mortality: A population-based cancer registry data analysis from 2000 to 2020. – *Cancer Commun (Lond)*. 2021 Aug 16. doi: 10.1002/cac2.12207.
10. Lu, H., Z. H. Huo, P. Gao, J. Chen, T. Li, Z. Y. Shi, L. Peng. Fluctuating asymmetry of dermatoglyphy in breast cancer patients. – *Acta Anat. Sinica*, **40**(1), 2009, 37-40.
11. Lu, H., Z. H. Huo, J. Dang, L. Peng, Z. Y. Shi, H. Y. Jiao. Dermatoglyphic patterns of hands in breast cancer. – *Acta Anat. Sinica*, **41**(5), 2010, 733-736.
12. Madhavi, D., S. Dorairaj, S. S. J. Dorairaj, H. Kommuru. Dermatoglyphic study in breast carcinoma patients. – *Int. J. Sci. Res.*, **5**(10), 2016, 837-840.
13. Metovic, A., J. Musanovic, S. Alicelebic, E. Pepic, S. Sljuka, M. Mulic. Predictive analysis of palmar dermatoglyphics in patients with breast cancer for small Bosnian-Herzegovinian population. – *Med. Arch.*, **72**(5), 2018, 357-361.
14. Musanovic, J., A. Metovic, E. Pepic, D. Kopic, E. Cosovic, D. Rebic, O. Lepara. Predictive values of quantitative analysis of finger and palmar dermatoglyphics in patients with breast cancer for Bosnian-Herzegovinian population. – *J. Evolution Med. Dent. Sci.*, **7**(24), 2018, 2855-2860.

15. **Mušanović, J., A. Metović, F. Husremović, S. Bejić, A. Hasković, A. Babić, S. Šljuka.** Digital dermatoglyphics in the evaluation of the genetic basis of breast cancer in Bosnian-Herzegovinian population - quantitative analysis. – *Med. glasnik (Zenica)*, **17**(1), 2020, 1-6.
16. **Natekar, P. E., F. M. DeSouza.** Fluctuating asymmetry in dermatoglyphics of carcinoma of breast. – *Indian J. Hum. Genet.*, **12**(3), 2006, 76-81.
17. **Oladipo, G. S., C. W. Paul, I. F. Bob-Manuel, A. D. Iboroma, H. B. Fawehinmi.** Study of digital and palmar dermatoglyphic patterns of Nigerian women with malignant mammary neoplasm. – *J. Appl. Biosci.*, **15**, 2009, 829-834.
18. **Paranjape, V., A. Kundalkar, A. V. Swamy, Y. Kulkarni.** Digital dermatoglyphics in carcinoma of breast. – *Int. J. Cur Res. Rev.*, **7**(21), 2015, 47-52.
19. **Raizada, A., V. Johri, T. Ramnath, D. Chowdhary, R. Garg.** A cross-sectional study on the palmar dermatoglyphics in relation to carcinoma breast patients. – *J. Clin. Diagn. Res.*, **7**(4), 2013, 609-612.
20. **Saberian, M., K. Mehrabani, H. R. Shahraki.** Clustering time trends of breast cancer incidence in Africa: a 27-year longitudinal study in 53 countries. – *Afr. Health Sci.*, **21**(1), 2021, 47-53.
21. **Sadoh, A. E., C. Osime, D. U. Nwaneri, B. C. Ogboghodo, C. O. Eregie, O. Oviawe.** Improving knowledge about breast cancer and breast self examination in female Nigerian adolescents using peer education: a pre-post interventional study. – *BMC Womens Health*, **21**(1), 2021, 328.
22. **Sariri, E., M. Kashanian, M. Vahdat, S. Yari.** Comparison of the dermatoglyphic characteristics of women with and without breast cancer. – *Eur. J. Obstet. Gynecol. Reprod. Biol.*, **160**(2), 2012, 201-204.
23. **Scutt, D., G. A. Lancaster, J. T. Manning.** Breast asymmetry and predisposition to breast cancer. – *Breast Cancer Res.*, **8**(2), 2006, R14. doi:10.1186/bcr1388.
24. **Sharma, R.** Global, regional, national burden of breast cancer in 185 countries: Evidence from GLOBOCAN 2018. – *Breast Cancer Res Treat.*, **187**(2), 2021, 557-567.
25. **Singh, D., B. R. Prabhakar, S. S. Bhalla.** Dermatoglyphic study in breast carcinoma. – *Indian J. Pathol. Microbiol.*, **22**(1), 1979, 27-32.
26. **Sridevi, N. S., C. R. Delphine Silvia, R. Kulkarni, C. Seshagiri.** Palmar dermatoglyphics in carcinoma breast of Indian women. – *Rom. J. Morphol. Embryol.*, **51**(3), 2010, 547-550.
27. **Sukre, S. B., M. Laeeque, A. Mahajan, S. N. Shewale.** Dermatoglyphics in the identification of women either with or at risk of breast cancer. – *Int. J. Basic Med. Sci.*, **3**(5), 2012, 160-165.
28. **Sung, H., J. Ferlay, R. L. Siegel, M. Laversanne, I. Soerjomataram, A. Jemal, F. Bray.** Global cancer statistics 2020: GLOBOCAN estimates of incidence and mortality worldwide for 36 cancers in 185 countries. – *CA Cancer J. Clin.*, **71**(3), 2021, 209-249.
29. **Thornhill, R., A. P. Møller.** Developmental stability, disease and medicine. – *Biol. Rev. Camb. Philos. Soc.*, **72**(4), 1997, 497-548.
30. **Xue, H., R. Qiao, L. Yan, S. Yang, Y. Liang, Y. Liu, Q. Xie, L. Cui, B. Cao.** The correlation between potential “anti-cancer” trace elements and the risk of breast cancer: a case-control study in a Chinese population. – *Front. Oncol.*, **11**, 2021, 646534.
31. **Yaneva, G. A.** Medico-dermatoglyphic study of fingerprints and palmar prints in women with breast cancer in North-Eastern Bulgaria. PhD thesis. Varna, Medical University “Prof. Paraskev Stoyanov” of Varna, 2018. 144 p. (in Bulgarian).
32. **Yaneva, G., G. Ingilizova.** Main line patterns of palmar dermatoglyphics in female breast cancer patients. – *MOJ Anat. Physiol.*, **5**(6), 2018, 345-347.
33. **Yaneva, G., I. Maslarski.** Palmar dermatoglyphic traits on hypothenar and thenar in breast cancer patients. – *Acta morphol. anthropol.*, **25**(3-4), 2018, 165-170.
34. **Yaneva, G.** Breast cancer epidemiology in Northeast Bulgaria. – *Sci. Works Union of Scientists in Bulgaria-Plovdiv*, **22**, 2019, 394-397.
35. **Yaneva, G.** Modern prevention of breast cancer. – *Sci. Works Union of Scientists in Bulgaria-Plovdiv*, **22**, 2019a, 389-393.

36. **Yaneva, G.** Study of dermatoglyphic fluctuating asymmetry in female breast cancer patients. – *Acta morphol. anthropol.*, **26**(1-2), 2019b, 84-89.
37. **Yaneva, G., N. Petrova, D. Ivanov.** Finger papillary traits in Bulgarian female breast cancer patients. – *J. IMAB Annu. Proc. Sci Papers*, **26**(1), 2020, 2998-3004.
38. **Yaneva, G., S. Slavov, I. Kostov, D. Ivanov.** Quantitative dermatoglyphic patterns in female breast cancer patients. – *J. IMAB Annu. Proc. Sci. Papers*, **28**, 2022 (in press).
39. **Yiangou, K., K. Kyriacou, E. Kakouri, Y. Marcou, M. I. Panayiotidis, M. A. Loizidou, A. Hadjisavvas, K. Michailidou.** Combination of a 15-SNP polygenic risk score and classical risk factors for the prediction of breast cancer risk in Cypriot women. – *Cancers (Basel)*, **13**(18), 2021, 4568.

Author Guidelines

Acta morphologica et anthropologica is an open access peer review journal published by Bulgarian Academy of Sciences, Prof. Marin Drinov Publishing House.

Corporate contributors are Bulgarian Academy of Sciences, Institute of Experimental Morphology, Pathology and Anthropology with Museum and Bulgarian Anatomical Society.

Acta morphologica et anthropologica is published in English, 4 issues per year.

The journal accepts manuscripts in the following **fields**: experimental morphology, cell biology and pathology, anatomy and anthropology.

Publication types: original articles, short communications, case reports, reviews, Editorial, letters to the Editors.

Acta morphologica et anthropologica is the continuation of *Acta cytobiologica et morphologica*

The **aim** of the Journal is to disseminate current interdisciplinary biomedical research and to provide a forum for sharing new scientific knowledge and methodology. The general editorial policy is to optimize the process of issuing and distribution of *Acta morphologica et anthropologica* in line with modern standards for scientific periodicals focusing on content, form, and function.

Scope – experimental morphology, cell biology and pathology (neurobiology, immunobiology, tumor biology, environmental biology, reproductive biology, etc.), new methods, anatomy and pathological anatomy, anthropology and paleoanthropology, medical anthropology and physical development.

Acta morphologica et anthropologica is published twice a year as one volume with 4 issues. For the first two issues (1-2) the deadline for manuscript submission is March 15th and for the next two issues (3-4), the deadline is September 15th. Electronic version for issues 1-2 is uploaded on the website till June 30th and for issues 3-4 – till December 30th.

Contact details and submission

Manuscript submission is electronical only. The manuscripts should be sent to the Managing Editor's e-mail address ygluhcheva@hotmail.com with copy to iempam@bas.bg

All correspondence, including notification for Editor's decision, requests for revision, is sent by e-mail.

Article structure

Manuscripts should be in English with total length not exceeding 10 standard pages, line-spacing 1.5, justified with 2.5 cm margins. The authors are advised to use Microsoft Word 97-2003, Times New Roman, 12 pt throughout the text. Pages should be numbered at the bottom right corner of the page.

The article should be arranged under the following headings: Introduction, Material and Methods, Results, Discussion, Conclusion, Acknowledgements and References.

Title page – includes:

- **Title** – concise and informative;
- **Author(s)' names and affiliations** – indicate the given name(s) and family name(s) of all authors. Present the authors' affiliation addresses below the names. Indicate all affiliations with a lower-case superscript after the author's name and in front of the appropriate address. Provide the full postal address information for each affiliation, including the country name.
- **Corresponding author** – clearly indicate who will handle the correspondence for refereeing, publication and post-publication. An e-mail should be provided.
- **Abstract** – state briefly the aim of the work, the principal results and major conclusions and should not exceed 150 words. References and uncommon, or non-standard abbreviations should be avoided.
- **Key words** – provide up to 5 key words. Avoid general, plural and multiple concepts. The key words will be used for indexing purposes.

Introduction – state the objectives of the work and provide an adequate background, avoiding a detailed literature survey or summary of the results.

Material and Methods – provide sufficient detail to allow the work to be reproduced. Methods already published should be indicated as a reference: only relevant modifications should be described.

Results – results should be clear and concise.

Discussion – should explore the significance of the results in the work, not repeat them. A combined *Results and Discussion* section is often appropriate. Avoid extensive citation and discussion of published literature.

Conclusions – the main conclusions of the study should be presented in a short section.

Acknowledgements – list here those individuals who provided help during the research and the funding sources.

Units – please use the International System of Units (SI).

Math formulae – please submit math equations as editable text, not as images.

Electronic artwork – number the tables and illustrations according to their sequence in the text. Provide captions for them on a separate page at the end of the manuscript. The proper place of each figure in the text should be indicated in the left margin of the corresponding page. **All illustrations (photos, graphs and diagrams)** should be referred to as “figures” and given in abbreviation “Fig.”, and numbered in Arabic numerals in order of its mentioning in the manuscript. They should be provided in grayscale as JPEG or TIFF format, minimum 300 dpi. The illustrations should be submitted as separate files.

References – they should be listed in alphabetical order, indicated in the text by giving the corresponding numbers in parentheses. The “References” should be typed on a separate sheet. The names of authors should be arranged alphabetically according to family names. In the reference list titles of works, published in languages other than English, should be translated, original language must be indicated at the end of reference (e.g., [in Bulgarian]). Articles should include the name(s) of author(s), followed by the full title of the article or book cited, the standard abbreviation of the journal (according to British Union Catalogue), the volume number, the year of publication and the pages cited, for books – the city of publication and publisher. In case of more than one author, the initials of the second, third, etc. authors precede their family names. Ideally, the names of all authors should be provided, but the usage of “et al” after the fifth author in long author lists will also be accepted.

For articles: **Davidoff, M. S., R. Middendorff, G. Enikolopov, D. Riethmacher, A. F. Holstein, D. Muller.** Progenitor cells of the testosterone-producing Leydig cells revealed. – *J. Cell Biol.*, **167**, 2004, 935-944.

Book article or chapter: **Rodriguez, C. M., J. L. Kirby, B. T. Hinton.** The development of the epididymis. – In: *The Epididymis – from molecules to clinical practice* (Eds. B. Robaire, B. T. Hinton), New York, Kluwer Academic Plenum Publisher, 2002, 251-269.

Electronic books: **Gray, H.** *Anatomy of the human body* (Ed. W.H.Lewis), 20th edition, NY, 2000. Available at <http://www.Bartleby.com>.

PhD thesis: **Padberg, G.** Facioscapulohumeral diseases. *PhD thesis*, Leiden University, 1982, 130 p.

Website: National survey schoolchildren report. National Centre of Public Health and Analyses, 2014. Available at <http://ncphp.government.bg/files>

Page charges

Manuscript publication is free of charges.

Ethics in publishing

Before sending the manuscript the authors must make sure that it meets the Ethical guidelines for journal publication of *Acta morphologica et anthropologica*.

Human and animal rights

If the work involves the use of human subjects, the authors should ensure that work has been carried out in accordance with *The Code of Ethics of the World Medical Association* (Declaration of Helsinki). The authors should include a statement in the manuscript that informed consent was obtained for experimentation with human subjects. The privacy rights of human subjects must always be observed.

All animal experiments should comply with the *ARRIVE guidelines* and should be carried out in accordance with the U.K. Animals (Scientific procedures) Act, 1986 and the associated guidelines *EU Directive 2010/63/EU* for animal experiments, or the National Institutes of Health guide for the care and use of Laboratory animals (NIH Publications No. 8023, revised 1978) and the authors should clearly indicate in the manuscript that such guidelines have been followed.

Submission Details

Acta morphologica et anthropologica is published twice a year as one volume with 4 issues. For the first two issues (1-2) the deadline for manuscript submission is March 15th and for the next two issues (3-4), the deadline is September 15th. Electronic version for issues 1-2 is uploaded on the website till June 30th and for issues 3-4 – till December 30th.

Manuscript submission is electronical only.

The manuscripts should be sent to the Managing Editor email address ygluhcheva@hotmail.com with copy to iempam@bas.bg

All correspondence, including notification for Editor's decision, requests for revision, is sent by e-mail.

Submission declaration

Submission of the manuscript implies that the work described has not been published previously, is not considered under publication elsewhere, that its publication is approved by all authors, and that if accepted, it will not be published elsewhere in the same form, in English or in any other language, including electronically, without the informed consent of the copyright-holder.

Contributors

The statement that all authors approve the final article should be included in the disclosure.

Copyright

http://www.iempam.bas.bg/journals/acta/Author%20Copyright%20Agreement_last.pdf

Upon acceptance of an article, the authors will be asked to complete a “**Copyright Transfer Agreement**”.

http://www.iempam.bas.bg/journals/acta/Copyright_Transfer_Agreement_Form_AMA.doc

Peer review

Once a manuscript is submitted, the Managing Editor (or the Editor-in-Chief) briefly checks the manuscript for conformance with the journal's Focus, Scope, Policies and style requirements and decide whether it is potentially suitable for publication and can be processed for review, or rejected immediately, or returned to the author for improvement and re-submission.

Manuscripts are peer-reviewed by the Editors, Editorial Board members, and/or external experts before final decisions regarding publication are made. The entire editorial workflow is performed in the following steps:

1. The submitted manuscript is checked in the editorial office whether it is suitable to go through the normal peer review process.
2. If deemed suitable, the manuscript is sent to 2 reviewers for peer-review. The choice of reviewers depends on the subject of the manuscript, the areas of expertise of the reviewers, and their availability.

3. Each reviewer will have 2 weeks to provide evaluation of the manuscript. The Editor may recommend publication, request minor, moderate or major revision, or provide a written critique of why the manuscript should not be published (rejected).
4. In case only one reviewer suggests rejection of the manuscript, the latter is subjected to additional evaluation by a third reviewer.
5. The manuscript will be published in a revised form provided that the authors successfully answer the critics received. The Editor-in-Chief is the final authority on all editorial decisions.

Open Access

This journal provides immediate open access to its content on the principle that making research freely available to the public supports a greater global exchange of knowledge.

After acceptance

Proof correction

The corresponding author will receive proofs by e-mail in PDF format and will be requested to return it with any corrections within two weeks.

